AALTO UNIVERSITY
SCHOOL OF SCIENCE AND TECHNOLOGY
Faculty of Engineering and Architecture
Master`s Programme in Civil and Environmental Engineering
Soil mechanics and Foundation Engineering

KATI SUHONEN

CREEP OF SOFT CLAY

Master`s Thesis submitted on 07/01/2010

SUPERVISOR: Prof. Pauli Vepsäläinen
INSTRUCTOR: PhD. Minna Karstunen

AALTO UNIVERSITY
SCHOOL OF SCIENCE AND TECHNOLOGY
Faculty of Engineering and Architecture

ABSRACT OF THE MASTER'S THESIS

Author: Thesis:	Kati Suhonen Creep of soft clay	
Date: Chair:	3.12.2009 Soil mechanics and Foundation Engineering	Number of pages: 103+appendices Code: Rak-50
Supervisor: Instructor:	Professor Pauli Vepsäläinen PhD. Minna Karstunen	
Keywords:	Creep, consolidation, modelling, EVP-SCLAY1S, ACM, parameters, triaxial test, oedometer test, stress, strain, time-dependent behaviour	

This thesis is a part of the four year (2009-2012) project called "Modelling progressive failure of embankments and slopes" which is funded by the Academy of Finland. The project is a collaboration project between the Helsinki University of Technology and the University of Strathclyde, and it has been established in order to develop reliable, economic and user-friendly analysis methods for practical geotechnical design.

The aim of this thesis was to gather more test data on the behaviour of Finnish soft clay and that way improve the definition of the parameters of EVP-SCLAY1S model and ACM model. These two models were developed by Karstunen and her co-workers as a part of a previous project funded by the Academy of Finland. EVP-SCLAY1S and ACM models take into account anisotropy and time-dependent viscoplastic strain and, in addition, EVP-SCLAY1S is also able to take into account destructuration.

In this work the values for the parameters of these models were defined with the help of laboratory tests on clay samples from Otaniemi. The testing program included oedometer and undrained triaxial tests on natural and reconstituted samples as well as triaxial consolidation tests on natural samples.

It was noticed in oedometer tests that there was only a minor difference between critical state values of natural and reconstituted samples. Hence the clay in Otaniemi is not very structured and there are two possible reasons: samples were disturbed or from dessicated layer. From the triaxial consolidation tests same critical state parameters as from oedometer tests were possible to define but values were not comparable.

In triaxial tests the influence of strain rate on strength parameters was small. Strength parameters were very similar for test groups performed with strain rates 0,06%/h, 0,6%/h and 6%/h. In tests performed with highest strain rate 6%/h, the strain rate effect on strength parameters was clear. In individual tests, where strain rate was altered during the test, higher strain rate significantly strengthened the sample.

AALTO YLIOPISTO **DIPLOMITYÖN**
TEKNILLINEN KORKEAKOULU **TIIVISTELMÄ**
Insinööritieteiden ja arkkitehtuurin tiedekunta

Tekijä: Diplomityö:	Kati Suhonen Creep of soft clay	
Päivämäärä: Professuuri:	3.12.2009 Maamekaniikka ja pohjarakennus	Sivumäärä: 103+appendices Koodi: Rak-50
Valvoja: Ohjaaja:	Prof. Pauli Vepsäläinen PhD. Minna Karstunen	
Avainsanat:	Viruma, konsolidoituminen, mallintaminen, EVP-SCLAY1S, ACM, kolmiaksiaalikoe, ödometrikoe, jännitys, muodonmuutos	

Tämä työ on osa neljävuotista (2009-2012) Suomen Akatemian rahoittamaa projektia ”Modelling progressive failure of embankments and slopes”. Projekti on tehty yhteistyössä Teknillisen korkeakoulun ja Strathclyden yliopiston kesken ja sen tarkoituksena on kehittää luotettavia, taloudellisia ja käyttäjä-ystävällisiä laskentamenetelmiä käytännön geotekniseen suunnitteluun.

Työn tarkoituksena oli kerätä testitietoa suomalaisten pehmeiden savien käyttäytymisestä ja näin helpottaa EVP-SCLAY1S- ja ACM-mallin parametrien määrittämistä. Karstunen ja kollegat kehittivät kyseiset mallit osana edellistä Suomen Akatemian rahoittamaa projektia. EVP-SCLAY1S- ja ACM-mallit ottavat huomioon anisotropian ja viskoplastiset muodonmuutokset sekä lisäksi EVP-SCLAY1S huomioi myös rakenteen vaikutuksen.

Tässä työssä kyseisten mallien parametrit määritettiin laboratoriokokeiden avulla Otaniemen savesta. Koeohjelmaan kuului suljettuja kolmiaksiaalikokeita ja ödometrikokeita luonnontilaisille ja rakennetuille näytteille sekä kolmiaksiaalisia konsolidointikokeita luonnontilaisille näytteille.

Ödometrikokeissa havaittiin, että luonnontilaisten ja rakennettujen näytteiden kriittisen tilan parametrien arvojen välillä oli hyvin pieni ero. Otaniemen saven rakenne ei täten vaikuta parametrien arvoihin juurikaan. Tämä voi aiheutua näytteiden häiriintymisestä tai siitä, että näytteet ovat kerroksesta, joka on altistunut kuivumis- ja kastumissykleille. Kolmiaksiaalisista konsolidointikokeista määritettiin samoja kriittisen tilan parametreja kuin ödometrikokeista, mutta arvot eivät olleet verrattavissa.

Kolmiaksiaalikokeissa muodonmuutosnopeuden vaikutus lujuusparametreihin oli pieni. Lujuusparametrit olivat hyvin samanlaisia testiryhmille, jotka oli suoritettu nopeuksilla 0,06%/h, 0,6%/h ja 6%/h. Suurimmalla muodonmuutosnopeudella 6%/h suoritetuissa kokeissa muodonmuutosnopeuden vaikutus lujuusparametreihin oli selkeä. Yksittäisissä kokeissa, joissa muodonmuutosnopeutta vaihdeltiin kokeen aikana, korkeampi muodonmuutosnopeus selvästi lujitti näytettä.

PREFACE

I would like to thank Professor Pauli Vepsäläinen and PhD. Minna Karstunen for the quidance that they have given me for this Master`s thesis. Special compliments I would like to say to Lic. Sc. (Tech.) Matti Lojander for his valuable time and priceless advice. Also the help of Jarmo Vihervuori and Matti Ristimäki was essential in order to carry out laboratory tests and for that I`m thankful. I also present thanks to the whole personnel of the Laboratory of Soil Mechanics and Foundation Engineering at the Helsinki University of Technology.

Then, last but not least, I would like to thank Bosse and the rest of my family for their encouragement during this half of the year. In addition, I feel great gratitude to my friends Laura and Linda for their understanding and peer support.

Espoo, the 7th of January 2010

Kati Suhonen

LIST OF SYMBOLS

Roman letters

A	Area of the sample [cm^2]
°C	Degree celcius
C_α	Secondary compression index
C_c	Compression index
C_r	Recompression index
C_s	Swelling index
c'	Effective cohesion
c_u	Undrained shear strength [kPa]
c_v	Coefficient of consolidation [m^2/s]
Cl-%	Clay content
e	Void ratio
e_0	Initial void ratio
e_{eoc}	Void ratio at the end of primary consolidation
$\dot{e}$	The rate of change of void ratio
f_d	Viscoplastic potential function , represented by the dynamic loading surface
G	Shear modulus
H	Drainage length [m]
H_{EOP}	Height at the end of primary consolidation
h_0	Initial height of the sample [cm]
Hm-%	Organic content
I_P	Plasticity index [%]
K	Elastic bulk modulus
K_0	Coefficient of the earth pressure at rest
k	Permeability [m/s]
k_1	Slope of the failure line
M	Compression modulus [kPa]
M_0	Model parameter from Embankco model, compression modulus for $\sigma_v' < \sigma_c'$ [kPa]
M_L	Model parameter from Embankco model, compression modulus for $\sigma_c' \le \sigma_v' \le \sigma_l'$ [kPa]

$M(\sigma')$ Oedometer modulus [kPa]

M' Model parameter from Embankco model, modulus number for $\sigma_v' > \sigma_L'$ [kPa]

m Modulus number

m_v Coefficient of compressibility

m_1 Modulus number (normally consolidated)

m_2 Modulus number (overconsolidated)

N Viscosity index (or strain rate coefficient)

p Mean stress [kPa]

p' Mean effective stress [kPa]

p'_{eq} Equivalent mean stress [kPa]

p_{mi} The size of intrinsic yield surface

p_m^d The size of dynamic loading surface

p_m^s The size of static yield surface

p_p' Isotropic preconsolidation pressure [kPa]

q Deviatoric stress [kPa]

q_0 Interception point with failure line and q-axis

R Time resistance [s]

r_s Time resistance number

S_p The final primary settlement of the structure [m]

S_r Degree of saturation [%]

S_t Sensitivity

S(t) The primary settlement of the structure [m]

T_v Time factor

t Time [s]

t' Effective creep time [s]

t_r Reference time [s]

t_{eop} Time at the end of primary consolidation [s]

U_p The degree of consolidation

u Pore water pressure [kPa]

u_{cr} Pore water pressure due to creep effects [kPa]

V Volume [m^3]

v Spesific volume

v_λ Ordinate of λ-line with p=1 kPa

w Water content [%]

w_L Liquid limit [%]

w_P Plastic limit [%]

z Depth [m]

Greek letters

α Rotational hardening parameter

α_d Deviatoric fabric tensor

α_s The coefficient of secondary consolidation

α_0 The initial rotation of the ellipse

$\beta_{\alpha s}$ The coefficient of change in secondary consolidation

β_k Model parameter from Embankco model, factor that express the decrease of permeability with compression

β_1 Stress exponent (normally consolidated)

β_2 Stress exponent (overconsolidated)

γ Unit weight [kN/m^3]

γ_w Unit weight of the water [kN/m^3]

$\dot{\gamma}^c$ Deviatoric creep strain rate [1/s]

δ_{ij} Kronecker delta

ε Strain [%]

ε_{cr} Creep strain [%]

ε_c^e Elastic strain during primary consolidation [%]

ε_c^{cr} Creep strain during primary consolidation [%]

ε_{ac}^{cr} Creep strain after primary consolidation [%]

ε_v Vertical strain [%]

ε_v^{vp} Viscoplastic volumetric strain [%]

ε_{vol}^c Volumetric creep strain [%]

$\dot{\varepsilon}$ Strain rate [1/s]

$\dot{\varepsilon}^{e}$ Elastic strain rate [1/s]

$\dot{\varepsilon}_{cr}$ Creep strain rate [1/s]

$\dot{\varepsilon}_{ij}$ *(i,j)* component of the total strain rate tensor [1/s]

$\dot{\varepsilon}^{e}_{ij}$ Elastic component of strain rate[1/s]

$\dot{\varepsilon}^{vp}_{ij}$ Viscoplastic component of the strain rate [1/s]

$\dot{\varepsilon}_{v}$ Vertical strain rate [1/s]

η Stress ratio

η_{K_0} Stress ratio at K_0-state

κ Slope of the overconsolidation (unloading) line in v:ln (p) plane

κ^{*} Modified swelling index

λ Slope of the normal consolidation line in v:ln (p) plane

λ_i The slope of the intrinsic normal compression curve in the $e - \ln \sigma_v^{`}$ plane

λ^{*} Modified compression index

M Stress ratio at critical state

M_C Stress ratio at critical state

μ Fluidity parameter

μ^{*} Modified creep index

$\nu^{'}$ Effective Poisson`s ratio

ξ Soil constant controlling the absolute rate of destructuration

ξ_d Soil constant controlling the relative effect of viscoplastic deviatoric strains in destroying the bonds

ρ_s Spesific gravity [g/cm^3]

$\sigma^{'}$ Effective stress [kPa]

$\sigma^{'}_{ij}$ Actual effective stress [kPa]

$\sigma^{'}_{c}$ Preconsolidation pressure [kPa]

$\sigma^{'}_{L}$ Model parameter from Embankco model, the effective stress where the compression modulus begins to increase [kPa]

σ'_p Preconsolidation pressure [kPa]

σ'_v Vertical effective stress [kPa]

$\dot{\sigma}_d$ Deviatoric stress rate tensor

σ_1, σ_3 Principal stresses [kPa]

τ Reference-time

τ_c Intercept with the time axis of the straight creep line

φ' Effective friction angle

χ Scalar variable describing the amount of particle bonding

χ_0 The initial amount of bonding

ω Soil constants that control the rate of rotation

ω_d Soil constants that control the rate of rotation

ϕ'_{cv} Critical-state friction angle

$\Phi(F)$ overstress function representing the difference between the loading surface and the static yield surface as normalized overstress

ABREVIATIONS

ACM Anisotropic creep model for soft soils

CRS constant rate of strain

CSS current stress surface

EOP end of primary consolidation

EVP elastoviscoplastic

ICM isotropic creep model

IL increment loading

LIR load increment ratio

MCC Modified Cam Clay model

NCS normal consolidation surface

OCR overconsolidation ratio

REC reconstituted sample

1. INTRODUCTION

This work is a part of the three year project called “Modelling progressive failure of embankments and slopes”, which is funded by The Academy of Finland. The project is a collaboration project between the Helsinki University of Technology and the University of Strathclyde. The aim of the project is to develop a numerical tool for modelling the delayed behaviour of structured clays under embankment loading.

The design methods used in geotechnical engineering are often over-conservative and raw and in some cases also unsafe. This, in addition to the fact that densely populated coastal areas in Finland, as well as in some parts of Europe, Northern America and Asia, are covered with extremely soft and sensitive clay deposits, require design tools that provide safe and economical design and construction.

The behaviour of soft sensitive clay is remarkably complicated and thus the modelling requires plenty of efforts. A significant degree of anisotropy is exhibited by natural clays. Anisotropy has developed during clays deposition, sedimentation, consolidation history and following straining [Tavenas & Leroueil 1977, Burland 1990]. Natural soils also exhibit some apparent bonding, which will be progressively lost during straining [Leroueil & Vaughan 1990, Burland 1990]. This process is referenced as destructuration [Leroueil et al. 1979]. In addition, the time dependent stress-strain relationship, which has a major influence on the shear strength and the preconsolidation pressure, is one important feature of natural clays [Bjerrum 1967, Mesri & Godlewski 1977, Vaid & Campanella 1977, Graham et al. 1983, Leroueil et al. 1985, 1988, Sheahan et al. 1996]. In order to develop sophisticated design methods, which could take into account all these major features of soft natural clays, two new constitutive models to model the viscous behaviour of soil was developed by Karstunen and her co-workers [Karstunen 2008]. These two new models: an elastoviscoplastic model EVP-SCLAY1S and a viscose model ACM, were developed as a part of the former project funded by The Academy of Finland. However, the performance of EVP-SCLAY1S and ACM still needs to be improved. Further information about models can be found in Chapter 3.

The purpose of this work was to improve the performance of EVP-SCLAY1S and ACM models with a large testing program of HUT clay. The first objective was to compose literature survey about different consolidation theories and models in order to understand the basics of the modelling the behaviour of soft clays. The second objective was to perform oedometer tests on both natural, undisturbed samples and reconstituted samples in order to define the stress state of the clay and define critical state parameters, which are included in EVP-SCLAY1S and ACM models. The third objective was to perform triaxial consolidation tests to be able to define yield points and critical state parameters. The fourth objective was to carry out undrained triaxial tests in order to research the influence of strain rate variation to strength parameters of soft clay. The laboratory test results can be found in Chapter 6 and conclusions and recommendations for further work are presented in Chapter 7.

.

2. CONSOLIDATION MODELS AND THEORIES

2.1 Terzaghi´s one dimensional consolidation theory

The classical theory of consolidation was first introduced in 1925 in Terzaghi´s book *Erdbaumechanik* [Ortigao J.R 1995]. Still today, this theory forms the foundation of one dimensional consolidation theory. Purpose of the theoretical study of consolidation is setting up of an equation from which the pressure and void ratio values are possible to determine at any point and at any time in a stratum of consolidating soil of any thickness [Taylor 1948].

The classical consolidation theory is based on the assumption that there is a unique relationship between effective stress and strain independent of time. Terzaghi also assumes that the modulus and the permeability are constants with time. For high plastic clays the assumption that the relationship between stress and strain, or void ratio, is independent of time is a rough simplification since those clays allocate a large amount of time dependent strains [Claesson 2003]. Moreover, in the theory it is assumed that seepage flow and deformation of soil layer occur in the same direction. Skeleton of the consolidating soil layer affects on the settlement rate not until the secondary consolidation and primary and secondary consolidation are assumed to occur consecutively [Korhonen 1985].

Terzaghi´s one dimensional consolidation equation:

$$\frac{\partial u}{\partial t} = \frac{M}{\gamma_w} \cdot \frac{\partial}{\partial z}\left(k \cdot \frac{\partial u}{\partial z} \right) \tag{2.1}$$

or if k does not vary with depth,

$$\frac{\partial u}{\partial t} = c_v \frac{\partial^2 u}{\partial z^2} \tag{2.2}$$

Where the coefficient of consolidation is defined as:

$$c_v = \frac{k \cdot M}{\gamma_w} \tag{2.3}$$

Where k is permeability [m/s]

M compression modulus [kPa]

u pore water pressure [kPa]

z depth [m]

γ_w unit weight of water [kN/m^3]

Equation (2.2) is eligible when following assumptions are fulfilled:

The soil is homogenous and saturated
The validity of Darcy´s law
The flow of pore water flow and the strain are one-dimensional
The change in pore water pressure equals to change in effective stress
The pore water and soil particles are incompressible
The strain is solely dependent on the effective stress

Terzaghi introduced the first oedometer device and test procedure in 1925. In this procedure the specimen is loaded step-wise, each load step doubling the previous value as long as the excess pore pressure has dissipated. Duration of 24 hours is quite common for clays. This procedure is commonly referred to as a standard incremental load oedometer test and it is still widely used [Claesson 2003]. In this test the cylindrical sample can move only in the direction of its vertical axis, and only in this direction pore air and pore water can be pressed out [Suklje 1969].

Terzaghi presented a model for calculating the degree of consolidation in 1936. The degree of consolidation can be determined by calculating the time factor T_v:

$$U_p = \frac{S(t)}{S_p} \tag{2.4}$$

$$T_v = \frac{c_v}{H^2} \cdot t \tag{2.5}$$

Where U_P is the degree of consolidation for primary settlement at time t

S(t) the primary settlement of the structure at time t

S_p the final primary settlement of the structure at time t

c_v coeffient of consolidation [m^2/s]

H drainage length [m]

t time [s]

The relationship between the degree of consolidation U_p and time factor T_v is shown in Figure 2.1

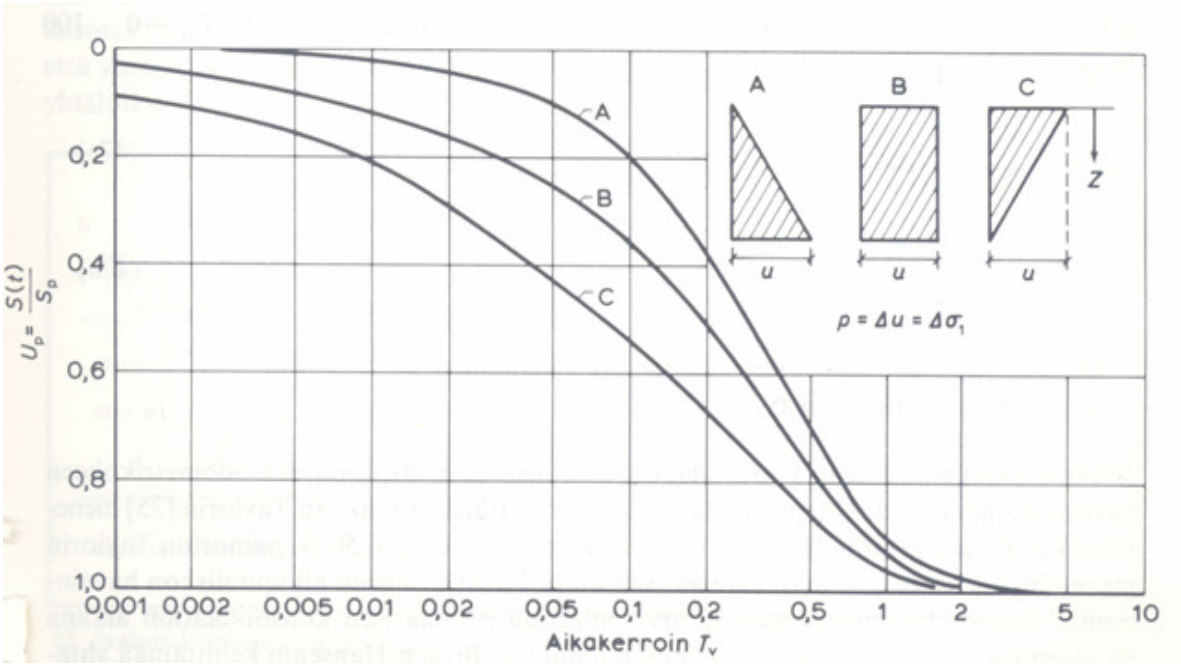

Figure 2.1 *Relationship between degree of consolidation and time factor. The three polygrams and curves correspond to three different cases of excess pore pressure and drainage conditions. [Reproduced after Terzaghi & Peck 1948]*

In 1936 Casagrande suggested an oedometer test procedure for determining the end of primary consolidation, EOP, of each load increment when the dissipation of excess pore pressure is complete. Casagrande´s test procedure suggest that time-strain dependency is plotted in a semilogarithmic diagram. The EOP is evaluated as the intersection point between the two tangents of the curve as shown in Figure 2.2

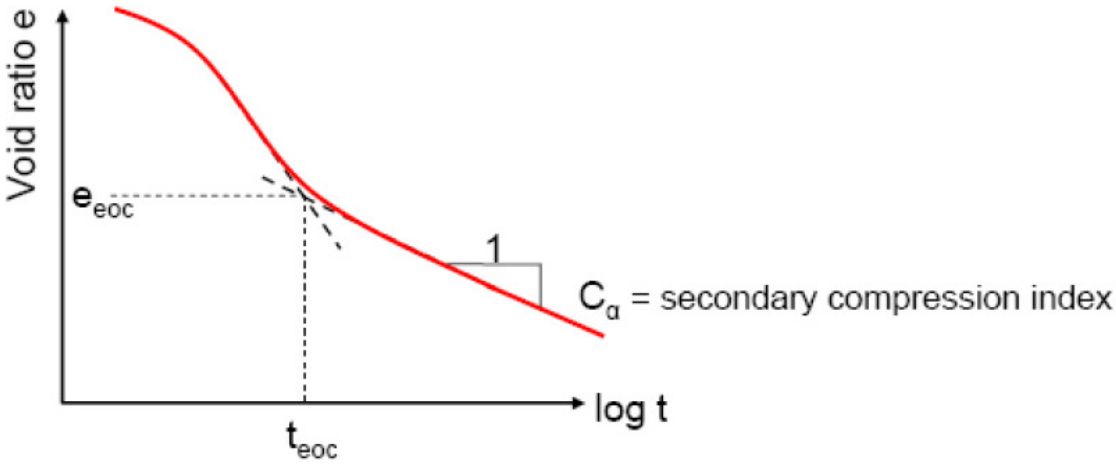

Figure 2.2 *Casagrande method of determining EOP, 100% primary consolidation.*

Taylor suggested in 1948 another widely used method of determining the EOP. In Taylor´s method the strain is plotted versus the square root of time.

2.2 Early models for consolidation including creep effects

In the literature the consolidation process has almost always been divided into primary and secondary consolidation when dealing with consolidation models. The basic hypothesis is that the primary consolidation occurs during an increase in the effective stress and a concurrent decrease in excess pore pressure and volume. The secondary consolidation process is been defined as a decrease in volume under constant effective stress. Creep strains were separated from the primary consolidation and hence regarded equal to secondary consolidation for a long time [Claesson 2003].

Originally calculations of the consolidation settlements were based on Terzaghi´s theory which was assumed to be valid during primary consolidation [Larsson 1986]. According to Buisman (1936) secondary compression and possibly creep effects started after the full excess pore pressure dissipation had occurred, and proceeded at a continuously decreasing rate as the secondary settlement was assumed to be a linear function of the logarithm of time.

The first theory where creep effects were at least partly involved in primary consolidation process was formulated by Taylor and Merchant in 1940. Taylor developed a first model for a general variation of void ratio e, versus effective stress σ' and time t, two years later, in 1942 [Taylor 1942]. To be exact it was two different theories, A and B, that Taylor generated for one-dimensional strained state. It is presumed in theory A, that primary and secondary consolidation takes place consecutively. Whereas, according to theory B primary and secondary consolidation occurs at least partly simultaneous.[Hoikkala 1991].

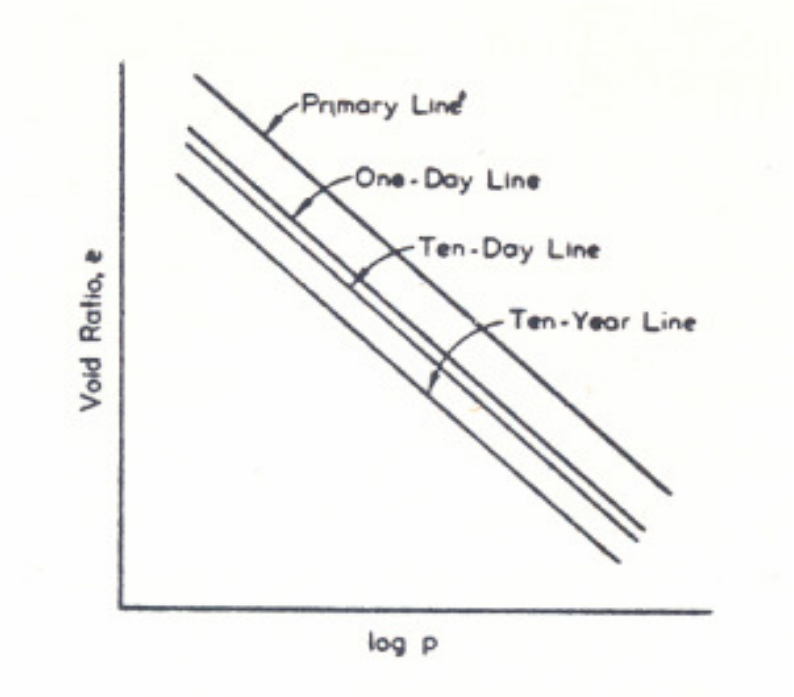

Figure 2.3 *Relationship between void ratio and effective stress for different times [Taylor 1942]*

Suklje, in 1957, was the first one to introduce a more general model where creep strains also were assumed to occur during primary consolidation [Claesson 2003]. According to Sulkje term "creep" is used to express the increase of deformation with time at constant effective stress [Suklje 1969]. Basic assumption in Suklje´s model is that the void ratio-effective pressure relation continuously changes with rate of deformation [Larsson 1986]. Relationship between effective stress, void ratio and strain rate defined the form of the consolidation curve and this relationship was demonstrated by a set of isotaches. Isotaches can be defined as graphs relating effective stresses to void ratios for certain constant consolidation speeds as shown in Figure 2.4. [Suklje 1969]

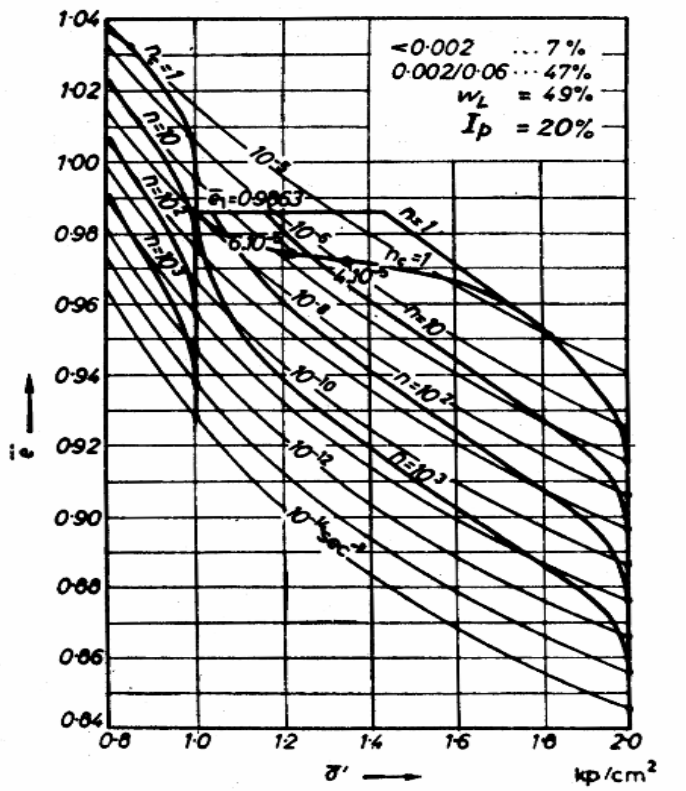

Figure 2.4 *Set of isotaches and compression curves of normally consolidated clay for a suddenly applied load $\Delta\sigma$ = (2,0-1,0)kp/cm^2 and various layer thicknesses $h = nh_1$, $2h_1$ = 3,585cm [Reproduced after Suklje 1957].*

It was originally Sulkje, who suggest that the behaviour of clay at one dimensional consolidation is controlled by a unique relationship between effective stress, void ratio and strain rate. The model developed by Suklje assumes that primary consolidation and creep effects are not two separate processes and thus creep occurs during entire consolidation process, not only after the dissipation of excess pore pressure. Suklje also suggested in his model that the time-dependent strains are influenced by the thickness of the clay layer, permeability and drainage conditions. [Claesson 2003].

2.3 The Bjerrum model

Bjerrum presented in 1967 a conceptual model, which assumes that primary consolidation and creep strains are not divided into separate processes. Bjerrum model´s assumptions are very similar to assumptions of Suklje´s model. Bjerrum model is primarily intented for settlements that have developed over a long period of time, i.e. a period of time in a geologi-

cal perspective. Normally engineers are concerned with a shorter period of time, usually 50-100 years or shorter. However, it is essential in engineering practice that the design takes into consideration of the time delay caused by the permeability and the drainage conditions.

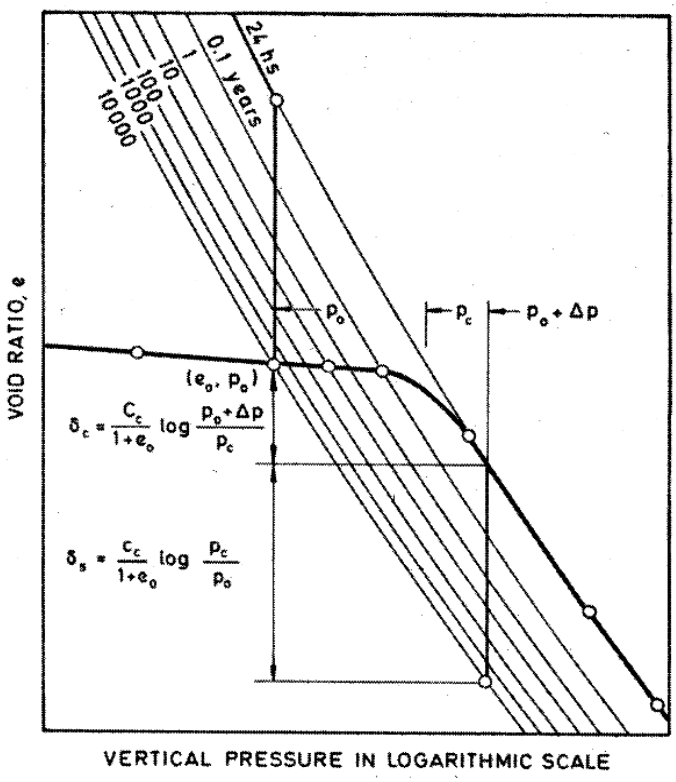

2.5 Figure *Diagram describing the Bjerrum model. Series of parallel time lines describing the compressibility and shear strength of clay, which shows delayed consolidation. [Bjerrum 1967]*

The purpose of the Bjerrum model was to explain the apparent preconsolidation pressure and overconsolidation ratio OCR, resulting from geological ageing. The model also accounts for settlements and creep effects occurring over time, though the preconsolidation pressure has not been exceeded [Claesson 2003]. A series of paraller “time lines” were proposed to represent a) multistage loading (MSL) tests with alternate durations, b) delayed compression at constant effective stress under engineering structures, c) aging in natural deposits [Yin & Graham 1989]. In figure 2.5 the relationship between void ratio, pressure (effective stress) and time is represented by a series of parallel time lines on the vertical pressure-void ratio diagram. Each of these lines represents the equilibrium void

ratio for different values of effective stress at a specific time of sustained loading [Flaate 2003].

Bjerrum separated strains into instant and delayed compression and utilized “time lines” to model reduced creep rates resulting from the increased duration of loading. In figure 2.6 assumed compression development of a clay layer with time for an applied load is represented. In this figure it is assumed that the applied load is transferred instantaneously to the clay structure, i.e. as effective stress. This is designated instant compression and the broken lines show how the strains would occur if the pore water in saturated clay could be disregarded. The subsequent compression that occurs under unchanged effective stress, is the delayed compression. The effective stresses will gradually increase due to the viscosity of water, when the excess pore pressure dissipates and thus compression will occur along the solid line. [Claesson 2003]

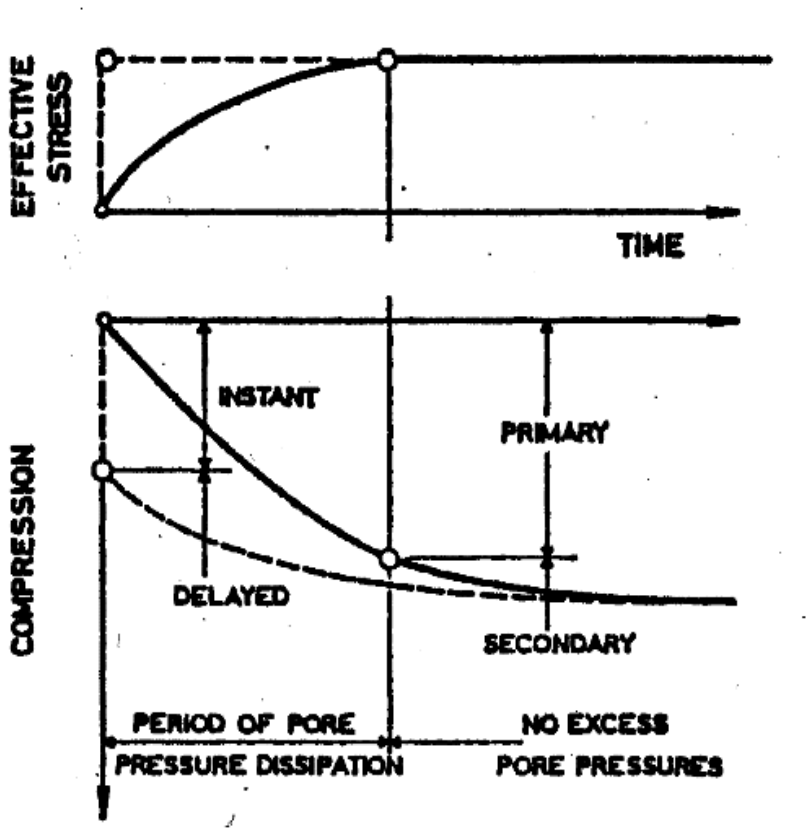

Figure 2.6 *Definition of the two parts of settlements, instant and delayed compression, compared with primary and secondary compression illustrated by the broken and the solid line respectively [Bjerrum 1967].*

In 1967 Bjerrum presented that there is an apparent relation between undrained shear strength and preconsolidation pressure. It is assumed that this relation remains unchanged at changing void ratio (or strain). Thereby, a decrease in void ratio or increasing strains, increases the undrained shear strength. According to Bjerrum the magnitude of the over-consolidation ratio, OCR, depends on the plasticity of the clay and its geological history. [Claesson 2003]

2.4 The creep parameters C_α and α_s

In 1942 Taylor introduced a commonly used parameter for describing the creep behaviour of clay, *secondary compression index*, C_α, which is defined as:

$$C_\alpha = \frac{\Delta e}{\Delta \log(t)} \tag{2.6}$$

where e is void ratio

t time

In Sweden the commonly used creep parameter is the *coefficient of secondary consolidation*, α_s, which is defined as:

$$\alpha_s = \frac{\Delta \varepsilon_{cr}}{\Delta \log(t)} \tag{2.7}$$

where α_s is the coefficient of secondary compression

ε_{cr} creep strain

t time

The *coefficient of secondary consolidation* α_s relates to the *secondary compression index* C_α and the only difference in definition of these two parameters is that α_s is defined as a

function of strain, ε, and C_α as a function of void ratio, e [Claesson 2003]. The relationship between creep parameters can be described as:

$$\alpha_s = \frac{C_\alpha}{1+e_0} \tag{2.8}$$

where $1+e_0$ is the specific volume, V

e_0 the initial void ratio

Figure 2.7 illustrates the evaluation of α_s and C_α from an incremental loading (IL) test.

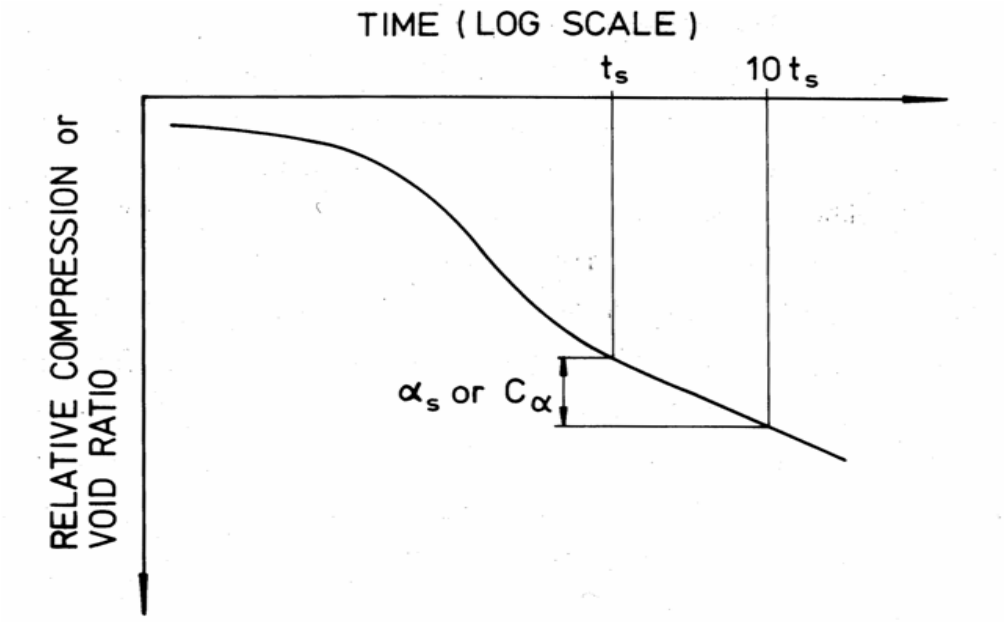

Figure 2.7 *Evaluation of α_s and C_α from an incremental loading test [Larsson 1986).*

The creep behaviour is very often described by the coefficient of secondary compression α_s, but it has been proved that α_s is not a constant [Larsson 1986]. α_s varies from load step to load step in incremental oedometer tests and variation of α_s with strain is illustrated in Figure 2.8. The coefficient $\beta_{\alpha s}$ specifies the change in α_s with increasing strain.

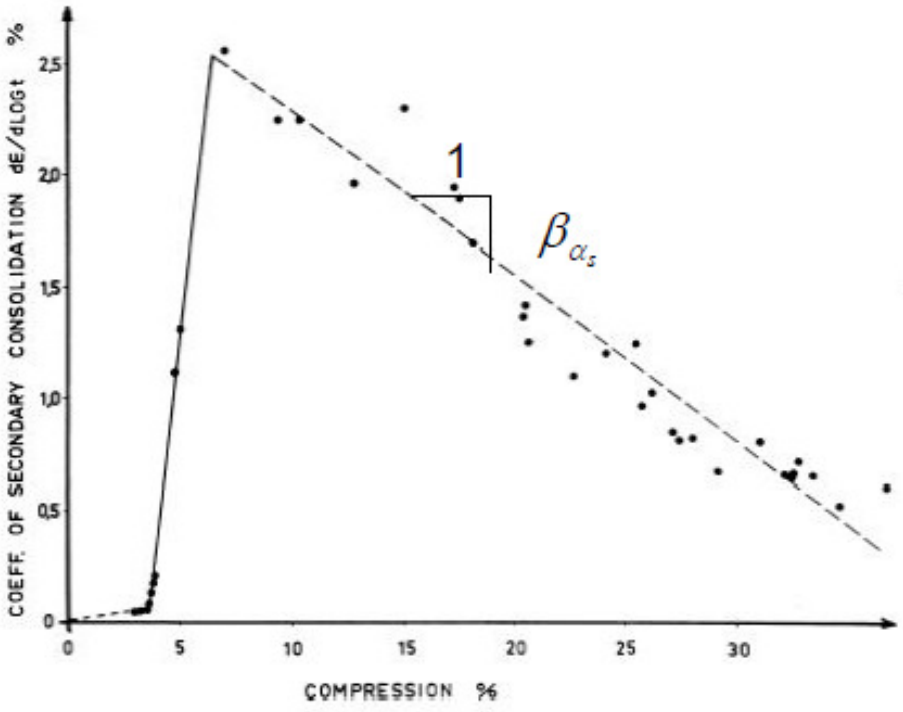

Figure 2.8 *The model of the coefficient of secondary compression* α_s*, according to Swedish practice [Larsson 1986].*

2.5 The time resistance concept

In 1969 Janbu introduced another parameter that describes creep behaviour, the time resistance R. Since in actual creep the excess pore pressure is zero, if one believes in theory A, it is possible to consider time t as an action and creep strain as a reaction. Time resistance is then defined as:

$$R = \frac{dt}{d\varepsilon} \tag{2.9}$$

Where R is time resistance [s]

ε strain

Thus time resistance *R* is the tangent of time - strain graph. In laboratory tests it has ocurred that the time resistance *R* of clays increases linearly with time after particular time

t_0. [Länsivaara 2001] This is illustrated in Figure 2.9. Thereafter the relation may be expressed as:

$$R = r_s \cdot (t - t_r) \ , \ t > \ t_0 \tag{2.10}$$

Where r_s is time resistance number

t time

t_r reference time

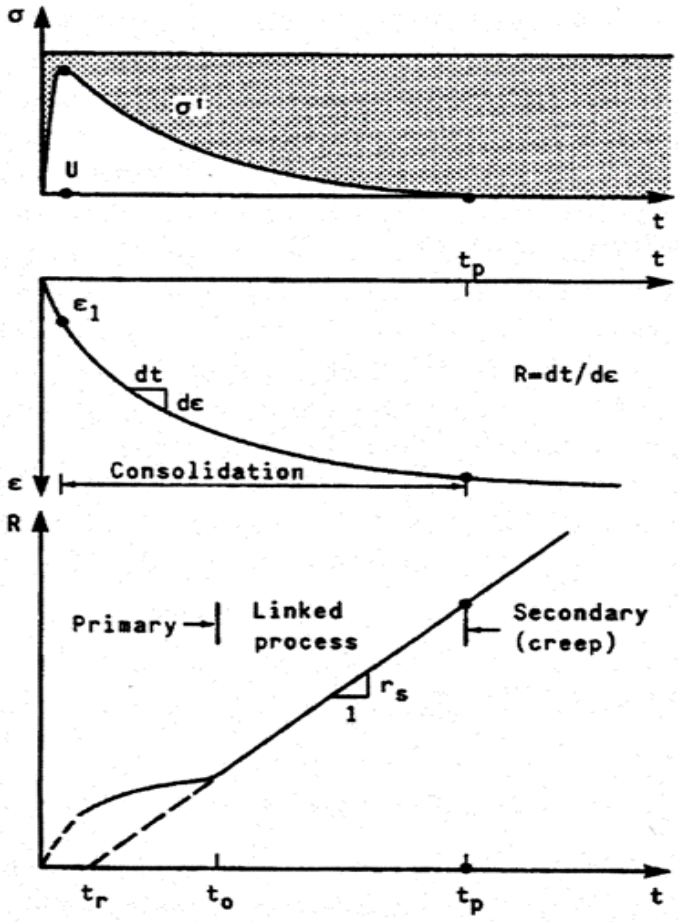

Figure 2.9 *Definitions for time-resistance R and time-resistance* r_s *[Janbu 1998].*

Thus the creep strain rate $\dot{\varepsilon}$ at time *t* is equal to the inverse of the time resistance *R:*

$$\dot{\varepsilon}_{cr} = \frac{\partial \varepsilon_{cr}}{\partial t} = \frac{1}{R} = \frac{1}{r_s \cdot (t - t_r)} \tag{2.11}$$

where $\dot{\varepsilon}_{cr}$ is the creep strain rate[1/s]

ε_{cr} the creep strain

The strain due to creep is discovered by integration of equation (2.11) from t_0 to *t,* resulting to equation (2.12):

$$\Delta\varepsilon_{cr} = \frac{1}{r_s}\ln\frac{t-t_r}{t_0-t_r} \tag{2.12}$$

where t_0 is time when the R-t curve approaches a straight line

From equation (2.12), the time resistance number, r_s, can be determined as:

$$\frac{1}{r_s} = \frac{\partial\varepsilon_{cr}}{\partial\ln t} \tag{2.13}$$

Eventually, the relationship between the time resistance number and the coefficient of secondary consolidation is defined as:

$$\alpha_s = \frac{\partial\varepsilon_{cr}}{\partial\log(t)} = \frac{\partial\varepsilon_{cr}}{\partial\ln(t)}\cdot\frac{\partial\ln(t)}{\partial\log(t)} = \frac{\partial\varepsilon_{cr}}{\partial\ln(t)}\cdot\ln 10 \tag{2.14}$$

$$\alpha_s = \frac{\ln 10}{r_s} \approx \frac{2{,}3}{r_s} \tag{2.15}$$

2.6 Relationship between parameters for primary and secondary consolidation

Compression index C_c is commonly used parameter to describe the compression behaviour of clay for effective stresses greater than the preconsolidation pressure. The *compression index* C_c is defined as:

$$C_c = \frac{\Delta e}{\Delta \log \sigma`} \tag{2.16}$$

or

$$C_c = \frac{\Delta e}{\log \frac{\sigma` + \Delta \sigma`}{\sigma`}} \tag{2.17}$$

where e is void ratio

σ' effective vertical stress

In 1977 Mesri and Godlewski presented that there is relationship between the *secondary compression index* C_α and the *compression index* C_c. This relationship is valid for any type of soil and for all combinations of time, effective stress and void ratio. The relationship is defined as:

$$\frac{C_\alpha}{C_c} = \text{constant} \tag{2.18}$$

According to Mesri and Castro (1987) for major part of inorganic clays the relationship equals:

$$\frac{C_\alpha}{C_c} = 0.04 \pm 0.01 \tag{2.19}$$

Janbu specified in 1985 the relationship between the modulus number, m, and time resistance number, r_s, as:

$$\frac{C_\alpha}{C_c} = \frac{m}{r_s} \tag{2.20}$$

where $m = \frac{M(\sigma`)}{\sigma`}$

$M(\sigma')$ is the oedometer modulus [kPa]

σ' the effective vertical stress [kPa]

It is assumed that the stiffness of the clay increases linearly with stress in the normally consolidated area, i.e $M = m \cdot \sigma'$. This assumption is in agreement with the concept of Janbu´s tangent modulus (1963).

As shown in this chapter, the three creep parameters have some significant differences but are however strongly related to each other.

2.7 The relationship between effective stress, strain and strain rate

Leroueil et al. performed a comprehensive study of different tests on various types of clays in 1985. The aim of this study was to determine the rheological behaviour of soft clays. According to Leroueil et al. the rheological behaviour of one-dimensional consolidation of clays is controlled by a unique relationship between stress, strain and strain rate $(\sigma' - \varepsilon - \dot{\varepsilon})$. It is possible to describe this relationship with two functions. The first function defines the relationship between the preconsolidation pressure and the strain rate, equation (2.21) and the second function describes the normalized effective stress-strain curve by means of equation (2.22), see Figure 2.10:

$$\sigma'_p = f(\dot{\varepsilon}_v) \tag{2.21}$$

$$\frac{\sigma'_v}{\sigma'_p} = g(\varepsilon_v) \tag{2.22}$$

where σ'_p is the preconsolidation pressure

σ'_v the vertical effective stress [kPa]

ε_v the vertical strain

$\dot{\varepsilon}_v$ the vertical strain rate [1/s]

$f(\dot{\varepsilon}_v)$ a function of vertical strain rate

$g(\varepsilon_v)$ a function of vertical strain

This rheological model is analogous with Sulkje´s model (1957) which includes sets of isotaches.

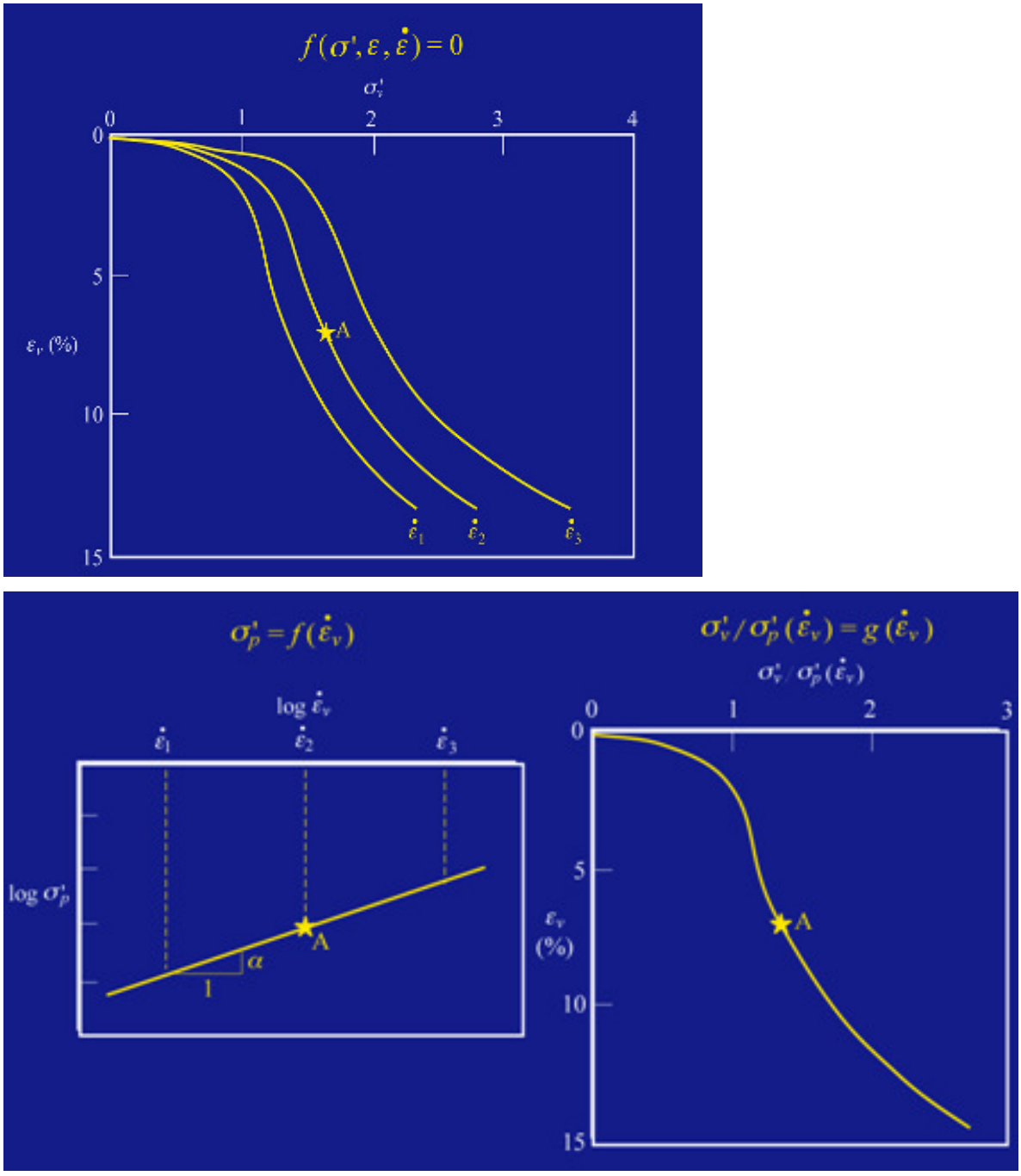

Figure 2.10 *Suggested model for natural clays [Leroueil et al. 1985].*

Many researchers, e.g. Sällfors (1975), Larsson (1981), Graham et al. (1983) and Leroueil et al. (1985), have recognized that the preconsolidation pressure is dependent on the strain rate. This behaviour can be observed by CRS-tests with different strain rates.

In 1995 Mesri et al. presented another important test result, which confirms the behaviour described. In this test the effective stress-strain curves of four different sub-layers of a 500 mm long sample were monitored. The stress-strain curves vary, depending on the distance of each sub-element to the drainage boundary. Sub-element 1 located close to the drainage surface showed higher strain rate than the other sub-elements. As a result it is stated that for a higher strain rate a higher magnitude of effective stress was obtained in the initial branch of the curve, i.e. the apparent preconsolidation pressure increased. Berre and Iversen reported analogous results already in 1972. In Figure 2.11 these results are presented and it is clearly shown how the consolidation process and the apparent preconsolidation pressure vary in the clay strata due to different drainage conditions. In Figure 2.11 the point of EOP seems to be equal for all the sub-elements. In 1985 Mesri and Choi proposed that there is a unique EOP e- $\log\sigma'$ curve for any soft clay. This statement is not, however, analogous to theories of Suklje (1957), Berre and Iversen (1972) and Yin and Graham (1996). They all concluded that the relationship between strain and effective stress at the EOP depends on the thickness of the clay specimen and layer.

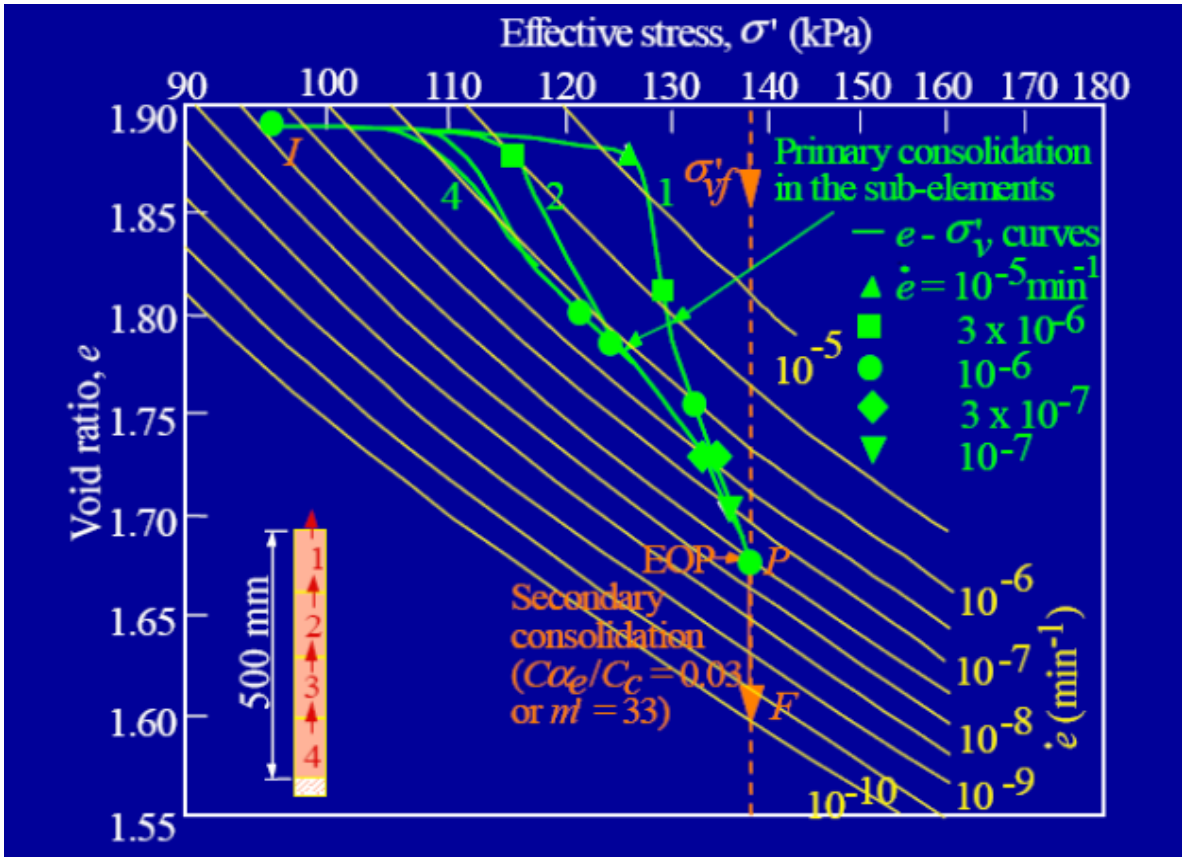

Figure 2.11 *Consolidation of St-Hilaire clay for pressure increment from 97 to 138 kPa (results from Mesri et al. (1995), reinterpreted and presented by Leroueil and Marques, 1996),* C_α *secondary compression index;* C_c *compression index;* $\dot{e}$ *rate of void ratio and* $m' = C_c / C_\alpha$.

Leroueil and Kim proposed a non-linear viscoplastic model for one-dimensional consolidation in 2001. In this model the strain is divided into two parts: elastic strains and viscoplastic strains and viscoplastic behaviour is modeled by a unique effective stress (σ_v')- viscous strain (ε_v) - viscous strain rate ($\dot{\varepsilon}_v$) relationship. This model is developed from the model presented by Leroueil at al. (1985) and it is described in detail by Kim & Leroueil (2001).

2.8 The effect of temperature on the compressibility

The behaviour of natural clay during consolidation is influenced by strain rate, as well as temperature. Especially in the normally consolidated range and in terms of the magnitude of the preconsolidation pressure, the temperature is important factor. Many authors, such

as Tidfors and Sällfors (1989) and Boudali et al. (1994), have investigated the influence of temperature on the compressibility of natural clays. Boudali et al (1994) suggested a generalization of the Leroueil´s model (1985), which takes the temperature into account.

In 1989 Tidfors and Sällfors discovered that the preconsolidation pressure for a high plastic clay decreases with 6 to 10% if the temperature increases from normal temperature in-situ $+7^{\circ}C$ to $20^{\circ}C$. Leroueil and Marques obtained analogous results in 1996. [Claesson P. 2003]

3. MODELS FOR SETTLEMENT CALCULATIONS INCLUDING CREEP EFFECTS

3.1 Introduction

In this chapter four different models for one-,two- and three-dimensional settlement analysis including creep effects for settlement calculation are briefly described. These four models have been chosen amongst various models.

The basic equation for all four models is Terzaghi´s classic equation for one dimensional consolidation, see section 2.1 and equation 2.2.

3.2 Embankco

In 1994 the Embancko computer program was developed by the Swedish National Road Administration (SNRA) and the Swedish Geotechnical Institute (SGI) [Bengtsson & Larsson 1994]. The Embankco program is based on a finite difference method and one-dimensional modelling [Takala 1995]. The aim of the Embankco program was to develop a competent computer program for prediction of settlements, including creep effects, in soft clays and fine grained soils beneath embankment constructions. With Embankco it is possible to calculate primary and secondary consolidation settlement in desired depth in embankment cross-section.[Bengtsson & Larsson 1994]

Originally the Embankco program is based on CONMULT code and through many sub-phases it has been developed into a new creep model [Claesson 2003]. In Embankco program the compressibility is described by the parameters, which are shown in table 3.1

Table 3.1 *The Embankco compression parameters*

Parameter	**Description**
$\sigma_c^{`}$ [kPa]	Preconsolidation pressure
$\sigma_L^{`}$ [kPa]	Effective stress where the compression modulus begins to increase
M_0 [kPa]	Compression modulus for $\sigma_v^{`} < \sigma_c^{`}$
M_L [kPa]	Compression modulus for $\sigma_c^{`} \le \sigma_v^{`} \le \sigma_l^{`}$
$M^{`} = \Delta M / \Delta\sigma^{`}$	Modulus number for $\sigma_v^{`} > \sigma_L^{`}$

The permeability is defined by the parameter k and factor β_k, which express the decrease on permeability with compression. In Figure 3.1 evaluation of compression and permeability properties is introduced.

Parameter β_k is defined as:

$$\beta_k = \frac{-\Delta \log k}{\Delta \varepsilon} \tag{3.1}$$

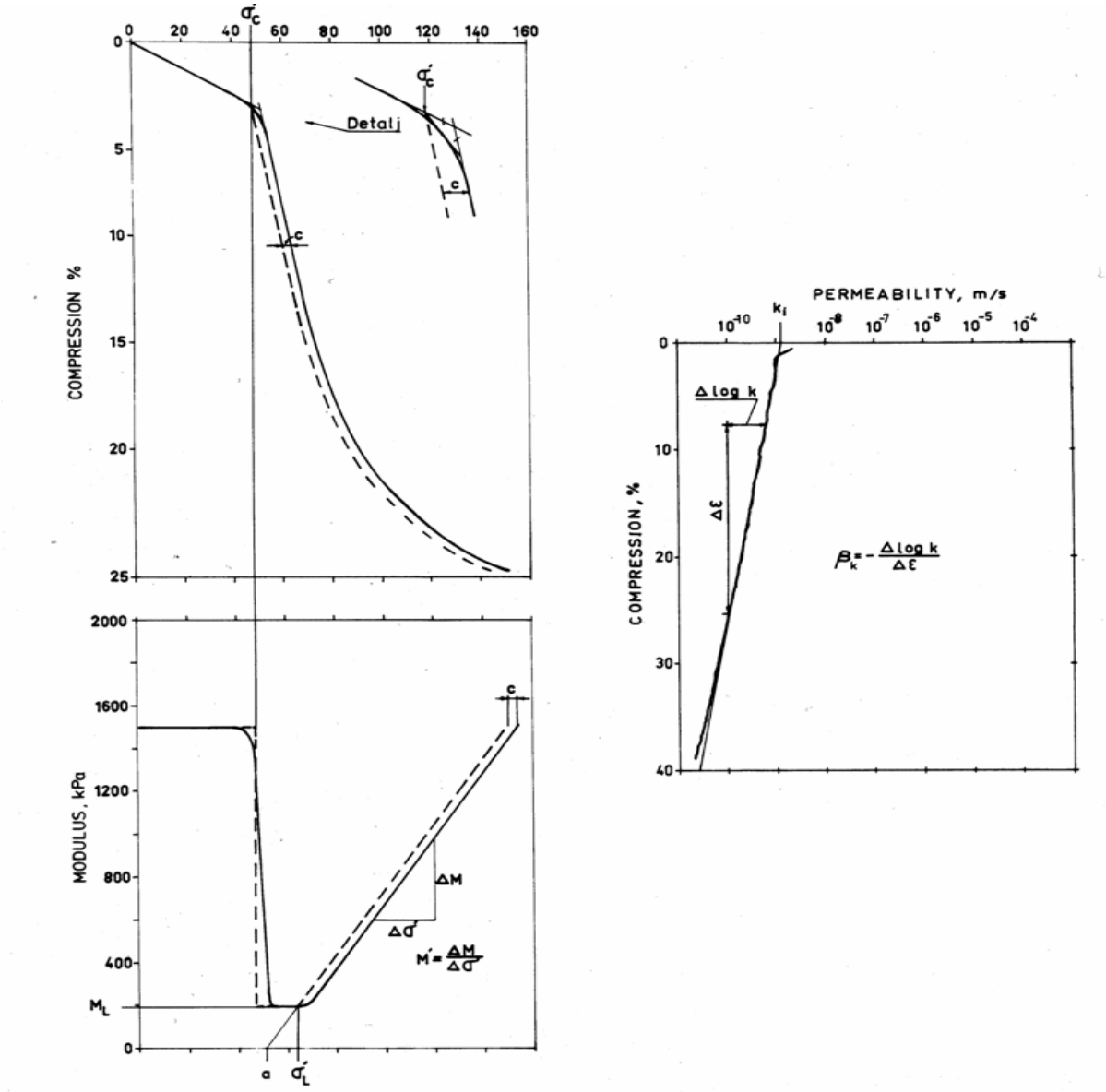

Figure 3.1 *Evaluation of compression and permeability properties from CRS-test results [Larsson 1986].*

The secondary consolidation parameters, the coefficient of secondary compression α_s and the coefficient $\beta_{\alpha s}$ are evaluated from incremental load oedometer tests, unlike the primary consolidation parameters that are evaluated from constant rate of strain (CRS) -tests [Takala 1995].The coefficient of secondary compression α_s describes the creep behaviour and it is defined as:

$$\alpha_s = \frac{\Delta\varepsilon_{cr}}{\Delta\log(t)} \tag{3.2}$$

α_s varies with strain and this behaviour is described in Section 2.4.

Diminuation of pore water pressure is calculated according to the Terzaghi´s consolidation theory in Embankco. Creep produces additional pore water pressure and due to that term u_{cr} is added to the classical consolidation equation [Larsson et al. 1993].

$$\frac{\partial u}{\partial t} = \frac{M}{\gamma_w} \cdot \frac{\partial}{\partial z}(k \cdot \frac{\partial u}{\partial z}) - \frac{\partial u_{cr}}{\partial t} \tag{3.3}$$

where ∂u_{cr} is an increase in pore water pressure due to creep effects. This term is obtained by first determining the strain due to creep, that would have occurred if the soil was freely drained, equation (3.4). Finally, the resulting increase in pore pressure is calculated with equation (3.5)

$$\Delta\varepsilon_{cr} = \int_{t}^{t_1} \frac{\alpha_s}{2{,}3} \frac{dt}{t} \tag{3.4}$$

$$\Delta u_{cr} = \Delta\varepsilon_{cr} \cdot M \tag{3.5}$$

There are three characteristic features of the model. First is that the soil parameters are updated after each time increment. Second feature is that the excess pore water pressure due to creep effects is restricted to the dissipation for the calculated time increment according to equation (3.3) i.e. $\partial u / \partial t \leq 0$. Third feature is that the model does not consider creep effects when the strain rate exceeds value $\dot{\varepsilon} = \alpha_s \cdot 5 \cdot 10^{-6}$ [1/s]. That value corresponds to the standard strain rate at which the oedometer stress-strain curve is evaluated in Sweden. [Claesson 2003]

The Embancko program has been used for 15 years now in the design of embankment constructions and certified to have a good reliability in the prediction of settlements. It has also

been tested several times. However, there are some uncertain factors in that program also. When the effective stress increases close to the value of preconsolidation pressure, the calculation results can depend on the chosen number of sub-layers and the excess pore pressure may exceed the initial pore pressure. It is also found that when using Embankco, a minor change in the parameters results in large differences in calculated settlements after long period of times when dealing with time-dependent settlements. [Claesson 2003]

Nowadays, the Embankco model is also used as an alternative settlement calculation method in the computer program GeoCalc. In the Geocalc program Embankco model is called as Swedish settlement calculation method [Novapoint]. This method is originally based on the tangent modulus concept that was introduced by Janbu in 1963 [Janbu 1967]. In Figure 3.2 The Swedish settlement calculation method and relationship between compression modulus M_0 and effective stress $\sigma`$ is introduced.

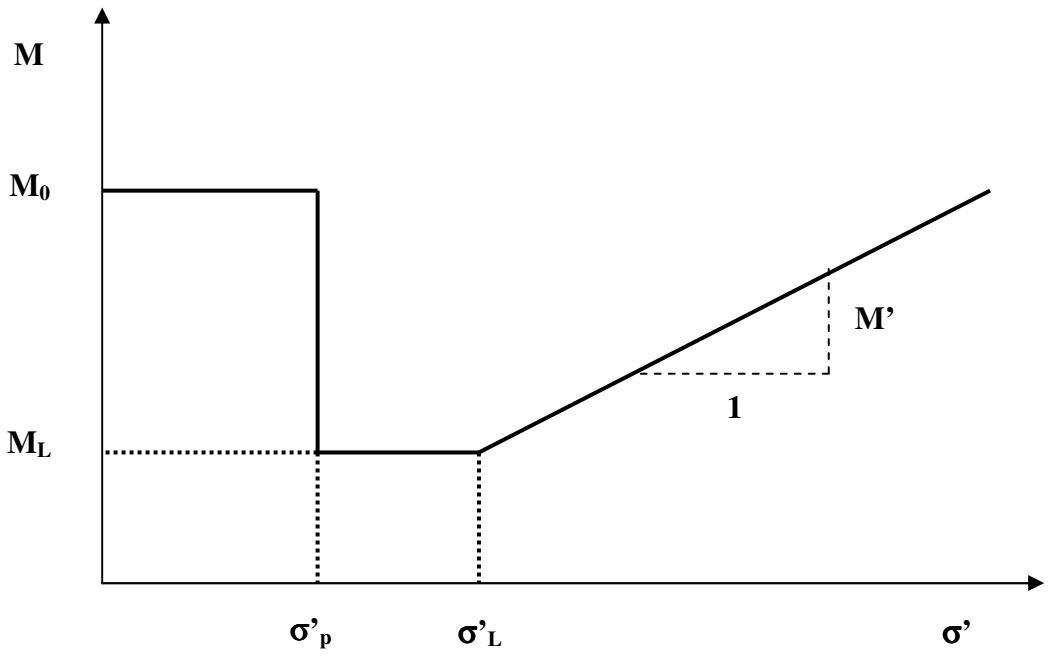

Figure 3.2 *The Swedish settlement calculation method. The relationship between compression modulus and effective stress. [Novapoint]*

3.3 Plaxis – Soft –Soil-Creep model, version 8.0

In 1987 the development of Plaxis began at the Technical University of Delft. Originally the goal was to develop a user-friendly 2D finite element code for the analysis of river embankments on the soft soils of the lowlands of Holland. However, the program has been continuously developed and nowadays it covers most areas of geotechnical engineering. The Plaxis version 8 includes a three-dimensional model including creep effects. Soft Soil Creep model has been improved, by researchers like Bjerrum, Garlanger, Mesri and Leroueil, year by year. The model was implemented in Plaxis in 1998 by Vermeer et al. and Neher & Vermeer. [Brinkgreve et al.2004].

The basic assumption in the Soft-Soil-Creep model is that all inelastic strains are considered to be creep. In the one-dimensional model the total strain is defined by equation (3.6) and the parameters are represented in Figure 3.3 and Figure 3.4.

$$\varepsilon = \varepsilon_c^e + \varepsilon_c^{cr} + \varepsilon_{ac}^{cr} = -A \cdot \ln\left(\frac{\sigma`}{\sigma`_0}\right) - B \cdot \ln\left(\frac{\sigma`_{pc}}{\sigma`_{p0}}\right) - C \cdot \ln\left(\frac{\tau_c + t`}{\tau_c}\right) \tag{3.6}$$

where ε_c^e is the elastic strain during primary consolidation

ε_c^{cr} the creep strain during primary consolidation

ε_{ac}^{cr} the creep strain after primary consolidation

τ_c the intercept with the time axis of the straight creep line, see Fig.3.4

$t`$ effective creep time, see Fig. 3.4

and $$\varepsilon_c^e = \frac{C_r}{(1+e_0)\cdot \ln 10} = \frac{\kappa}{V} \tag{3.7}$$

$$\varepsilon_c^{cr} = \frac{(C_c - C_r)}{(1+e_0)\cdot \ln 10} = \frac{\lambda - \kappa}{V} \tag{3.8}$$

$$\varepsilon_{ac}^{cr} = \frac{C_\alpha}{(1+e_0)\cdot \ln 10} = \frac{1}{r_s} \tag{3.9}$$

Where C_r = recompression index

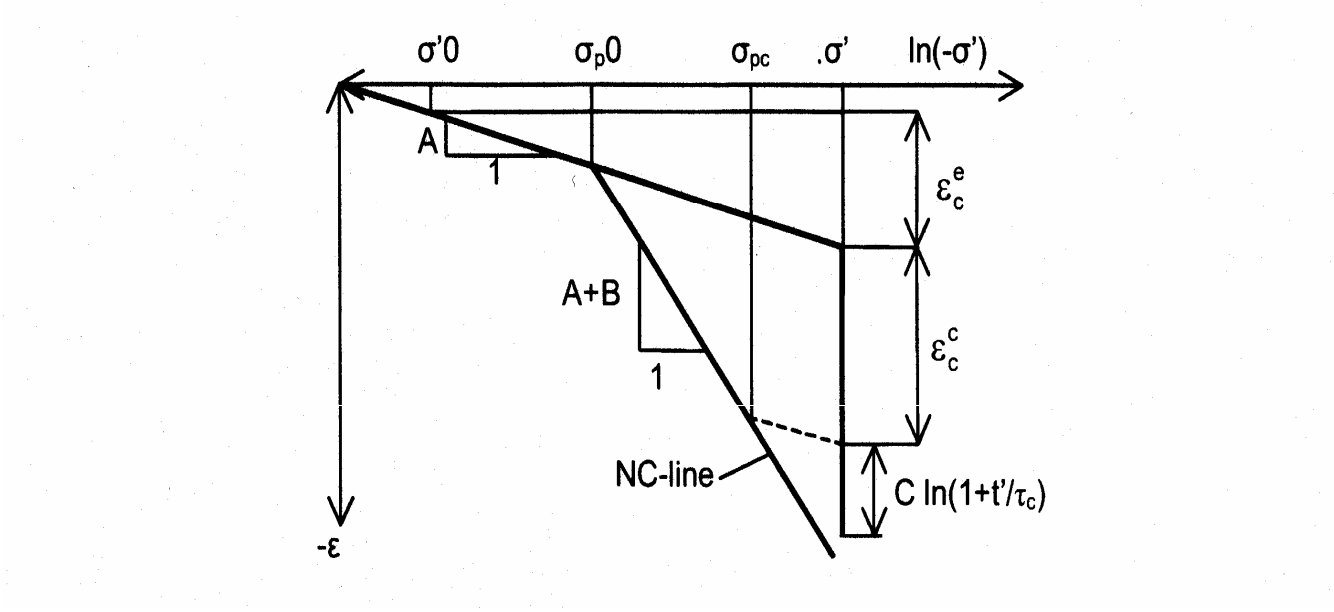

Figure 3.3 *Idealised stress-strain curve from oedometer test with the strain increment divided into an elastic and a creep component [Brinkgreve et al. 2004].*

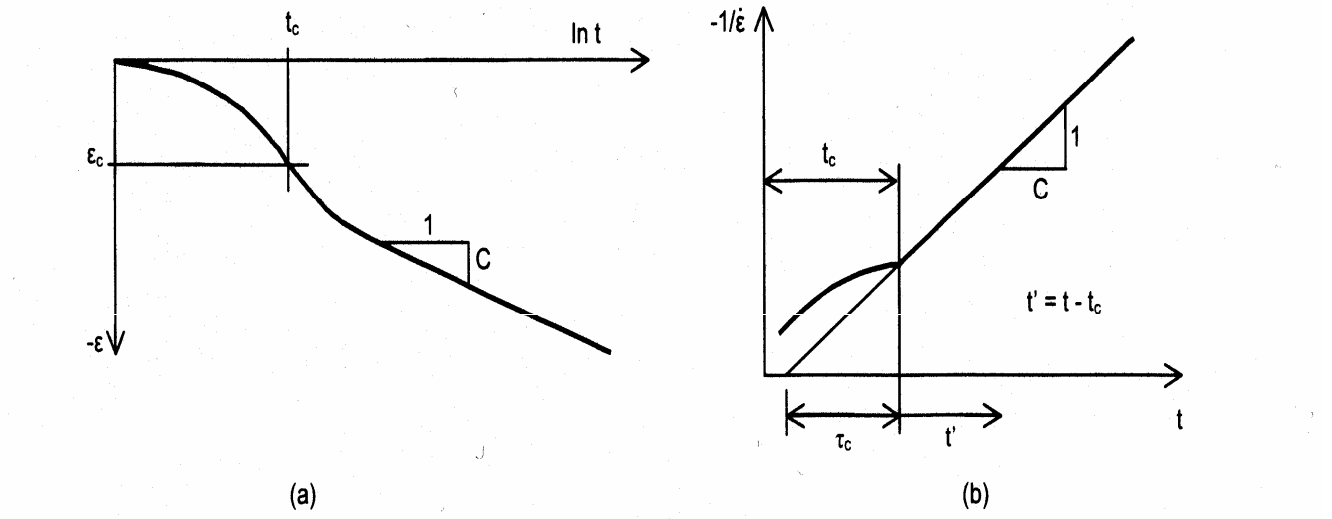

Figure 3.4 *Definition of C and the relevant time parameters from standard oedometer test [Brinkgreve et al. 2004].*

The differential equation is then derived as:

$$\dot{\varepsilon} = \dot{\varepsilon}^{e} + \dot{\varepsilon}^{cr} = -A\frac{\dot{\sigma}}{\sigma} - \frac{C}{\tau_c + t} \tag{3.10}$$

The Soft-Soil-Creep model is recommended to be used for calculations concerning normally consolidated clays, clayey silts and peat. For lightly overconsolidated soft clay the

model may not describe the natural behaviour with sufficient accuracy, especially for loads that implies a final effective stress around the preconsolidation pressure. In this model the creep parameter C is given as a constant. [Brinkgreve et al. 2004]

3.4 Anisotropic creep model for soft soils (ACM)

In 1997 Vermeer and co-workers developed an isotropic creep model (ICM) based on ellipses of Modified Cam Clay. The model was validated by comparing laboratory tests and complex boundary value problems and the performance was good. The model was implemented into a commercial finite element code and it has been widely used for geotechnical design. However, it has been acknowledged that particle orientation of naturally deposited soils plays a significant role when modelling mechanical behaviour of soft soils and cannot be neglected. Wheeler at al. (2003) enhanced the time-independent Modified Cam Clay model to an anisotropic formulation, using the fabric tensor approach for the anisotropic elastoplastic model S-CLAY1. Based on Wheeler et al´s (2003) model the anisotropic creep model for soils ACM has been developed by introducing a rotational hardening law describing the evolution of anisotropy with volumetric and deviatoric creep strain rates [Leoni et al. 2008]. The aim of ACM- model is to model the rate-dependent behaviour of normally consolidated and lightly overconsolidated soft soils [Leoni et al. 2008].

In the ACM-model the elastic and creep parts are combined with an additive law, that express the total strain rate as combination of elastic and creep component, congruent with classical elastoplasticity [Leoni et al. 2009].

In Figure 3.5 the contours of volumetric creep strain rates, suggested by experimental results, are shown. Because of the shape of contours indicated by data, it is obvious that isotropic ellipses of Modified Cam Clay are not adequate to model shapes like that. A fabric tensor was included in the formulation to achieve a better match with experimental data [Leoni et al 2009].

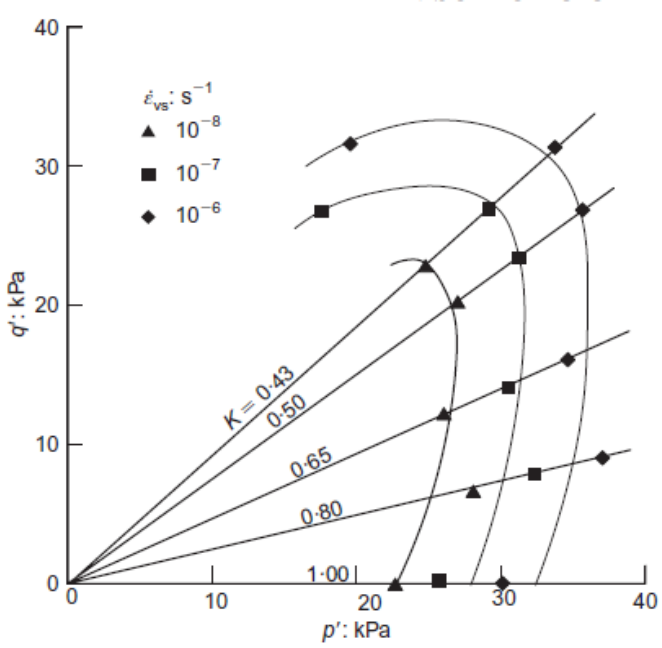

Figure 3.5 *Contours of volumetric creep strain rate for a natural soil [after Boudali,1995].*

In the cases when the stress state is cross-anisotropic, with no rotation of principal directions during the test, anisotropy can be defined by a scalar parameter. The experimental test has been performed in triaxial stress state in which the constitutive ellipses are rotated in $p` - q$ plane by an angle expressed by the scalar α. This is shown in Figure 3.6.

Basic equations

In the ACM model the first rotated ellipse defines the normal consolidation surface (NCS). The isotropic preconsolidation pressure $p`_p$ is the intersection where the vertical tangent to the ellipse and p´ axis converge [Leoni et al 2009]. The size of the ellipse increases with volumetric creep strains according to the hardening law and it is defined as:

$$p`_p = p`_{po} \cdot \exp\left(\frac{\varepsilon^c_{vol}}{\lambda^* - \kappa^*}\right) \tag{3.11}$$

where $\lambda^* = \lambda/(1+e^0)$ is modified compression index

$\kappa^* = \kappa/(1+e^0)$ modified swelling index

e^0 void ratio

In equation 3.11 the compression is positive because soil mechanics sign convention is used.

The second ellipse is called the current stress surface (CSS) and it passes through the point representing the actual effective stress $\sigma_{ij}^{'}$ (Fig. 3.6). The interception where the vertical tangent to the second ellipse and horizontal axis converge is the equivalent mean stress $p_{eq}^{'}$. The equivalent means stress can be considered as an isotropic measure of the current stress and it is defined as:

$$p_{eq}^{'} = p^{'} + \frac{(q - \alpha \cdot p^{'})^2}{(M^2 - \alpha^2) \cdot p^{'}} \tag{3.12}$$

where M is the stress ratio at critical state.

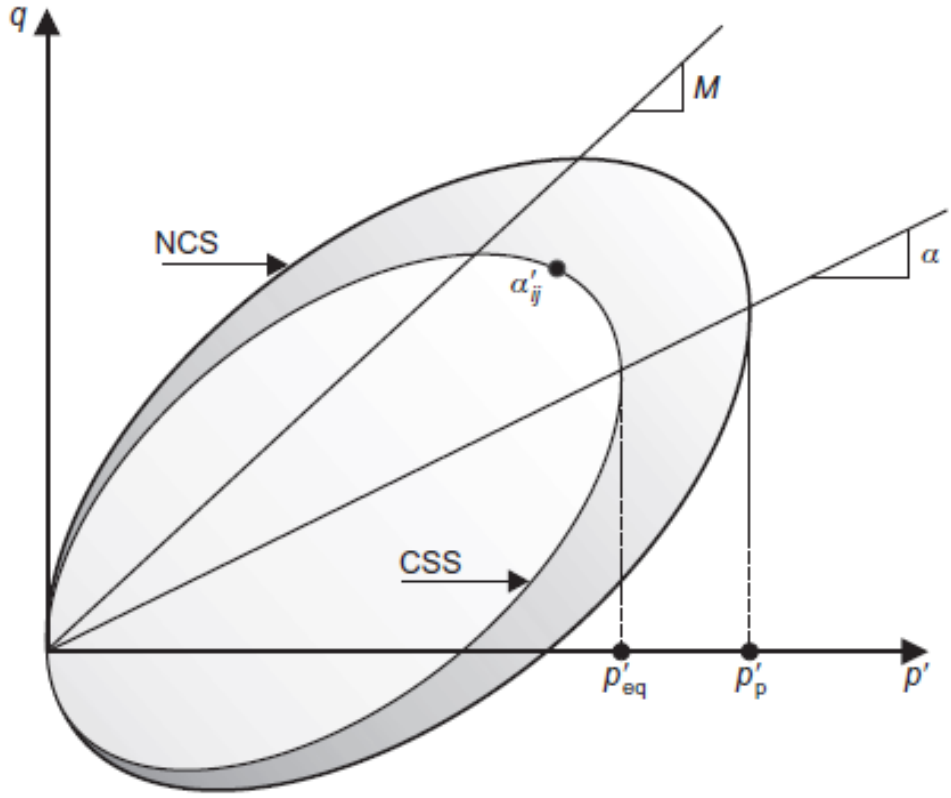

Figure 3.6 *Anisotropic creep model: current state surface (CSS) and normal consolidation surface (NCS) in triaxial stress space [Leoni et al. 2008]*

When p'_{eq} equals to p'_p the current stress lies on the normal consolidation surface and thus the soil is normally consolidated. The ratio p'_p / p'_{eq} is assumed as the isotropic overconsolidation ratio OCR^*, that gives a measurement of the distance between the current stress surface and the normal consolidation surface on the isotropic axis. [Leoni et al. 2008] The volumetric creep strain rate is given by the power law

$$\dot{\varepsilon}^c_{vol} = \frac{\mu^*}{\tau}\left(\frac{1}{OCR^*}\right)^{\beta} \quad \text{where } \mu^* = \frac{C_\alpha}{\ln 10(1+e_0)} \tag{3.13}$$

where μ^* is referred to as modified creep index

τ reference-time

The reference time is set to 24h if the NCS is found performing a standard 24h oedometer test. The deviatoric component of the creep strain rate vector results from the flow rule, which is assumed as associated for the sake of simplicity.[Leoni et al. 2009]

The scalar variable α in equation (3.12) functions like a rotational hardening parameter. The evolution of α is governed by creep strains according to the rotational hardening law:

$$\dot{\alpha} = \omega \left[\left(\frac{3q}{4p'} - \alpha \right) \dot{\varepsilon}_{vol}^{c} + \omega_d \left(\frac{q}{3p'} - \alpha \right) \dot{\gamma}^{c} \right] \tag{3.14}$$

where $\dot{\gamma}^{c}$ is the deviatoric creep strain rate, defined as $\dot{\gamma}^{c} = \frac{2}{3} \left| \dot{\varepsilon}_1^{c} - \dot{\varepsilon}_2^{c} \right|$ for triaxial stress space

ω, ω_d the soil constants that control the rate of rotation, related to basic soil parameters (parameter identification shown in subsequent sections)

The elastic part of the model is based on generalized Hooke´s law:

$$\dot{\sigma}_{ij}' = D_{ijhk} \dot{\varepsilon}_{hk}^{e} \tag{3.15}$$

where

$$D_{ijhk} = \frac{2Gv'}{1-2v'} \delta_{ij}\delta_{hk} + G(\delta_{ik}\delta_{jh} + \delta_{ih}\delta_{jk}) \tag{3.16}$$

where v' is the effective Poisson´s ratio, that is assumed to be a constant.
The shear modulus G is expressed as function of the modified swelling index κ^*:

$$G = \frac{E'}{2(1+v')} \qquad \text{and} \qquad E' = \frac{3p'(1-2v')}{\kappa^*} \tag{3.17}$$

Parameter identification

It is commonly assumed in geomechanics that an proper estimate of K_0 for normally consolidated soils is Jaky´s formula

$$K_0^{NC} \approx 1 - \sin\phi_{cv}^{'} \tag{3.18}$$

where $\phi_{cv}^{'}$ is the critical-state friction angle

A correlation between K_0^{NC} and the initial rotation of the ellipse α_0 is evident when the soil has been one-dimensionally consolidated. Assuming an associated flow rule and considering that the ratio between deviatoric and volumetric plastic strain rates is approximately $\frac{2}{3}$ in one -dimensional loading. As a result α_0 is defined as: [Wheeler et al. 2003]

$$\alpha_0 = \frac{\eta_0^2 + 3\eta_0 - M^2}{3} \tag{3.19}$$

where $\eta_0 = \frac{3(1 - K_0^{NC})}{(1 + 2K_0^{NC})}$ and $M = \frac{6\sin\phi_{cv}^{'}}{(3 - \sin\phi_{cv}^{'})}$

Wheeler et al. (2003) also proved that:

$$\omega_d = \frac{3}{8}\frac{4M^2 - 4\eta_0^2 - 3\eta_0}{\eta_0^2 - M^2 + 2\eta_0} \tag{3.20}$$

Hence, as it has been shown that the initial inclination α_0 and the shear rotation parameter ω_d are completely defined by the critical-state angle and thus do not need any calibration.

The parameter ω dominates the absolute rate at which the normal consolidation surface rotates with viscous straining. A similar parameter is found in many other anisotropic

models for example models by Pestana & Whittle (1999) and Dafalias et al.(2006). In these models procedures and laboratory tests are suggested to calibrate parameter ω. However, Zentar et al. (2002) suggested ω to be a function of the compression index λ, thus the calibration is not required and the determination of the parameter simplifies. The derivation of the equation for rotation parameter is not demonstrated in this thesis and for further details, the interested reader is referred to Leoni et al. (2008). The rotation parameter can be defined as

$$\omega = \frac{1}{\lambda^*} \ln \frac{10M^2 - 2\alpha_0 \omega_d}{M^2 - 2\alpha_0 \omega_d} \tag{3.21}$$

where parameters α_0 and ω_d are determined by the critical state angle, as specified by equations (3.19) and (3.20). Thus ω solely depends on the modified compression index λ^* and on the critical state angle, and the value for parameter ω can be determined via equation (3.21) without calibration. In Table 3.2 all the soil parameters needed in ACM model are introduced.

Table 3.2 *The ACM soil parameters*

λ^*	κ^*	μ^*	$v`$	M_c	ω	ω_d	α_0

The anisotropic consolidation model has been implemented in a finite element code and several validation tests have been performed. The response of the model in undrained triaxial tests has been compared with the corresponding results obtained with the elasto-plastic S-CLAY1 model. The results are promising and ACM showed good numeral predictions when comparing the numerical results with in situ measurements. [Leoni et al. 2008, Leoni et al. 2009, Leoni & Vermeer 2009]. The most attractive feature in ACM model is that all the parameters involved in the anisotropic formulation have a clear physical meaning and thus calibration and non-standard laboratory tests are not required. In order to expand the applicability of ACM model the future work involves incorporation of small-strain stiffness, bonding and destructuration. [Karstunen et al .2008]

3.5 The elasto - viscoplastic model EVP-SCLAY1S

The elasto-viscoplastic model EVP-SCLAY1S is a constitutive model that accounts for viscosity, anisotropy and destructuration. EVP-SCLAY1S is based on the overstress theory of Perzyna [Perzyna, 1963, 1966] and elasto-plastic model S-CLAY1S [Karstunen et al. 2005]. It is also considered as an extension of the elasto-viscoplastic model EVP-MCC, that was developed by Yin & Hicher (2008) [Stapelfeldt et al.2009]. The total strain rate is composed of the elastic and viscoplastic strain rates according to Perzyna´s theory:

$$\dot{\varepsilon}_{ij} = \dot{\varepsilon}^{e}_{ij} + \dot{\varepsilon}^{vp}_{ij} \tag{3.22}$$

where $\dot{\varepsilon}_{ij}$ denotes the *(i,j)* component of the total strain rate tensor and the superscripts *e* and *vp* imply the elastic and the viscoplastic components.

Similarly to MCC, S-CLAY1S and ACM models, the elastic behaviour is assumed to be isotropic. The viscoplastic strain rate $\dot{\varepsilon}^{vp}_{ij}$ is assumed to obey an associated flow rule with respect to the dynamic loading surface:

$$\dot{\varepsilon}^{vp}_{ij} = \mu \langle \Phi(F) \rangle \frac{\partial f_d}{\partial \sigma'_{ij}} \tag{3.23}$$

where μ is the fluidity parameter

$\Phi(F)$ the overstress function representing the difference between the dynamic loading surface and the static yield surface as normalized overstress

f_d the viscoplastic potential function , represented by the dynamic loading surface

σ' the effective stress tensor

An exponential type of scaling function is adopted to control the magnitude of the viscoplastic strain rate:

$$\mu\langle\Phi(F)\rangle = \mu\left\{\exp\left[N\cdot\left(\frac{p_m^d}{p_m^s}-1\right)\right]-1\right\} \tag{3.24}$$

where N is the viscosity index (or strain rate coefficient)

p_m^d the size of dynamic loading surface

p_m^s the size of static yield surface

An elliptical surface is adopted as the static yield surface from Wheeler et al. (2003) and it relates to the current state of preconsolidation:

$$f = \frac{3}{2}\left[\sigma_d^{'} - p^{'}\alpha_d\right]:\left[\sigma_d^{'} - p^{'}\alpha_d\right] - \left(M^2 - \frac{3}{2}[\alpha_d]:[\alpha_d]\right)\left(p_m^s - p^{'}\right)p' = 0 \tag{3.25}$$

where α_d is a deviatoric fabric tensor

M the slope of the critical state line

[ ]:[ ] double dot product

For the special case of a cross-anisotropic sample, the scalar parameter $\alpha = \sqrt{3/2(\alpha_d : \alpha_d)}$ defines the inclination of the ellipse of the yield curve in q-p'-plane as shown in Figure 3.7a. The dynamic loading surface has identical shape with static yield surface but a different size p_m^d. For determining the dynamic loading surface Eq. 3.25 is rewritten as:

$$f_d = \frac{\frac{3}{2}\left[\sigma_d - p^{'}\alpha_d\right]:\left[\sigma_d - p'\alpha_d\right]}{\left(M^2 - \frac{3}{2}[\alpha_d]:[\alpha_d]\right)p'} + p' - p_m^d = 0 \tag{3.26}$$

The intrinsic yield surface is also assumed to have similar shape, with size determined via p_{mi}, which is related to the size of the static yield surface with bonding parameter χ (Fig 3.7a). The expansion of the intrinsic yield surface, which represents the intrinsic hardening

of the material, is assumed to be due to the inelastic volumetric strain ε_v^{vp}, analogous to the critical state models:

$$dp_{mi} = p_{mi}\left(\frac{1+e}{\lambda_i - \kappa}\right)d\varepsilon_v^{vp} \tag{3.27}$$

where λ_i is the slope of the intrinsic normal compression curve in the $e - \ln\sigma_v^{'}$ plane for a stress path at constant stress ratio involving no change of anisotropy (e.g. isotropic loading of an isotropic sample, or oedometer test on a reconstituted sample, see Fig. 3.7b). κ is the slope of the swelling-line and *e* is the void ratio.

The rotational hardening law is based on the formulation proposed by Wheeler et al. (2003) and it describes the development or erasure of anisotropy caused by viscoplastic strains. Volumetric as well as deviatoric viscoplastic strains influence the rotation of the yield curve:

$$d\alpha_d = \omega\left[\left(\frac{3\sigma_d}{4p^{'}} - \alpha_d\right)\left\langle d\varepsilon_v^{vp}\right\rangle + \omega_d\left(\frac{\sigma_d}{3p^{'}} - \alpha_d\right)d\varepsilon_d^{vp}\right] \tag{3.28}$$

where the soil constant ω controls the rate at which the components of the deviatoric fabric tensor heads towards their current target values, which depend on the stress path. ω_d controls the relative effect of viscoplastic deviatoric strains in rotating the yield and loading surfaces.

A scalar state variable χ describes the amount of particle bonding. The variable χ is changing due to bond degradation ultimately to zero, similarly to the S-CLAY1S model [Karstunen et al. 2005]:

$$d\chi = -\xi \cdot \chi \cdot \left(\left|d\varepsilon_v^{vp}\right| + \xi_d \cdot d\varepsilon_d^{vp}\right) \tag{3.29}$$

where the soil constant ξ controls the absolute rate of destructuration and ξ_d controls the relative effect of viscoplastic deviatoric strains in destroying the bonds. χ_0 is the initial

amount of bonding, which relates the sizes of the intrinsic yield surface and static yield surfaces as:

$$p_{m0} = (1+\chi_0)\, p_{mi0} \tag{3.30}$$

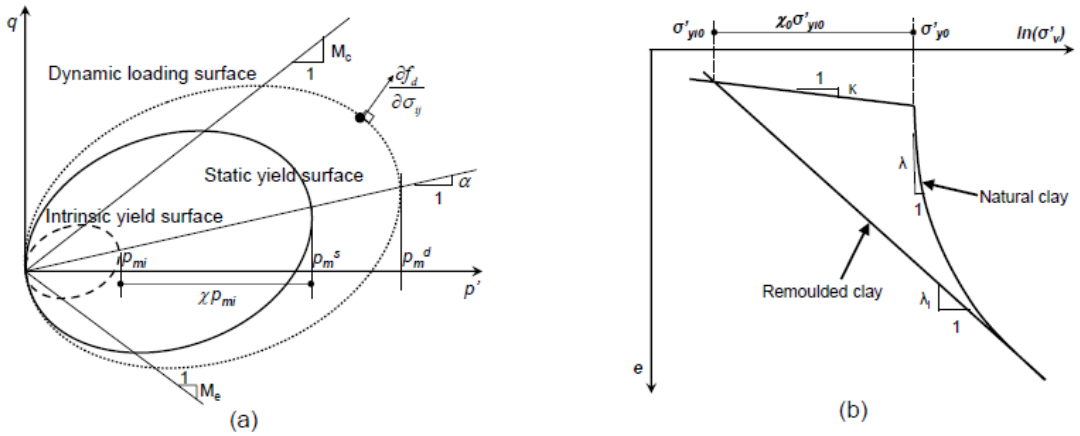

Figure 3.7 *Definition of surfaces and parameters of EVP-SCLAY1S model.*

Taking into account the elastic stress-strain relations, the constitutive equations of the EVP-SCLAY1S model for structured clays are derived as follows:

$$\dot{\varepsilon}_{ij} = \frac{1}{2G}\dot{\sigma}_d + \frac{\kappa}{3(1+e_0)p'}\dot{p}'\delta_{ij} + \mu\langle\phi(F)\rangle\left\{\frac{3[\sigma_d - p'\alpha_d] - \left([\alpha_d]:[\sigma_d - p'\alpha_d] + \frac{1}{2p'}[\sigma_d - p'\alpha_d]:[\sigma_d - p'\alpha_d]\right)\delta_{ij}}{\left(M^2 - \frac{3}{2}[\alpha_d]:[\alpha_d]\right)p'} + \frac{\delta_{ij}}{3}\right\} \tag{3.31}$$

where $\dot{\sigma}_d$ is the deviatoric stress rate tensor ($\sigma_d = \sigma'_{ij} - p'\delta_{ij}$); p' is the mean effective stress ($p' = \sigma'_{kk}/3$); G is the elastic shear modulus, which is related to the elastic bulk modulus ($K = (1+e)p'/\kappa$) by assuming a constant value of Poisson´s ratio v' ($G = 3(1-2v')K/2(1+v')$); δ_{ij} is Kronecker delta with $\delta_{ij} = 1$ for $i=j$ and $\delta_{ij} = 0$ for $i \neq j$.

Parameter identification

The common parameters of model λ, κ, e_0, M can be determined from triaxial and oedometer tests. The Poisson´s ratio v' and the soil permeability k are assumed to be constants during the consolidation and can be determined from standard laboratory tests. The viscosity parameters N and μ can be obtained from long-term oedometer tests

The preconsolidation pressure $\sigma_p^{'}$ is estimated from oedometer tests. The p_{m0} can be calculated with the Pre-Overburden Pressure ($\sigma_p^{'} - \sigma_{v0}^{'}$):

$$p_{m0} = p_i^{'} + \frac{(q_i - \alpha_0 p_i^{'})^2}{(M^2 - \alpha_0^2) p_i^{'}} \tag{3.32}$$

where $p_i^{'} = (1 + 2K_0)(POP + \sigma_{v0}^{'})/3$ and $q_i = (1 - K_0)(POP + \sigma_{v0}^{'})$. The coefficient of earth pressure at rest K_0 is determined by Jaky´s formula $K_0^{'} = 1 - \sin\phi_c^{'}$ for normally consolidated soil. The values for parameters α_0 and ω_d are determined from Wheeler et al´s (2003) equations in SCLAY1 model. The value for ω is estimated with equation proposed by Leoni et al. (2008). These equations are defined as:

$$\alpha_0 = \eta_{K0} - \frac{M^2 - \eta_{K0}^2}{3},\ \omega_d = \frac{3(4M^2 - 4\eta_{K0}^2 - 3\eta_{K0})}{8(\eta_{K0}^2 + 2\eta_{K0} - M^2)},\ \omega = \frac{1 + e_0}{\lambda} \ln\left(\frac{10M^2 - 2\alpha_0\omega_d}{M^2 - 2\alpha_0\omega_d}\right) \tag{3.33}$$

where $\eta_{K0} = 3M/(6 - M)$ and $\phi_c^{'} = \sin^{-1}(3M/(6 + M))$

The initial bonding χ_0 can be calculated from soil sensitivity: $\chi_0 = S_t - 1$. The values for soil constants ξ and ξ_d can be determined from isotropic consolidation tests combined with oedometer tests.

The EVP-SCLAY1S was implemented into 2D Plaxis v.8 as a user defined model. Because EVP-SCLAY1S is a hierarchical model, it is possible to switch on/off certain pa-

rameters, reducing the model to as EVP-SCLAY1 ($\chi_0 = \xi = \xi_d = 0$) and ultimately to EVP-MCC ($\alpha_0 = \omega = \omega_d = 0$ and $\chi_0 = \xi = \xi_d = 0$). The consolidation analyses of boundary value problem can be carried out in Plaxis by using the coupled consolidation analysis based on Biot´s theory with the proposed model. [Yin & Karstunen 2008]

Several validation tests have been performed to EVP-SCLAY1S and the performance has been good. There has been comparisons between the predictions of different models e.g. EVP-MCC, EVP-SCLAY1 and EVP-SCLAY1S. The advantages of EVP-SCLAY1S model are the ability to model primary, secondary and tertiary creep stages and possibility to predict negative visco-plastic strains associated with strain softening of the material and its numerical stability. A limitation of the model is analogous to all the models that are based on Perzyna´s theory: an increment of stress is required to launch visco-plastic straining while time-dependent models, like ACM, predict viscous strains even if there has been no change in stress [Karstunen et al. 2008]. Also the calibration of the viscosity parameters can be rather demanding [Yin & Hicher 2008]. However, when applying the model to practical boundary value problems, creep models of ACM type have the problem that they predict creep strains of major magnitude as a function of time even based on in situ stresses.

4. HUT CLAY

To investigate the validity of ACM- and EVP-SCLAY1S models and to determine the parameters for models an extensive testing programme was established. The HUT clay was appropriate for this study because the mechanical behaviour of HUT clay has been investigated closely since 1985 in the Helsinki University of Technology. Comprehensively the HUT clay has been researched in The Academy of Finland and EC funded projects. In these projects the behaviour of natural and reconstituted clay as well as the behaviour of clay stabilized with small amount of binder and the behaviour of deep stabilized clay have been in the focus of interest.

The deposit of HUT clay is situated very near the coast of the Baltic Sea in southern Finland. The location of HUT clay in map is shown in Figure 4.1. By nature the deposit of HUT clay is very similar to the other soft clay deposits in Finland and thus the results concerning the mechanical behaviour of HUT clay can partially be applied to generally describe Finnish clay deposits especially on coastal regions.

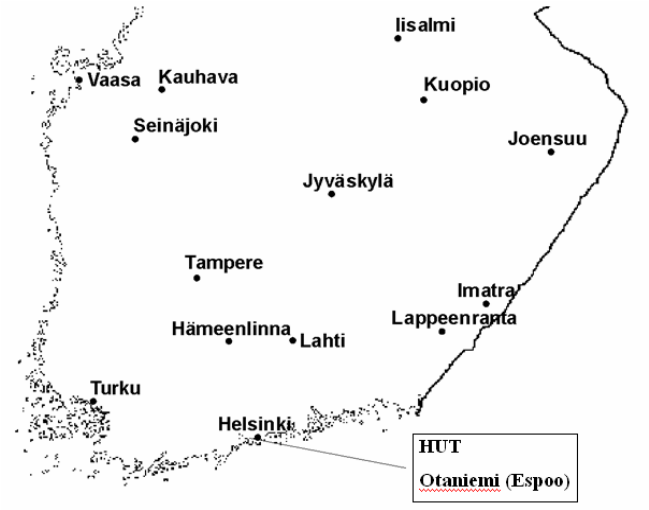

Figure 4.1 *Location of the HUT clay testing site.*

The deposition of soft clays in Finland occurred during the final stage of the last Ice Age (late-glacial sediments) or later (postglacial sediments). The evolutionary stages of the Baltic Sea created variation to the structure of the sedimentary deposits. It is possible to distinguish four main developmental stages, each representing different types of sediments. The major part of the oldest sediments deposited in the Baltic Ice Lake during the late-glacial period approximately 10 000-12 000 years ago. The general structure of the sediments became varved and diatactic as a result of the sedimentation in the vicinity of the continental ice sheet, primarily in fresh, cold water. In the second stage the sediments were deposited for the most part in the marine Yoldia Sea. Due to the salinity of the water the stratification of the sediments is weak, symmictic. However, variation in the prominence of the varves occurs as a consequence of mixing of fresh and saline water. Due to the land uplift, the connection of the Yoldia Sea with the ocean was broken and the Anculus Lake with fresh water was formed. The sediments deposited at this stage are homogenous in structure. The youngest sediments were largely deposited in the marine Littorina Sea. These sediments are almost homogenous in structure and occur primarily in coastal regions

[Gardemeister 1975]. However, these Littorina sediments have higher water content and organic content than older sediments [Ojala et al. 2007]. The Littorina sediments began to be deposited approximately 8000 years ago and the sedimentation still continues in the present basin of the Baltic Sea. Mineralogically the fine-grained Finnish sediments are illity clay that consist also considerably amounts of chlorite. There is no observed mineralogical variation between the geological types of sediments but a certain regional distribution can be observed. The mineralogical composition of the fine-grained Finnish sediments have been substantially affected by e.g. the interglacial sedimentary material, the preglacial weathering crust, the glacial rock powder, the underlying bedrock and the leaching and crystallization of the mineral under different sedimentation conditions [Gardemeister 1975].

The total thickness of the deposit of HUT clay is approximately 4-5 m and the ground water table is about 0,5 m below the surface. In this research concentration is aimed at the layer from depth 1,3 to 2,1 m. The layer´s static sounding resistance is 0,15 - 0,25 kN and on that account it was selected (Swedish weight sounding). The sampling depth was nearly the sea level. In this layer from depth 1,3 m to 2,1 m current stress is 13 – 17 kPa.

The geotechnical index properties of undisturbed HUT clay were determined by routine classification tests according to Finnish technical specification [SFS 179-2]. Some of the values were adopted from Hassan (2009).

Table 4.1 *Index properties of HUT clay, depth 1,3 - 2,1 m.*

Index property	**Notation**	**Value**
Water content	w %	65 - 79
Liquid limit	w_L %	71
Plastic limit	w_p %	30
Plasticity index	I_p %	41
Clay content	Cl - %	68 - 87
Organic content	Hm - %	0 - 0,3
Specific gravity	ρ_s	2,74 - 2,78 g/cm^3
Undrained shear strength(fall cone test)	c_u	8 - 14 kPa
Undrained shear strength(field vane test)	c_u	6 - 8 kPa
Sensitivity	S_t	10

5. LABORATORY TESTS

5.1 Sampling

In order to carry out the laboratory tests, the clay samples were taken from HUT test site. The undisturbed samples were taken with the help of Norwegian type piston sampler. Avoiding vibrations was fundamental to get as little disturbed samples as possible. HUT clay is so soft that piston sampler penetrated the ground with its own weight. First the cap of the sampler was pressed into ground and after that the piston was unlocked and guide pipe is pressed into ground. To ensure that the sample stayed in the piston sampler it was rotated two rounds so that the sample was cut. The diameter of the samples was 54 millimeters, which is too high for triaxial tests and because of that the samples had to be trimmed. Samples for trixial- and oedometer tests were chosen according to unit weigth and undrained shear strength and if those values differed from average the samples were used for reconstituted samples.

(a) *(b)*

***Figure* 5.1** *a) Norwegian type piston sampler b) Sampling*

5.2 Sample preparation

5.2.1 Sample preparation for oedometer tests

The dimensions of the samples used in oedometer tests were; the initial height $h_0 = 2{,}0\,\text{cm}$ and the surface area $A_0 = 20\,\text{cm}^2$. Both natural undisturbed samples and reconstituted samples were tested. The undisturbed samples were cutted straight from Norwegian type piston sampler, whereas the processing of the reconstituted samples was more complicated. Reconstituted samples were prepared according to Burland (1990) so that the natural clay was remoulded in water content of 1 to 1,5 times the liquid limit, and then consolidating the sample one-dimensionally. For the reconstituted samples the clay were taken from several points, 10 cm high pieces from tubes at a time. Approximately 2 kg of clay was mixed by using drilling machine (about 10 minutes) and three water content tests were performed from this mixed clay. After that water was added to the mixture several times, altogether the amount of added water was 625 ml. During water addition the mixture was constantly mixed with food mixer. When mixture reached smooth texture and preferred fluidity the mixing was stopped. The mixture was then poured to impermeable numbered sample tubes (REC 60 to REC 69) with porous stones and filter paper on the heads of the tube. Initial

heights of the samples in tubes were measured and tubes were placed under weights. The settlement in tubes was measured frequently. When the settlement of the samples was stabilized the samples were ready for oedometer and triaxial tests.

5.2.2 Sample preparation for triaxial and consolidation tests

High quality undisturbed and reconstituted samples were used for testing. The samples were taken with the Norwegian type piston sampler (see more precise description of the sampling in Chapter 5.1). The undisturbed samples had a diameter of 54 mm and in order to perform triaxial tests it had to be trimmed to hexadecagonal shape so that the diameter of the sample decreased to 50 mm. The samples were also cut to have the proper height, approximately $h_0 = 10$ cm. The preparation of the reconstituted samples was more demanding and it is described closely in Chapter 5.2.1. The samples were conserved in a temperature and humidity controlled room to guarantee the undisturbance.

5.3 Oedometer tests

5.3.1 Apparatus and experimental procedure

The testing program to research the creep behaviour of soft clay and to determine stress state of the soil and the critical state parameter values for proposed ACM- and EVP-SCLAY1S-models included largely the standard incremental loading tests. These tests were carried out according to CEN Technical Spesification [CEN ISO/TS 17892-5:fi] and the experimental procedure follows the international practice of oedometer testing.

The sample was placed at the steel ring, which was lubricated with silicone. The top and bottom of the specimen was placed in contact with porous papers and discs in order to guarantee the free vertical drainage of the pore water. The sample was loaded vertically through the moving piston. The principle of the loading was to double the applied load at each step compared to the previous one. For each loading the height of the sample (vertical deformation) was observed and plotted from the dial gauge with elongating time intervals, e.g. 6 s, 15 s, 30 s, 1 min, 2 min, 4 min etc. The oedometer apparatus is presented in Figure 5.2.

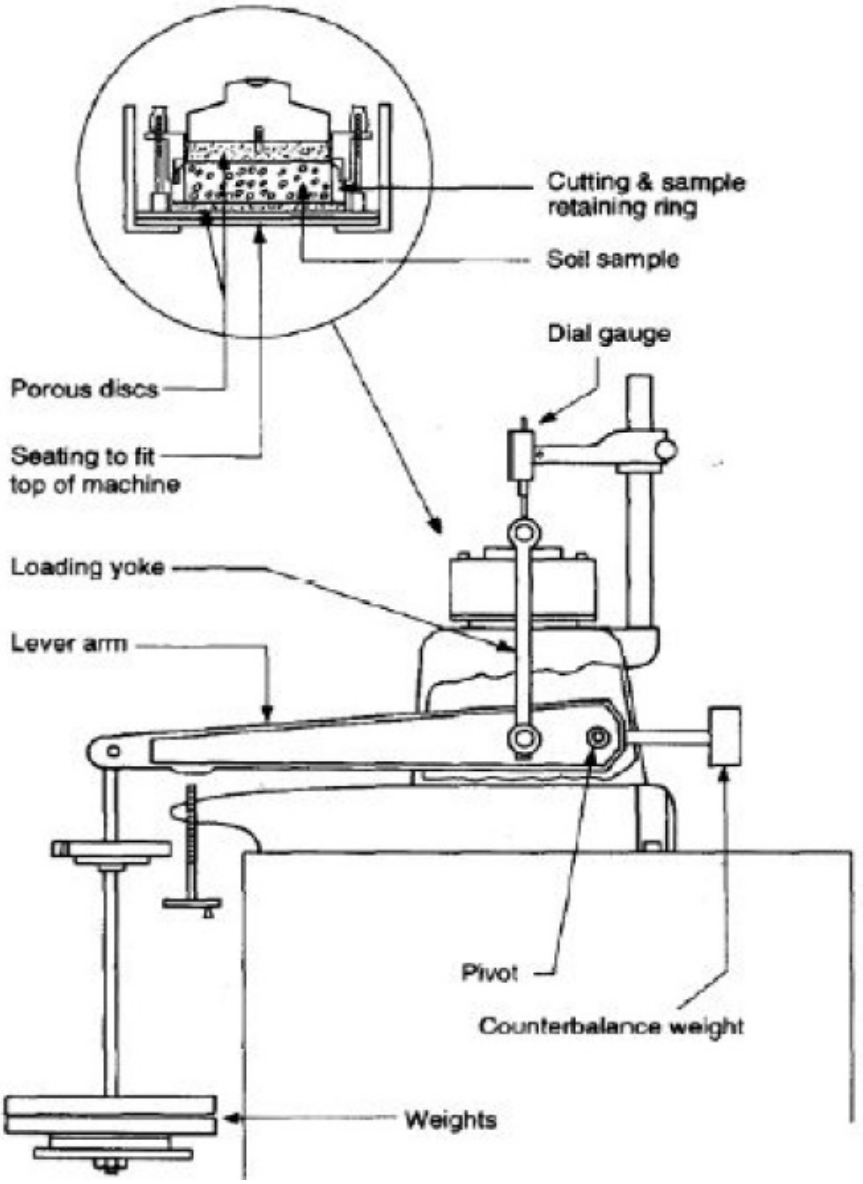

Figure 5.2 *Oedometer apparatus [Floquet V. 2006]*

In conventionally testing arrangement the duration of each load is 24 hours but in this research also the long-term tests were performed so that the duration of load step could be as long as 10 days. In figure 5.3 the oedometer test in laboratory is presented.

Figure 5.3 *The oedometer test in HUT laboratory.*

5.3.2 Test procedure

Altogether seven oedometer tests were performed; five tests for the undisturbed samples and two tests for the reconstituted samples. The duration of the loading step was one, two or ten days. The samples were loaded from 3,25 kPa to 200 kPa or from 3,25 kPa to 400 kPa. The tests for undisturbed samples are presented in Table 5.1 and the tests for reconstituted samples are presented in Table 5.2. For test 5610KREC also falling head measurement was performed, which is denoted by letter K.

Table 5.1 *The oedometer tests for undisturbed samples.*

Test number	**Sample**	**Depth [m]**	**Duration of the loading step**	**From(load) [kPa]**	**To(load) [kPa]**
5578	2009 - 2	1,92 - 1,95	1 d	3,125	400
5579	2009 - 2	1,89 - 1,91	10 d	3,125	400
5631	2009 - 9	1,88 - 1,90	1 d	3,125	200
5593	2009 - 7	1,92 - 1,94	1 d	3,125	200
5594	2009 - 7	1,90 - 1,92	7 d	3,125	400

Table 5.2 *The oedometer tests for reconstituted samples.*

Test number	Depth [m]	Duration of the loading step	From (load) [kPa]	To (load) [kPa]
5610KREC	1,3 - 2,1	2 d	3,125	400
5611REC	1,3 - 2,1	10 d	3,125	200

where REC denotes for reconstituted sample.

5.4 Triaxial- and consolidation tests

5.4.1 Apparatus and experimental procedure

The testing programme to investigate the influence of strain rate variation to the strength parameters included several undrained triaxial tests. Two additional triaxial consolidation tests were performed to determine the yield points and critical state parameters of HUT clay.

Spiral filter paper strips were attached around the sample to accelerate the rate of drainage during consolidation. The strips were installed so that the angle between the strips and the horizontal plane was 45 degrees. The remaining heads of the strips were folded to the top and bottom surfaces of the sample. Five strips were used on one sample, each having approximately a width of 5 mm.

On the both ends of the sample were porous discs that were saturated with water before installation. The porous disc and the cap were seamed together with a broad rubber ring. To assure that no air or water could permeate the joint, some silicone was spreaded between the rubber ring and the cap. The membrane covering the sample was attached with the caps by thin rubber rings to prevent the leaking of the joints. Some silicone was also used between the membrane and the cap. In Figure 5.4 the triaxial test in HUT laboratory is presented.

Figure 5.4 *Triaxial test in HUT laboratory*

In the consolidation stage the cell pressure was increased slowly (about in 15s) during the loading of the sample and after that the vertical load was added directly on the piston. The vertical strains were calculated on the grounds of the corresponding area of the sample.

All triaxial tests were done according to CEN Technical Specification [CEN ISO/TS 17892-9] from which further information can be found. The experimental procedure also follows the international practice of triaxial testing [Head 1992].

5.4.2 Test procedure

5.4.2.1 Triaxial consolidation tests

Two drained anisotropic consolidation test were executed to undisturbed samples. These tests took almost two months because of the low permeability of HUT clay (permeability

coefficient $k_i<1*10^{-9}$ m/s). These CAD - tests were done with different stress ratios that were kept constant through the first loading and unloading. CAD 5582 was loaded and unloaded with stress ratio 0,2 and CAD 5583 with stress ratio 0,7. The first loading continued until the stress reached value 50 kPa for CAD 5582 and value 48 kPa for CAD 5583 (approximately two times the p´-value of the initial yield point). The reloading and its unloading were done using stress ratio 0,7 for CAD 5582 and stress ratio 0,2 for CAD 5583.

Table 5.3 *Triaxial consolidation tests.*

Test number	Sample	Depth (m)	Loading η	Reloading η
CAD 5582	2009 - 2	1,58 - 1,69	0,2	0,7
CAD 5583	2009 - 2	1,47 - 1,58	0,7	0,2

5.4.2.2 Undrained triaxial tests

In undrained triaxial tests the sample was first consolidated undrained to approximately $\sigma_1 = \sigma_3 = 10 - 20$ kPa. The degree of saturation 100 % and certainty of impermeability of the system was verified by getting equal values for σ_3 and the maximum of pore water pressure $u_{w,\max}$. Then the consolidation to the σ_3-value of the shearing (see Table 5.4) was carried out drained by several load increments with stress ratio 0,4. The shearing was done undrained and with varying values of σ_3 and varying shearing rate to research the influence of different cell pressure and strain rate on strength properties of clay. Undrained triaxial tests were done to both undisturbed and reconstituted samples. Undrained triaxial tests to undisturbed samples are shown in Table 5.4 and to reconstituted samples in Table 5.5.

Table 5.4 *Undrained triaxial tests to undisturbed samples.*

Test number	Sample	Depth [m]	Loading σ_3 [kPa]	Strain rate [%/h]	Notes
CAUC 5580	2009 - 2	1,79 - 1,89	40	0,6	
CAUC 5581	2009 - 2	1,69 - 1,79	60	0,6	
CAUC 5591	2009 - 7	1,79 - 1,90	20	0,6	Broke
CAUC 5592	2009 - 7	1,68 - 1,79	20	6,0	
CAUC 5595	2009 - 5	1,83 - 1,94	20	0,6	Power failure
CAUC 5596	2009 - 5	1,72 - 1,83	40	6	Power failure
CAUC 5597	2009 - 5	1,50 - 1,61	40	0,06	
CAUC 5598	2009 - 5	1,61 - 1,72	20	0,06	
CAUC 5608	2009 - 7	1,79 - 1,68	60	6	
CAUC 5609	2009 - 7	1,57 - 1,68	60	0,06	

Table 5.5 *Undrained triaxial tests to reconstituted samples.*

Test number	Sample	Depth [m]	Loading σ_3 [kPa]	Strain rate [%/h]	Notes
CAUC 5602REC	REC 60	1,3 - 2,1	40	0,6	Broke?
CAUC 5603REC	REC 61	1,3 - 2,1	20	0,6	
CAUC 5606REC	REC 62	1,3 - 2,1	60	0,6	
CAUC5607REC	REC 63	1,3- 2,1	40	0,6	

where REC means reconstituted sample.

6. EXPERIMENTAL RESULTS

6.1 The oedometer test results

6.1.1 The index properties of oedometer samples

The index properties for undisturbed and reconstituted oedometer test samples were determined by classification tests according to Finnish Technical Spesification [SFS-179-2]. The index properties are shown in Table 6.1.

Table 6.1 *The index properties of oedometer samples.*

Test n:o	Point n:o	Tube n:o	Depth z [m]	A [cm^2]	h [cm]	γ_0 [kN/m^3]	w_0 [%]	e_0	S_r [%]
5578	2009-2	1	1,92-1,95	20	2	15,62	73,8	2,01	100
5579	2009-2	1	1,89-1,92	20	2	15,21	79	2,19	99,8
5593	2009-7	1	1,92-1,95	20	2	15,8	72,2	1,95	100
5594	2009-7	1	1,89-1,92	20	2	15,75	78	2,06	100
5631	2009-9	1	1,87-1,90	20	2	15,51	76,9	2,09	100
5610KREC		REC 64	1,3-2,1	20	2	15,52	78,6	2,12	100
5611REC		REC64	1,3-2,1	20	2	15,46	78,1	2,12	100

6.1.2 Determination of the consolidation parameters

Commonly the results of each loading stage of an oedometer test are plotted in a graph representing the dial gauge readings either as a function of square root of elapsed time, or as a function of the logarithm of elapsed time. From these curves the coefficient of consolidation (c_v) can be obtained using Taylor´s or Casagrande´s method. In addition the coeffient of secondary compression C_α and the characteristic end of primary consolidation EOP parameters (t_{EOP} , H_{EOP}) can be determined from these curves. In this research the EOP parameters have been determined according to Taylor´s 100%- method. Determination of

c_v and C_α is described in Figure 6.1 and Figure 6.2 for undisturbed sample and in Figure 6.6 and 6.7 for reconstituted sample.

The results of all the oedometer load stages are combined in one chart of void ratio as a function of the effective pressure. This graph is constructed on the basis of the calculated void ratios at the end of each load stages. From these results it is also possible to calculate the coefficient of compressibility ($m_v = \frac{\Delta e/(1+e_0)}{\Delta p}$, where Δe is the void ratio change for a pressure change Δp) for each load step. The coefficient of compressibility is used to predict the magnitude of settlement. In soft or sensitive clays the coefficient of compressibility results can be seriously affected by sample disturbance. The behaviour of clay under the load in oedometer is modelled with two models; Janbu´s model and compression index model. Janbus´s model pursue to model the bend of the curves plotted on the $e-\sigma_1$ graph and it is based on Janbu´s formula

$$\varepsilon_1 = \frac{1}{m_\beta}\left(\frac{\sigma}{\sigma_1}\right)^\beta + C \tag{5.1}$$

where β_1 and m_1 are parameters for normally consolidated part of curve ($\sigma_1 > \sigma_p^{'}$)

β_2 and m_2 parameters for overconsolidated part of curve ($\sigma_1 < \sigma_p^{'}$)

With curve fitting the parameters $m_1, \beta_1, m_2, \beta_2$ were attained. The compression index model utilizes two straight lines for determining the coefficients C_c and C_s. From these two methods the Janbu´s method is more commonly used in the Nordic countries, because the β_1-values tends to be so low that the functionality of semi-logarithmic scale is restricted. Janbu´s method for undisturbed sample is illustrated in Figure 6.3 and for reconstituted sample in Figure 6.8. Illustration of classical method is shown in Figure 6.4 for undisturbed sample and in Figure 6.9 for reconstituted sample.

The preconsolidation pressure is determined from Janbu´s method graph according to σ_p HUT-method. σ_p HUT-method was proposed by Aalto, Lojander and Ravaska in 2004. In this method the reloading curve is moved to point A for determining the preconsolidation pressure $\sigma_p^{'}$. Point A is in this case the nearest smaller point to the preconsolidation pressure. An intersection of the moved curve and the preloading curve is the preconsolidation pressure. In cases when the reloading curve is missing the return curve can be used. [Aalto et al. 2004]. This method is based on Ohde´s [1939] and Van Zelst´s [1948] concept. The method is illustrated in Figure 6.5 for undisturbed sample and in Figure 6.10. For undisturbed sample 5594 the preconsolidation pressure is 24 kPa and for reconstituted sample 5611REC it is 16 kPa. Preconsolidation pressures for different samples are possible to determine also according to Taylor´s method and these defined values are presented in Table 6.2.

Example 1:

In following example the determination of essential data from the test 5594 on the undisturbed sample from HUT is represented. This determination procedure is closely described earlier in this chapter. Used load increment ratio LIR=2.

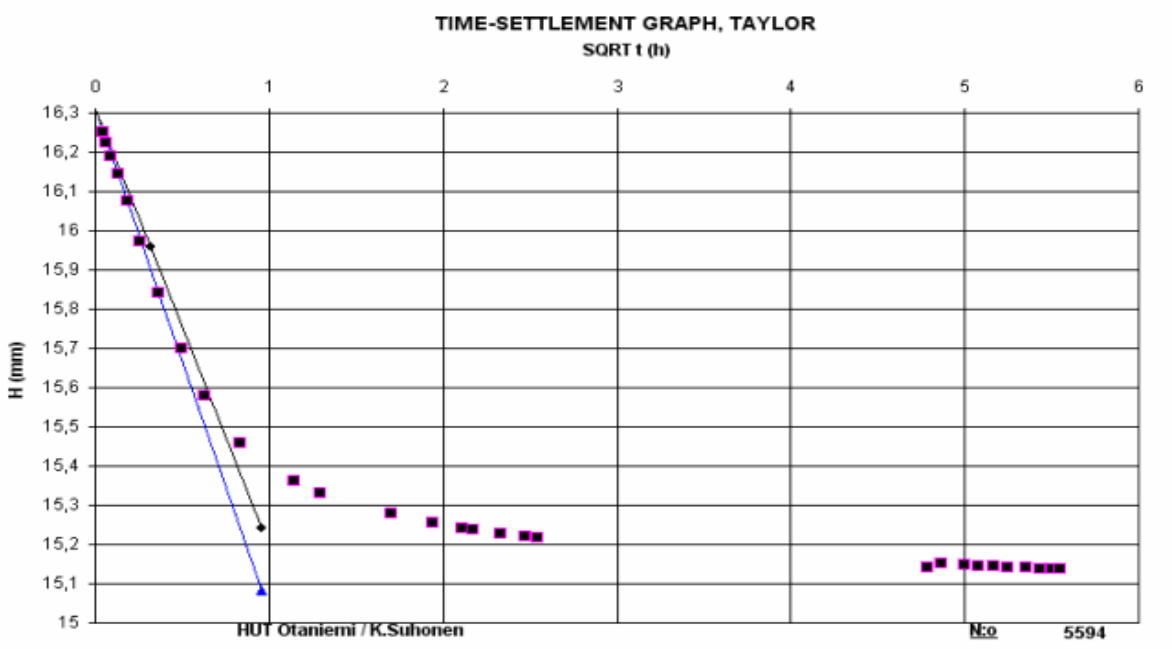

Figure 6.1 *Determination of characteristic EOP parameter, c_v, using Taylor´s method-Seventh load step: 100 ->200 kPa of HUT 5594, LIR = 2.*

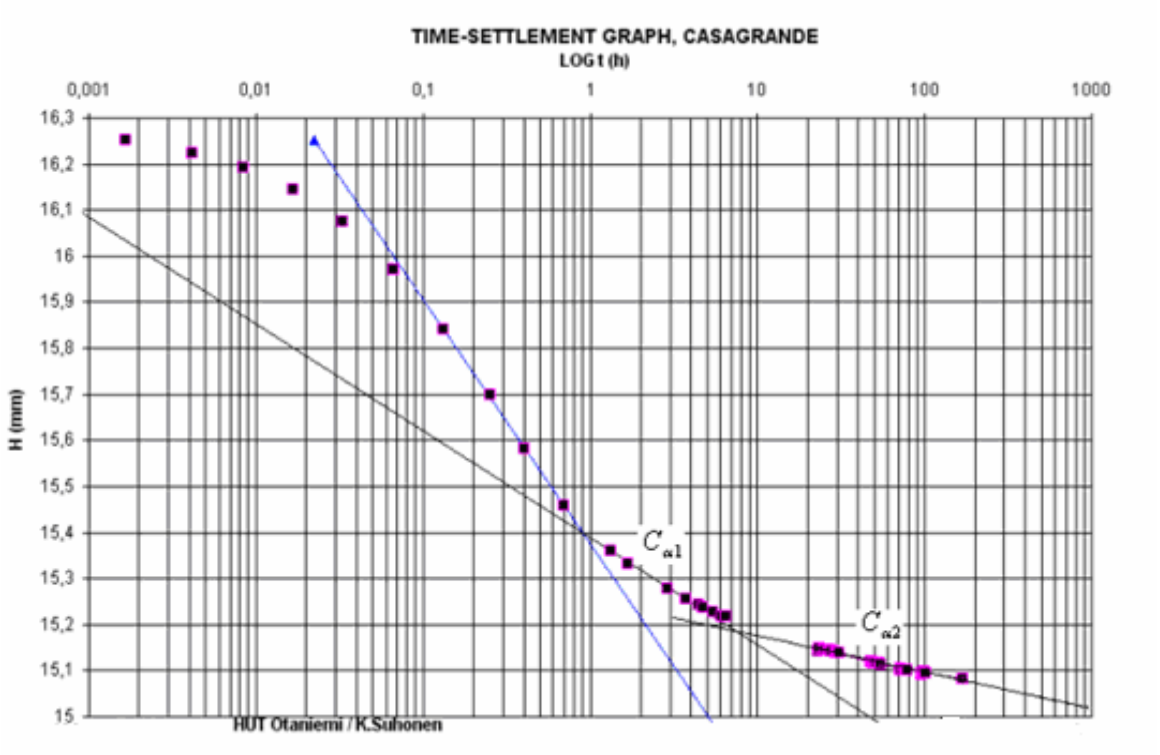

Figure 6.2 *Determination of the characteristic EOP parameters,* c_v *and* C_α *using Casagrande´s method- Seventh load step: 100→200 kPa of HUT 5594, LIR = 2.*

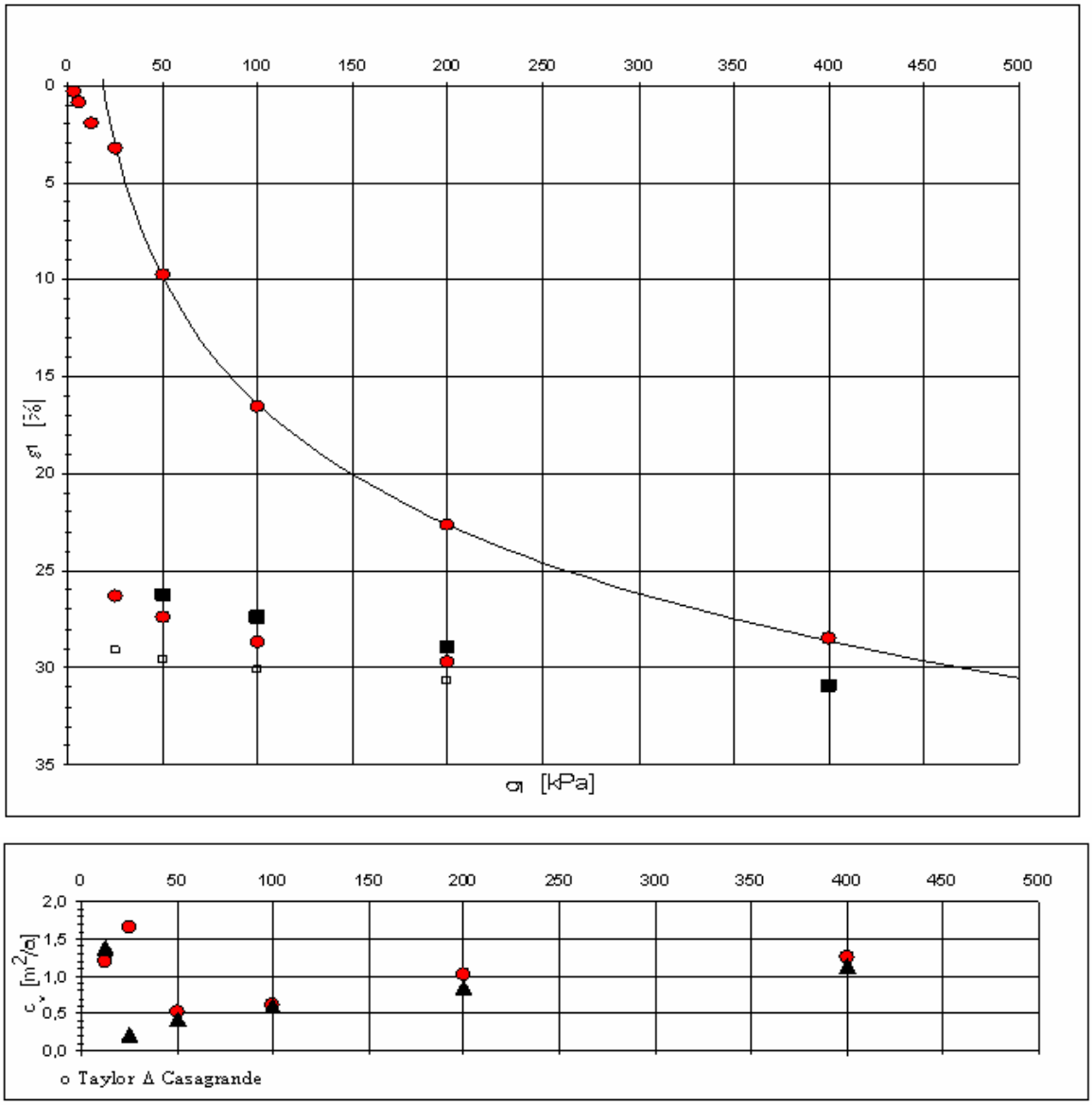

σ'_{vo} =20 kPa β_1=-0,05 β_2=0,4

σ_p =20 kPa m_1=10,95 m_2=52,01

Figure 6.3 *Janbu´s model to describe the behaviour of HUT 5594 and consolidation coefficients* c_v *for each load stage determined as mentioned before.*

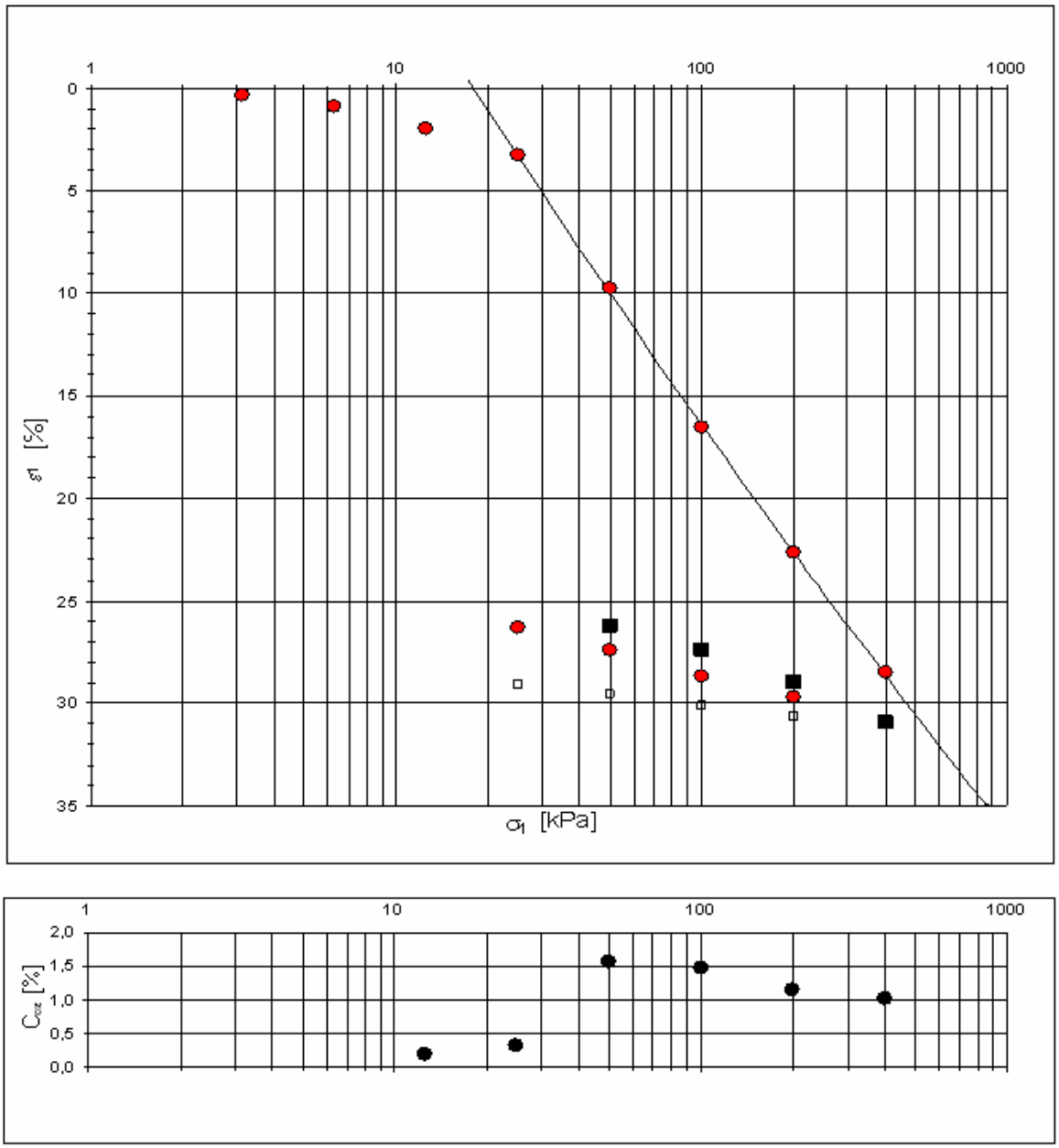

σ'_{vo} =20 kPa β_1=-0,05 β_2=0,4

σ_p =25 kPa m_1=10,95 m_2=52,01

Figure 6.4 *Compression index model to describe the behaviour of HUT 5594 and the coefficient of secondary consolidation* C_α *for each load step determined as mentioned before.*

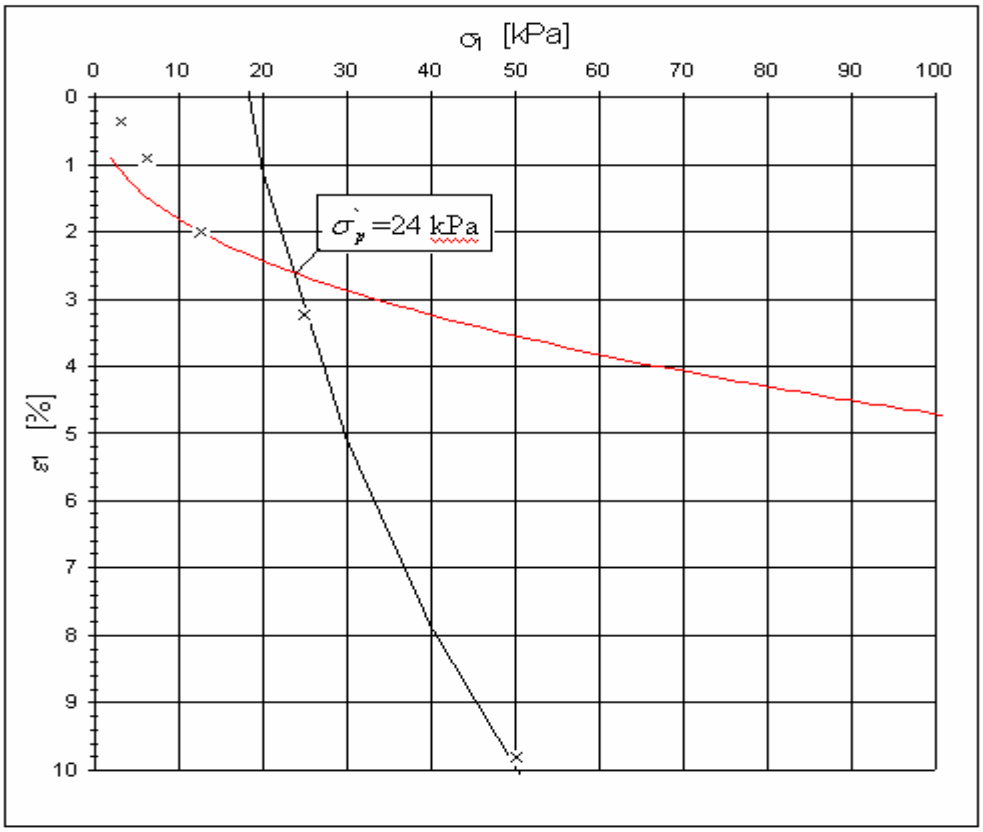

Figure 6.5 *Preconsolidation pressure determination on HUT 5594 according to HUT-method.*

Example 2:

In following example the determination of essential data from the test 5611REC on the reconstituted sample from HUT is represented. This determination procedure is closely described earlier in this chapter and it is similar to procedure for undisturbed sample, see Chapter 5.2.1. Used load increment ratio LIR = 2.

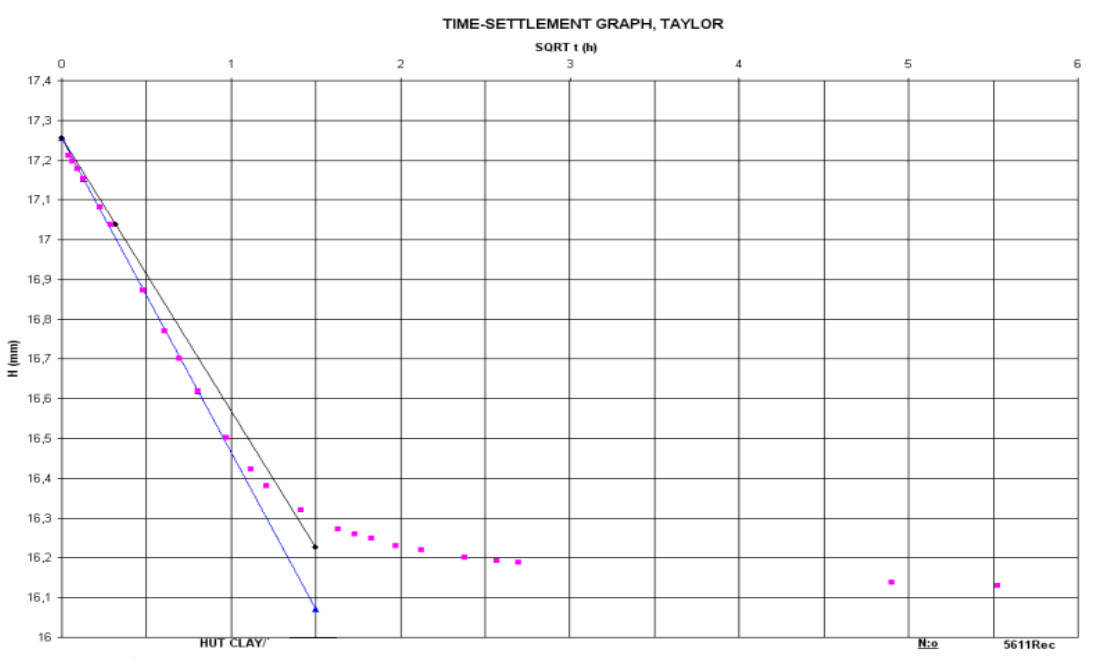

Figure 6.6 *Determination of characteristic EOP parameter, c_v, using Taylor´s method- Sixth load step: 50⟶100 kPa of HUT 5611REC, LIR = 2.*

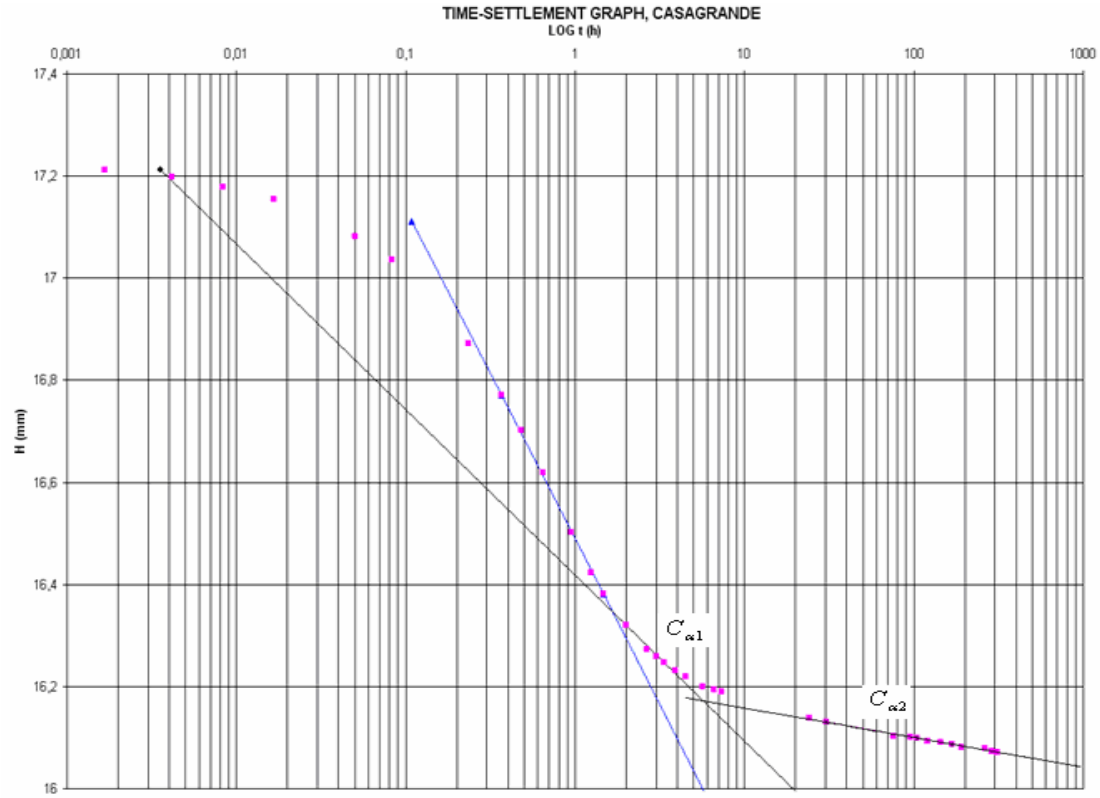

Figure 6.7 *Determination of the characteristic EOP parameters, c_v and C_α using Casagrande´s method- Sixth load step: 50->100 kPa of HUT 5611REC, LIR=2.*

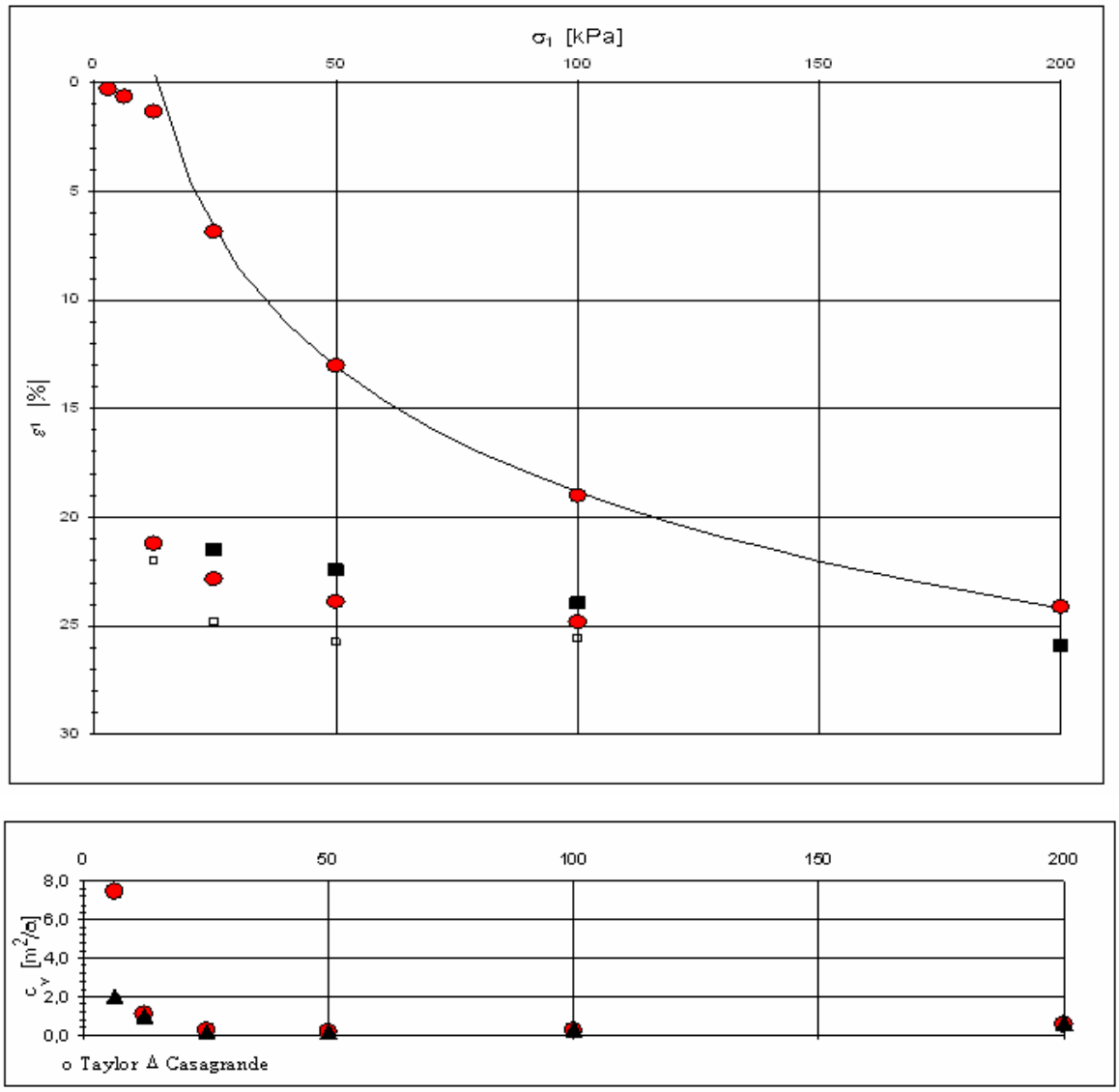

σ'_{vo} =15 kPa β_1=-0,110 β_2=0,685

σ_p =16 kPa m_1=12,49 m_2=36,53

Figure 6.8 *Janbu´s model to describe the behaviour of HUT 5611REC and consolidation coefficients* c_v *for each load stage determined as mentioned before.*

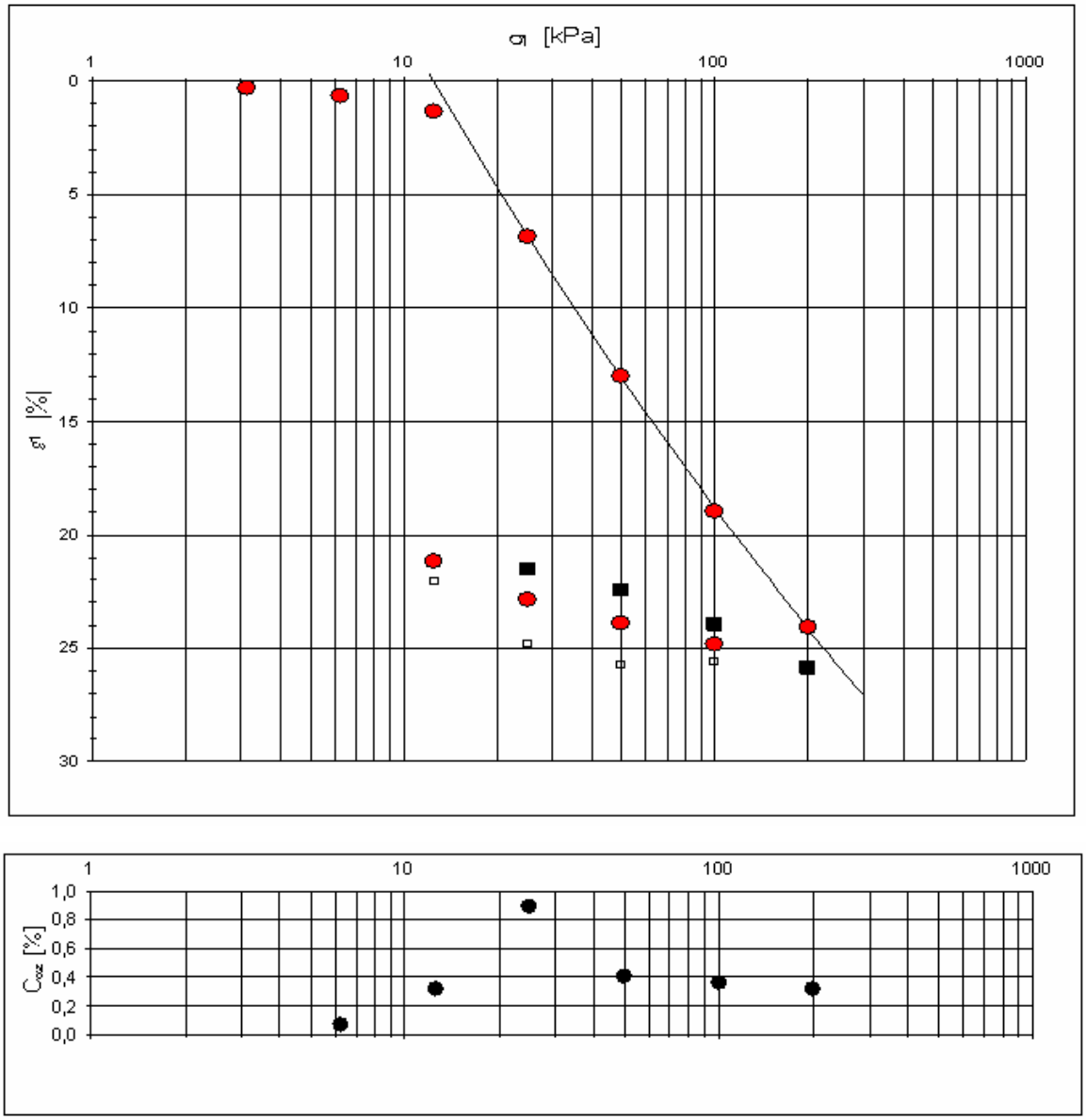

σ'_{vo} =15 kPa β_1=-0,110 β_2=0,685

σ_p =16 kPa m_1=12,49 m_2=36,53

Figure 6.9 *Compression index model to describe the behaviour of HUT 5611REC and the coefficient of secondary consolidation* C_α *for each load step determined as mentioned before.*

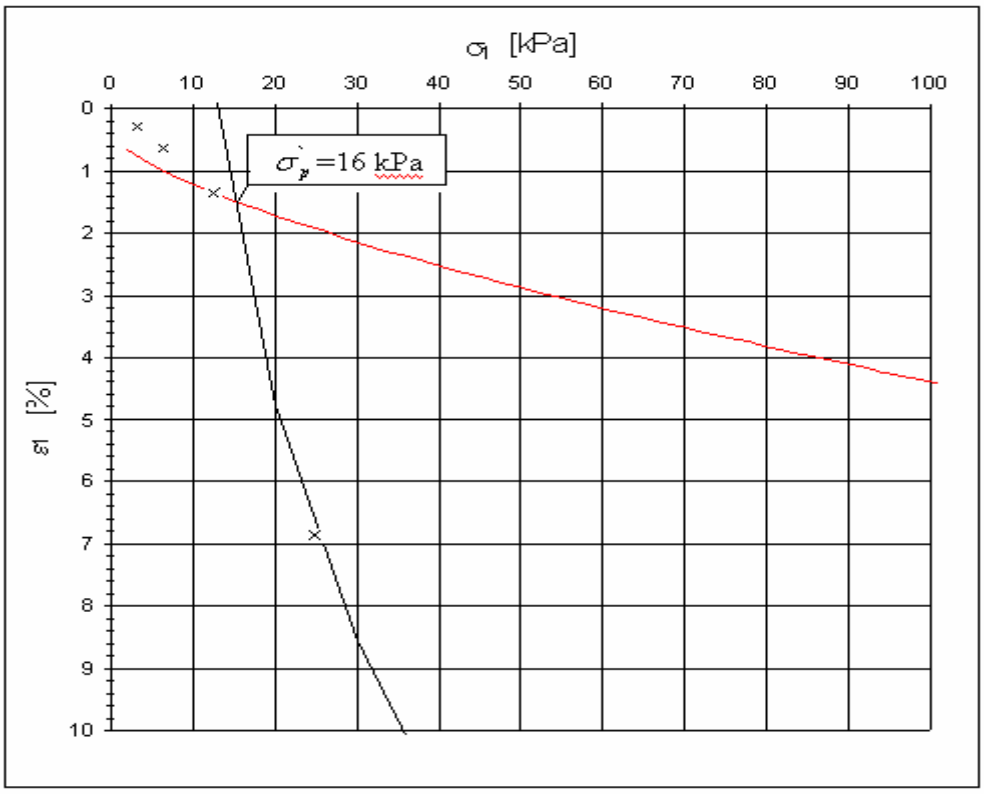

Figure 6.10 *Preconsolidation pressure determination on HUT 5611REC according to HUT-method.*

Table 6.2 *Defined preconsolidation pressures*

Test n:o	$\sigma`_p$ **[kPa]**
5578	17
5579	19
5593	20
5594	25
5610KREC	18
5611REC	16
5631	23

6.1.3. Determination of the parameters $\lambda, \kappa, \lambda^*, \kappa^*$ and v_λ

For EVP-SCLAY1S it is necessary to determine three parameters from oedometer tests; e_0, λ and κ. For precise definitions to these parameters see chapter 3.5. λ denotes the slope of the normal consolidation line in v:ln(σ_1) plane, κ denotes the slope of the over-consolidation line in v:ln(σ_1) plane and e_0 is the initial void ratio.

Even though the Janbu´s model is usually more accurate to simulate the behaviour of the Finnish clay, we are using parameters resulting from the compression index model when we are dealing with critical state models. e_0 is one of the index properties that is determined according to Finnish Technical Specification [SFS-179-2] and values for initial void ratios can be found in Table 6.1 (chapter 6.1.1). κ and λ values are extracted from the ln(σ_1)-v-graph, where v =1+e and denotes volumetric strain. An unloading-reloading process provides for the extraction of both parameters but in cases when such a process is not carried out the value of κ can be estimated in the range [λ/10; λ/5] [Floquet 2006]. In Figure 6.11 the determination of κ and λ is shown.

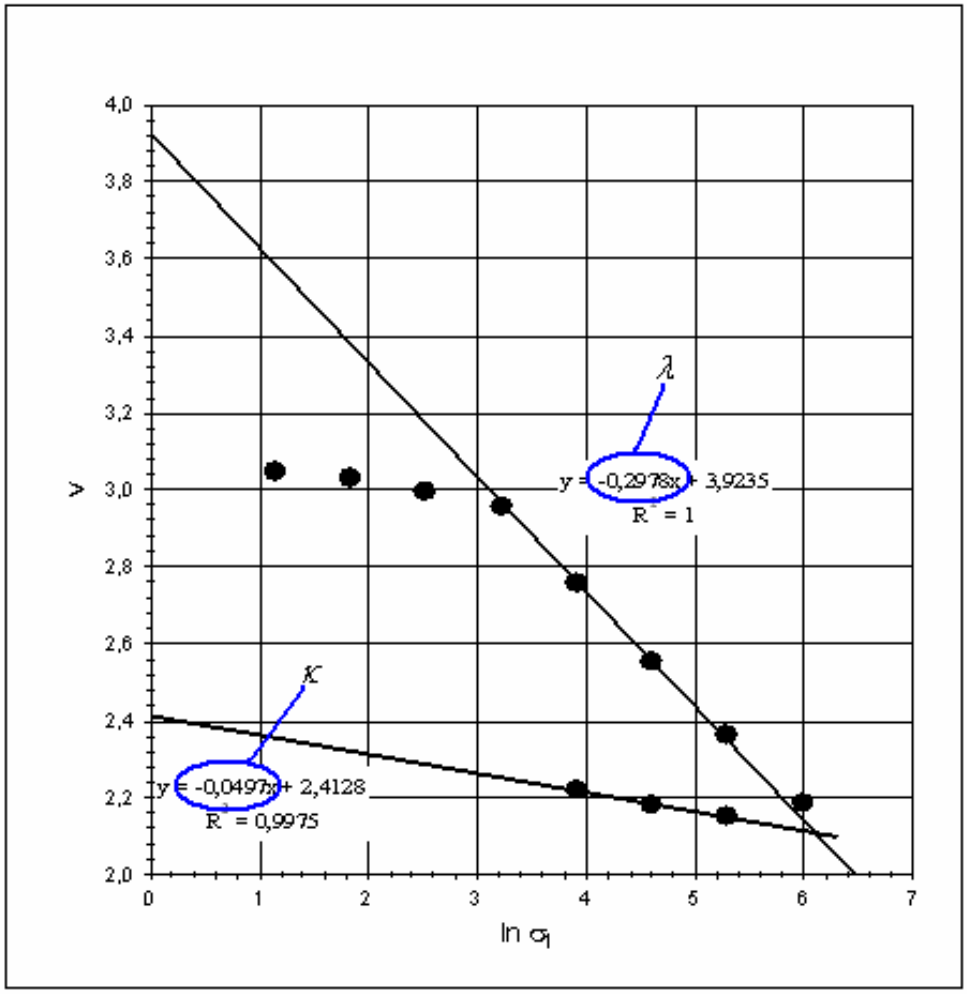

λ	κ
0,2978	0,0497

Figure 6.11 *Determination of lambda* λ *and kappa* κ *parameters on HUT 5594.*

For ACM model the modified compression index λ^*, the modified swelling index κ^* as well as the modified creep index μ^* has to be determined (Chapter 6.1.2.2). λ^* and κ^* are converted from λ and κ according to following formulas:

$$\lambda^* = \frac{\lambda}{1+e_0} \quad (6.1) \qquad \kappa^* = \frac{\kappa}{1+e_0} \quad (6.2)$$

Also the values for parameter v_λ can be determined as an ordinate to λ-line and thus it is extracted from the intersection point of the particular λ-line and v-axis. The equation $v_\lambda = v + \lambda \ln p$, describes the normal consolidation λ-line [Schofield & Wroth 1968].

Determined values for $\lambda, \kappa, \lambda^*, \kappa^*$ and v_λ are presented in Tables 6.3 - 6.7 for undisturbed samples and in Tables 6.8 and 6.9 for reconstituted samples.

Table 6.3 *Set of critical state parameters on HUT 5578.*

	λ	κ	λ*	κ*	ν_λ
Settlement at t ≈ 1 h	0,2433	0,0437	0,0808	0,0145	3,5888
Settlement at t ≈ 1 d	0,2524	0,0446	0,0838	0,0148	3,5932
Settlement at final time t ≈ 3 d	0,2524	0,0446	0,0838	0,0148	3,5962

Table 6.4 *Set of critical state parameters on HUT 5579.*

	λ	κ	λ*	κ*	ν_λ
Settlement at t ≈ 1 h	0,2862	0,0547	0,0898	0,0172	3,9668
Settlement at t ≈ 1 d	0,2801	0,0547	0,0879	0,0172	3,8908
Settlement at final time t ≈ 21 d	0,2737	0,0547	0,0859	0,0172	3,8420

Table 6.5 *Set of critical state parameters on HUT 5593.*

	λ	κ	λ*	κ*	ν_λ
Settlement at t ≈ 1 h	0,2669	0,0424	0,0808	0,0905	3,6930
Settlement at t ≈ 1 d	0,2669	0,0472	0,0905	0,0160	3,6930
Settlement at final time t ≈ 3 d	0,2808	0,0472	0,0952	0,0160	3,7226

Table 6.6 *Set of critical state parameters on HUT 5594.*

	λ	κ	λ*	κ*	ν λ
Settlement at t ≈ 1 h	0,2978	0,0497	0,0974	0,0163	3,9235
Settlement at t ≈ 1 d	0,296	0,0497	0,0968	0,0163	3,8704
Settlement at final time t ≈ 7 d	0,2907	0,0497	0,0951	0,0163	3,8335

Table 6.7 *Set of critical state parameters on HUT 5631.*

	λ	κ	λ*	κ*	ν λ
Settlement at t ≈ 1 h	0,2903	0,0386	0,0941	0,0125	3,8883
Settlement at t ≈ 1 d	0,3029	0,0386	0,0982	0,0125	3,8909
Settlement at final time t ≈ 3 d	0,2957	0,0386	0,0958	0,0125	3,8560

Table 6.8 *Set of critical state parameters on HUT 5610KREC.*

	λ	κ	λ*	κ*	ν λ
Settlement at t ≈ 1 h	0,2517	0,0427	0,0808	0,0137	3,7435
Settlement at t ≈ 1 d	0,2557	0,0427	0,0821	0,0137	3,7268
Settlement at final time t ≈ 3 d	0,2561	0,0427	0,0822	0,0137	3,7287

Table 6.9 *Set of critical state parameters on HUT 5611REC.*

	λ	κ	λ*	κ*	ν λ
Settlement at t ≈ 1 h	0,2592	0,0442	0,0831	0,0142	3,7308
Settlement at t ≈ 1 d	0,2614	0,0442	0,0838	0,0142	3,7217
Settlement at final time t ≈ 3 d	0,2623	0,0442	0,0841	0,0142	3,7161

Values of λ ranges from 0,25 to 0,27 to reconstituted samples and from 0,27 to 0,30 to natural samples. It can be seen from the results that the values of λ and λ^* are pretty similar for reconstituted samples and for undisturbed samples as well as values of κ and κ^*. The little smaller λ and λ^* values for reconstituted samples derive from degradation of bonding between particles, which is referred to as destructuration [Koskinen & Karstunen 2004]. In this case similar parameter values for reconstituted and undisturbed values would refer to disturbed samples or to samples taken from dessicated layer. It is also possible that HUT clay is not very structured clay. The behaviour of natural and reconstituted clays in ln(p´):v plot is presented in Figure 6.12. Between the λ and λ^* values for different settlement times there are no significant differences. The values of κ and κ^* remains constant for all settlement times. In ACM model the parameters has to be determined always from the 1d reference graph.

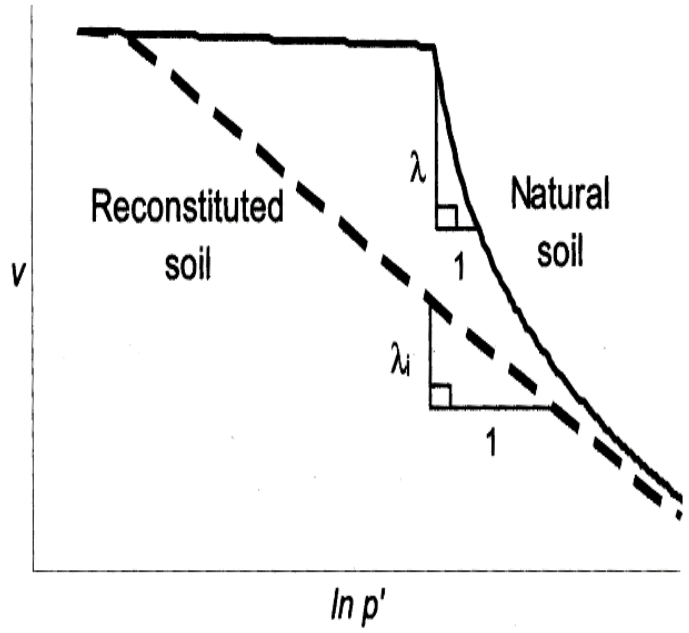

Figure 6.12 *Behaviour of natural and reconstituted clays.*

6.1.4 Determination of the parameters C_α, μ^* and k

The determination of the modified creep index μ^* is based on the extraction of the secondary compression index C_α from the oedometer test data. In this research $C_{\alpha\max}$ is used, which is processed as explained in Figure 6.13. There are two applicable methods for de-

termining $C_{\alpha \max}$, the method that is accordant to stress and method that is accordant to strain. Here method 1 ($\sigma_1 - C_{\alpha\varepsilon}$) is used and the user-defined curve is adopted because it is best-fitted in the set of observation points. In this method it is assumed that the secondary compression index is very low until a particular compression is reached and then it increases quickly up to a maximum value and after that it decreases slowly with compression, see Chapter 2.4, Figure 2.8. The critical compression where C_α starts to increase corresponds to an effective vertical stress of $0{,}8\sigma_p$ [Larsson 1981]. However, when dealing with HUT clay the point where the secondary consolidation commences could be $0{,}5\sigma_p$ since it is evident that C_α starts to increase rapidly before the point $0{,}8\sigma_p$. This behaviour is modelled in Figure 6.14, where it is supposed that C_α starts to increase in point $0{,}5\sigma_p$.

σ_{v0}`(kPa) = 15	β_1 = -0,110	β_2 = 0,685
σ_P (kPa) = 16	m_1 = 12,49	m_2 = 36,53

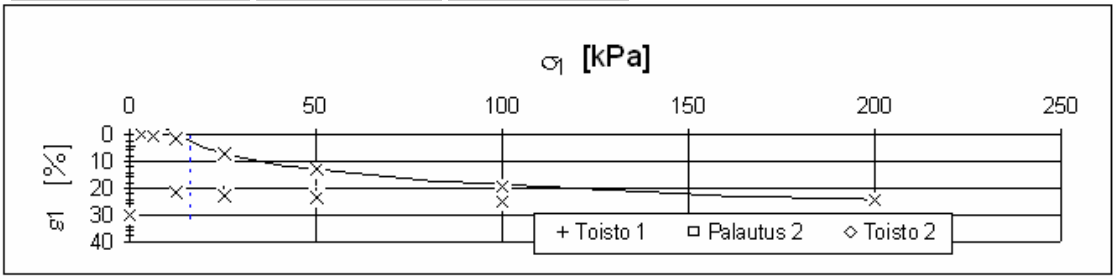

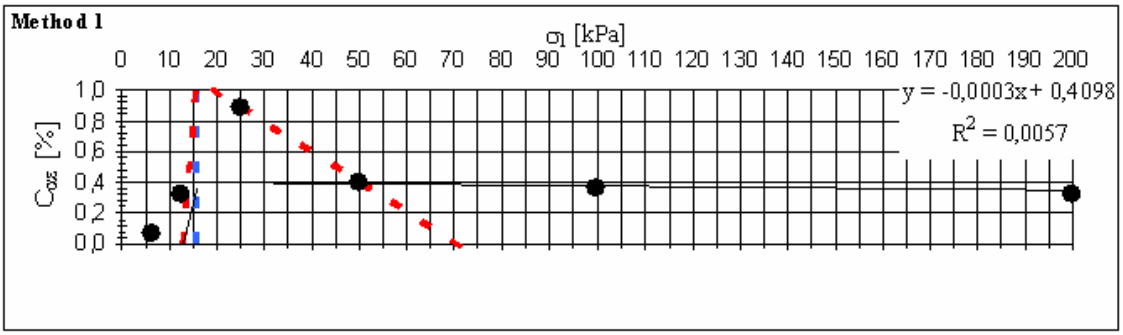

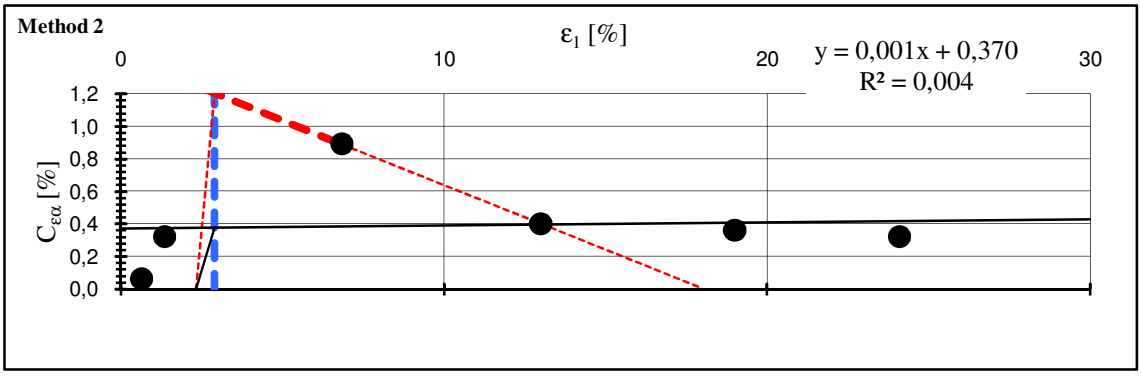

Secondary settlement parameters:

	Method 1 (s_1 - C_{ae}):			Method 2 (e_1 - C_{ae}):	
	Excel	User		Excel	User
$C_{ae\ max}$	0,36 %	1,07 %	$C_{ae\ max}$	0,38 %	1,20 %
$\alpha_{s\ max}$	0,011	0,033	$\alpha_{s\ max}$	0,012	0,038
β_{eas}	0,003 %/kPa	0,0196	β_{ea}	-0,002	0,080

Figure 6.13 *Determination of the parameters for secondary settlement on HUT 5611REC*

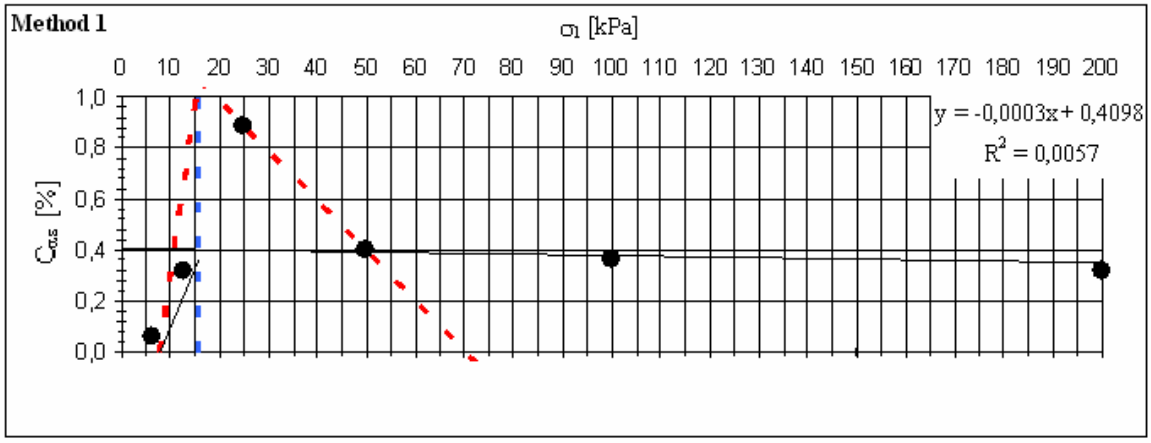

Figure 6.14 *The behaviour of* C_α *when the critical compression is* $0{,}5\sigma_p$.

After the determination of C_α it is possible to calculate the modified creep index according to following formula:

$$\mu^* = \frac{C_\alpha}{(1+e_0)\ln 10} \tag{6.3}$$

The values for μ^* are presented in Table 6.10. In this table also the permeability k_i is presented. k_i can be defined according to Taylor´s and Casagrande´s method which are illustrated in Figure 6.15.

Table 6.10 *Set of parameters* k, C_α, μ^*

Test	**Permeability**				**Secondary compression index**				**Modified creep index μ***
n:o	Taylor´s met.		Casagrande´s met.		s_1 - C_{ae}		e_1 - C_{ae}		
	k_1 *10^{-9} m/s	β_k	k_1 *10^{-9} m/s	β_k	C_{aemax}	β_{eas}	C_{aemax}	β_{ea}	
5578	0,4415	2,8650	0,4601	2,8916	1,1902	-0,0006	1,1719	-0,0054	0,1717
5579	0,6860	4,4148	0,5605	3,9727	1,1464	0,0044	1,2386	0,0358	0,1562
5593	0,4664	2,2765	0,5252	2,6363	1,2920	0,0021	1,3866	0,0247	0,1902
5594	0,5522	2,9738	0,4440	2,9501	1,6200	0,0020	1,7798	0,0320	0,2301
5631	0,5820	1,7808	0,3166	1,0051	1,0102	0,0026	1,0908	0,0218	0,1420
5610KRC	0,2988	1,9761	0,2711	2,2732	1,8052	0,0086	2,1844	0,0789	0,2513
5611REC	0,3958	4,2705	0,3181	3,4527	1,0664	0,0196	1,2049	0,0797	0,1484

It can be seen from the results that values for μ^* are fairly similar for all the undisturbed samples, excluding the test 5594. From this result it can be noticed that the Bjerrum´s time-lines are valid. μ^* values for reconstituted samples differ significantly, which can be due to different stress state.

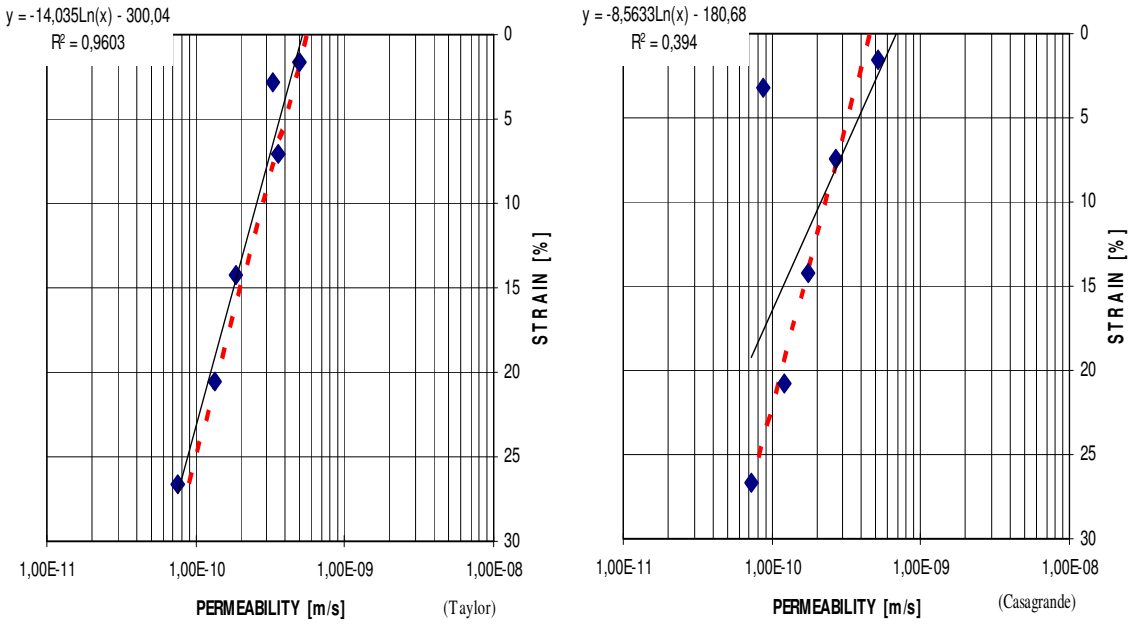

(a) *(b)*

Figure 6.15 *a) Determination of k_i according to Taylor´s method b) Determination of k according to Casagrande´s method*

6.2 The Triaxial Consolidation test results

6.2.1 Determination of the yield points, void ratios e_1, e_2 and maximum values for mean stress p and deviatoric stress q

The yield points were determined from the ln(p):v plots. The yield points were solved as an intersection points of overconsolidated and normally consolidated lines. Graham et al. (1983), for example, have used this method in their research. In cases when anisotropy changes significantly, parameter definition from ln(p):v plots may misquide and definitions would be safer to do by using linear graphs [Koskinen et al. 2003]. However, in these tri-axial consolidation tests the stress ratio were aimed to maintain constant.

The duration of the loading step was taken into account when determining the yield points. The most common duration of a loading step was 1 day but some loading steps were kept longer, even for 3 days. For these longer loading steps there are some visible time effects.

In Figure 6.16 in the beginning of the test the relatively small loading is kept for 3 days and as a consequence the sample absorbs water and the specific volume v increases. For larger loading steps the longer duration of loading steps causes the smaller values of the specific volume, which was taken into account while fitting the lines. The determination of the yield points is shown in Figures 6.16 and 6.17. In this context yield point refers to a yield point that is observed with particular stress ratio (for CAD5582 q/p is 0,2 and for CAD5583 q/p is 0,7).

The void ratios e_1 and e_2 are also determined from the intersection points of overconsolidated and normally consolidated lines. From the intersection point the specific volume is extracted and then according to formula v = 1+e, the void ratio is defined.

The maximum values for mean stress p and deviatoric stress q are determined from $p` - q$-graph, as a highest coordinates for first loading. This is shown in Figure 6.18 for CAD5582 test.

6.2.2 Determination of the parameters λ, κ, v_λ and $\frac{\Delta\varepsilon_s}{\Delta\varepsilon_v}$

The critical state parameters λ and κ were determined from ln(p):v plots. λ was determined for both first loading and the reloading. κ was determined for reloading. The determination of these parameters as slopes of the normal consolidation line and overconsolidation line is illustrated in Figures 6.16 and 6.17.

The parameter v_λ can be defined as an ordinate of λ-line when p= 1 kPa and it is extracted from the interception point of the particular λ-line and v-axis. It is useful to denote because it defines where the specimen´s state lies [Schofield & Wroth 1968].

$$v_\lambda = v + \lambda \ln p \tag{6.4}$$

The relationship $\frac{\Delta\varepsilon_s}{\Delta\varepsilon_v}$ between shear strain ε_s and volumetric strain ε_v describes the direction of the strain increment and can be defined as a slope of the line in ε_v - ε_s-plot. Determination of $\frac{\Delta\varepsilon_s}{\Delta\varepsilon_v}$-relationship is shown in Figure 6.19.

All the parameters that are discussed in chapter 6.2 can be found in Tables 6.11 - 6.13. In Table 6.11 the basic properties are shown, in Table 6.12 the parameters for loading and reloading are shown and in Table 6.13 the critical state parameters are defined.

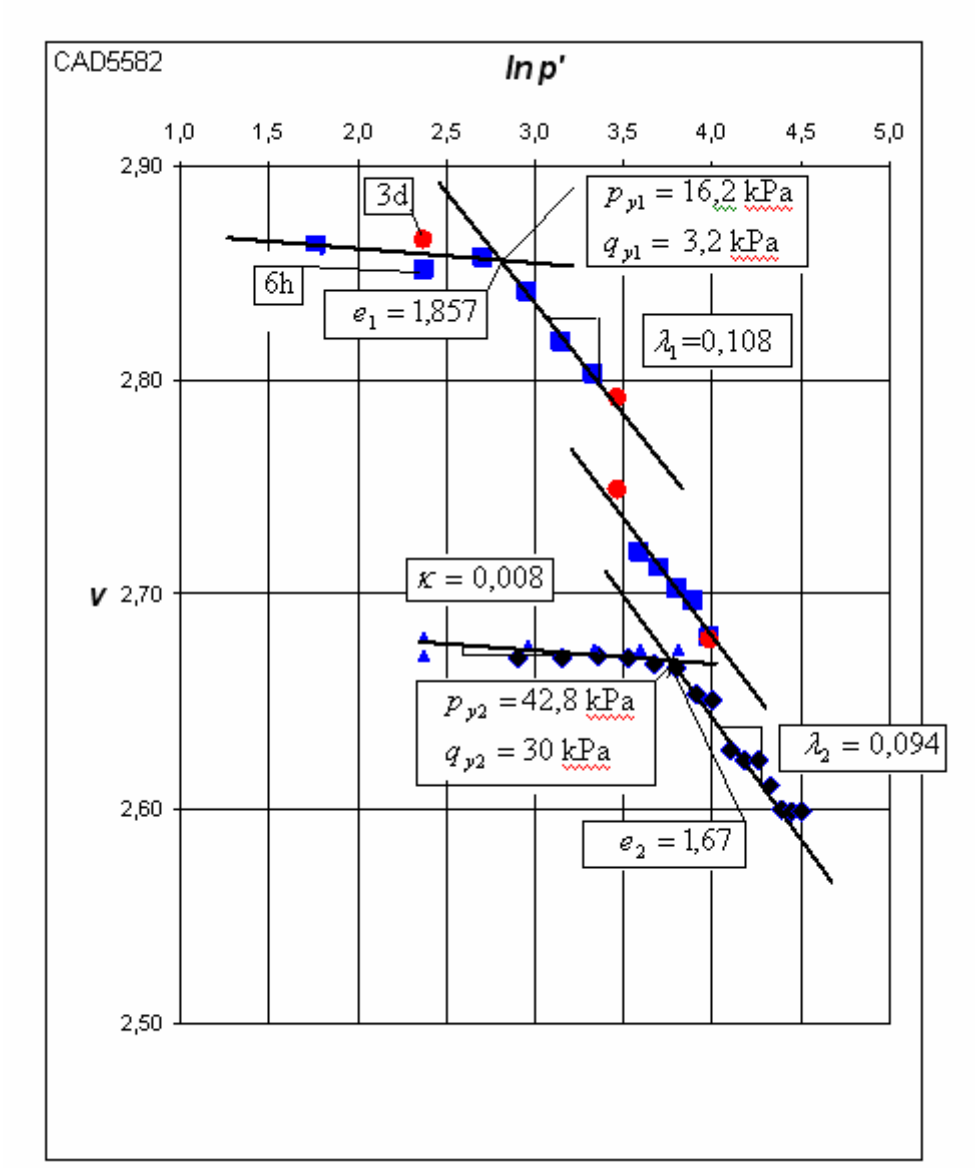

Figure 6.16 *Determination of the yield points and critical state parameters in triaxial consolidation test CAD5582.*

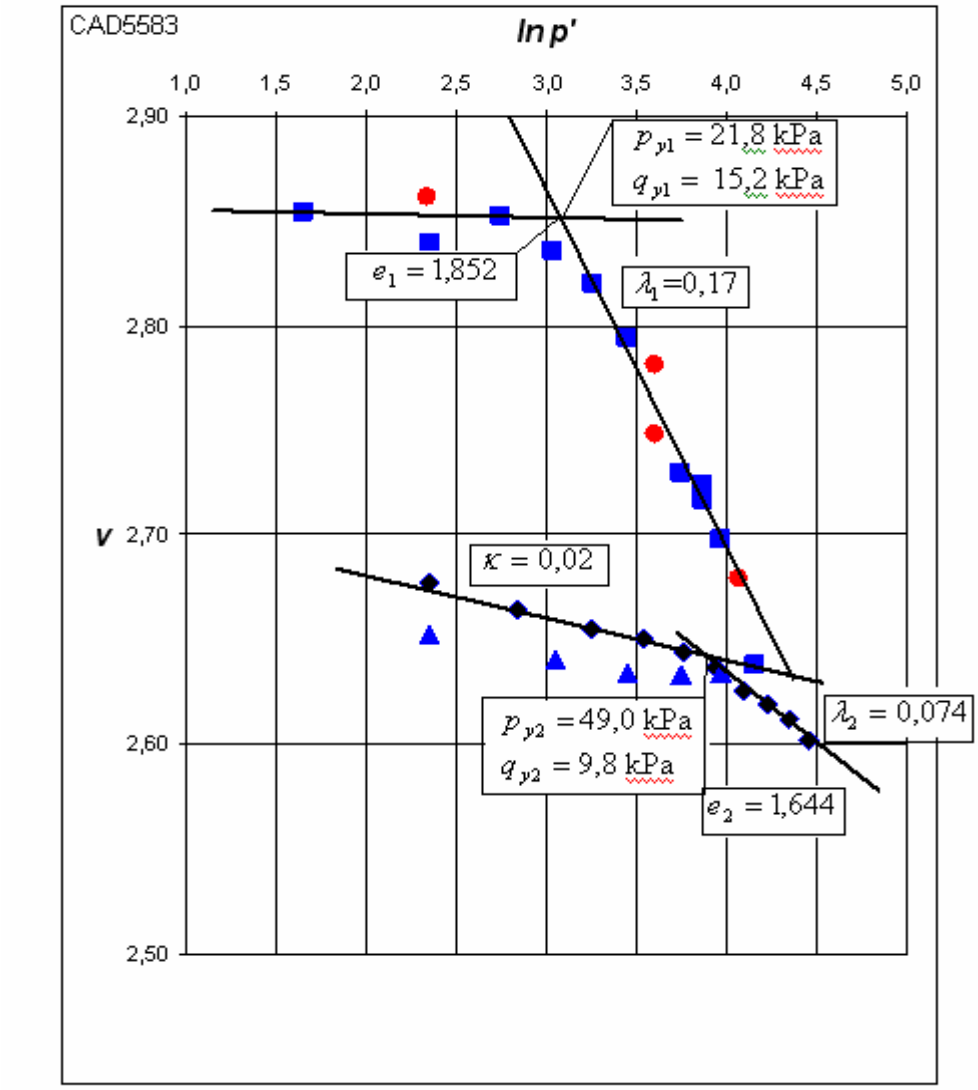

Figure 6.17 *Determination of the yield points and critical state parameters in triaxial consolidation test CAD5583.*

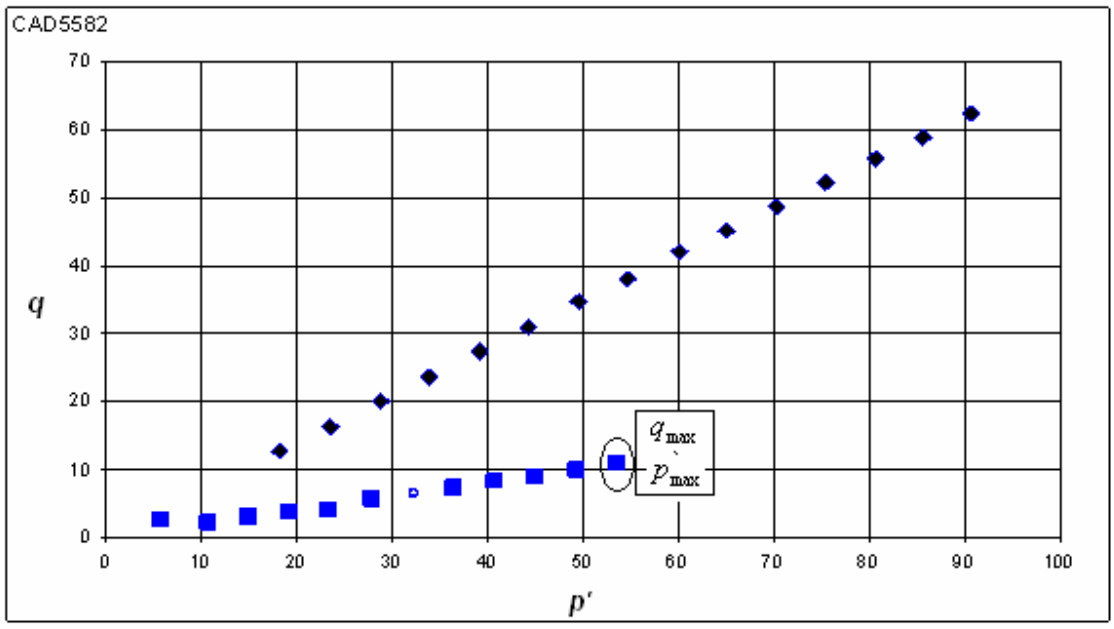

Figure 6.18 *Determination of the* q_{max} *and* p_{max} *in triaxial consolidation test CAD5582.*

Table 6.11 *Basic properties from consolidation tests.*

Test n:o	**Depth z** [m]	**Stress ratio** q/p	**Water content** w_0 [%]	**Bulk density** γ_0 kN/m^3	**Void ratio** e_0	**Satu-ration** S_r [%]	**Volume initial** V_0 [cm^3]	**Height initial** h_0 [cm]
CAD5582	1,58-1,69	0,2	74,1	16,22	1,905	100	198,95	10
CAD5583	1,47-1,58	0,7	68,5	15,7	1,905	100	198,95	10,00

Table 6.12 *Parameters for loading and reloading phases from consolidation tests.*

Yield Test n:o	p_{y1} kPa	q_{y1} kPa	e_1	p_{max} kPa	q_{max} kPa	**Reloading** q/p	p'_{y2} kPa	q_{y2} kPa	e_2
CAD5582	16,2	3,2	1,857	53,6	10,8	0,7	42,8	30,0	1,67
CAD5583	21,8	15,2	1,852	64,1	48,2	0,2	49	9,8	1,64

Table 6.13 *Critical state parameters from consolidation tests.*

Test n:o	λ_1	λ_2	κ	v_λ	$\Delta\varepsilon_s/\Delta\varepsilon_v$ **(after yield)**	$\Delta\varepsilon_s/\Delta\varepsilon_v$ **(reloading)**
CAD5582	0,108	0,094	0,008	3,156	-0,225	0,792
CAD5583	0,170	0,074	0,020	3,376	0,25	0,551

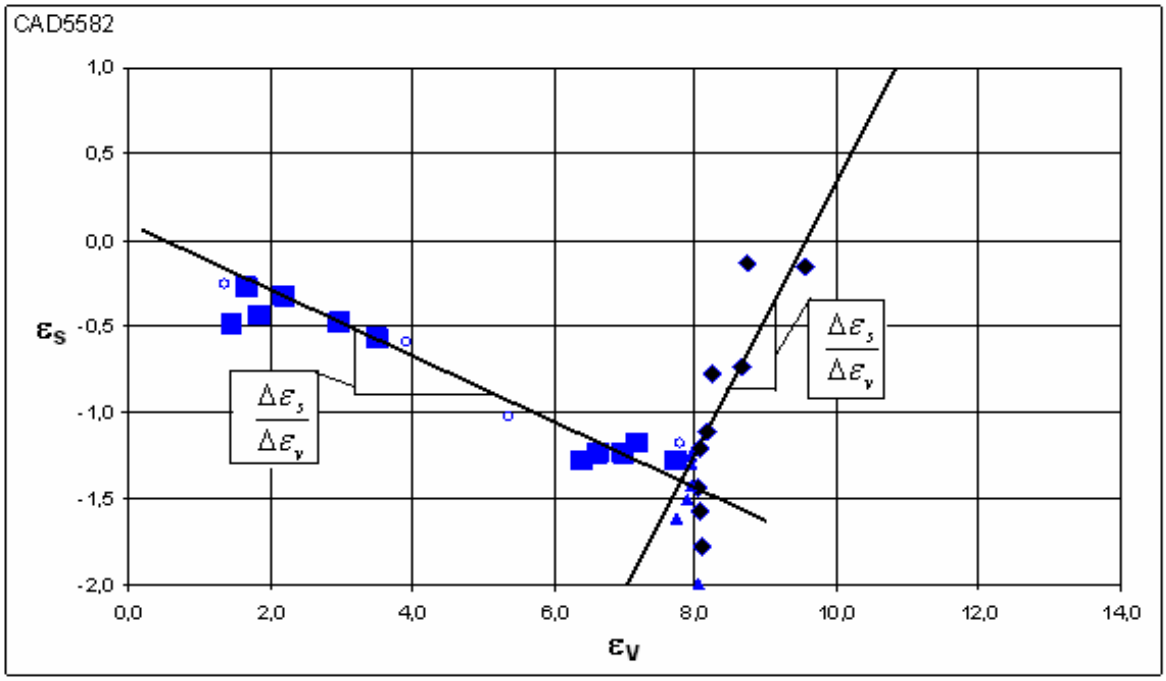

Figure 6.19 *Determination of the relationship between ε_s and ε_v on CAD 5582.*

As it can be seen from the results the values of λ and κ differ from each other and that is due to different stress ratios used in consolidation. As closely explained in Chapter 6.1.3 it is possible to define the values of λ and κ with the same procedure from oedometer tests as well. At least it might be logical to define the λ value from oedometer test results since oedometer tests are easier and much faster to carry out. In this research comparing the λ values determined from oedometer tests to values determined from triaxial consolidation tests is not accurate because in oedometer tests the consolidation takes place at K_0 state (radial deformations are not possible). Therefore, in this research the stress ratio in oedometer test signifies the η_{KO} = 0,5 in triaxial test (M = 1,2) whereas the stress ratios used in triaxial consolidation tests were 0,7 and 0,2

6.3 The Triaxial test results

6.3.1 Test-spesific description

6.3.1.1 Tests performed with strain rate $\dot{\varepsilon}$ = 0,06 %/h on undisturbed samples

Three undrained triaxial tests, CAUC 5597, CAUC 5598, CAUC 5609, were performed with strain rate $\dot{\varepsilon}$=0,06 %/h, which was the lowest strain rate that was used in this testing program. $\dot{\varepsilon}$ denotes axial strain rate and thus could be marked $\dot{\varepsilon}_1$ as well. Stress ratio was 0,4 in all the tests. As it can be seen from the Figure 6.20 a) the cell pressures were: CAUC 5598- 20 kPa, CAUC 5597- 40 kPa and CAUC 5609- 60 kPa.

In test CAUC 5598 shearing was stopped when strain ε_1 = 1,4 % and sample was allowed to relax. There was a short electricity breakdown when ε_1 = 1,41 % and after that shearing was started again with the initial strain rate $\dot{\varepsilon}$ = 0,06 %/h . When ε_1 = 3,9 % the strain rate was increased to $\dot{\varepsilon}$ = 0,6 %/h and again when ε_1 = 7,15 % the strain rate was reset to initial strain rate $\dot{\varepsilon}$ = 0,06 %/h. When ε_1 = 8,16 % shearing was stopped for 10 minutes and started again after that with strain rate $\dot{\varepsilon}$ = 0,6 %/h. When the ε_1 had dropped to 7,5 %, shearing was stopped and sample relaxed. The shearing action of the sample occurred when ε_1 was approximately 3,88 %.

In test CAUC 5597 shearing was continued with strain rate $\dot{\varepsilon}$ = 0,06 %/h until the ε_1 reached the value 1,6 % when shearing was stopped and sample relaxed. There was a short electricity breakdown when ε_1 = 1,65 % and after that shearing was started again with the initial strain rate $\dot{\varepsilon}$ = 0,06 %/h . The shearing action occurred approximately when ε_1 was 3,2 %. The shearing rate was increased to $\dot{\varepsilon}$ = 0,6 %/h when ε_1 = 4,8 % and again reset to iniatial strain rate $\dot{\varepsilon}$ = 0,06 %/h when ε_1 = 8,1%. Shearing was stopped when ε_1 = 9,3% and allowed to relax for 10 minutes and after that shearing was started again with shearing

rate $\dot{\varepsilon}$ = 0,6 %/h. Shearing continued until ε_1 had dropped to 8,6 % and then sample was allowed to relax.

In test CAUC 5609 shearing was carried with strain rate $\dot{\varepsilon}$ = 0,06 %/h through the whole test. The shearing action occurred as a barrel shaped sample when ε_1 = 3,5 %, but more clearly sample fractured when ε_1 = 11 % and then shearing was stopped.

In Figures 6.20 a) and 6.20 b) the behaviour of samples in triaxial tests is presented when strain rate was 0,06 %/h. In Figure 6.20 b) the failure line is illustrated. The position of failure line has been determined with the similar method that has been used in practical design. First the q_{max}-value for the tests in same series was detected and then fitted the failure line according to these values. Also strains in failure point were checked and it was ensured that the strains were reasonable, because samples are not usable if they are already broken. Any membrane correction has not been performed. Also the graphs describing the behaviour of pore pressure have been used to define the failure line. Graphs ε_1-u_w, ε_1-q and ε_1-q/p can be found in appendices. The position of the critical state line has been defined according to numerous earlier performed drained triaxial tests on HUT clay. According to these tests the slope of the critical state line M=1,2. When defining failure line and critical state line, the results that were generated when samples shape was clearly deformed, were not used in determination. Definitions for failure lines and critical state lines was performed with this procedure in Figures 6.20 b), 6.21b), 6.22b) and 6.23b).

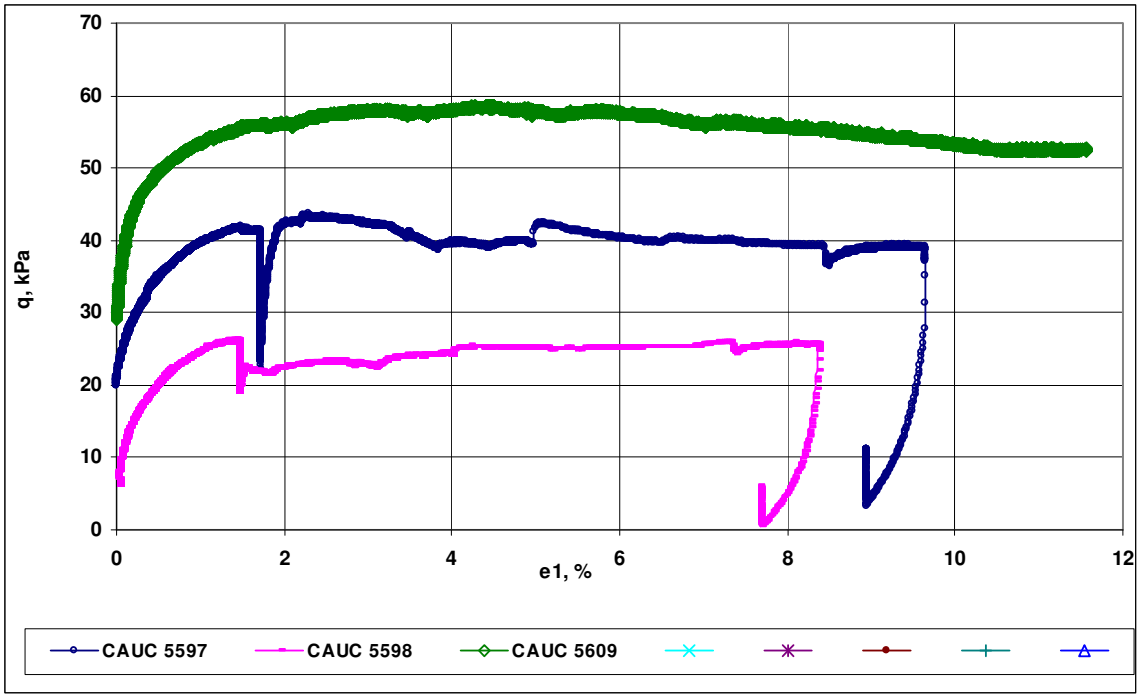

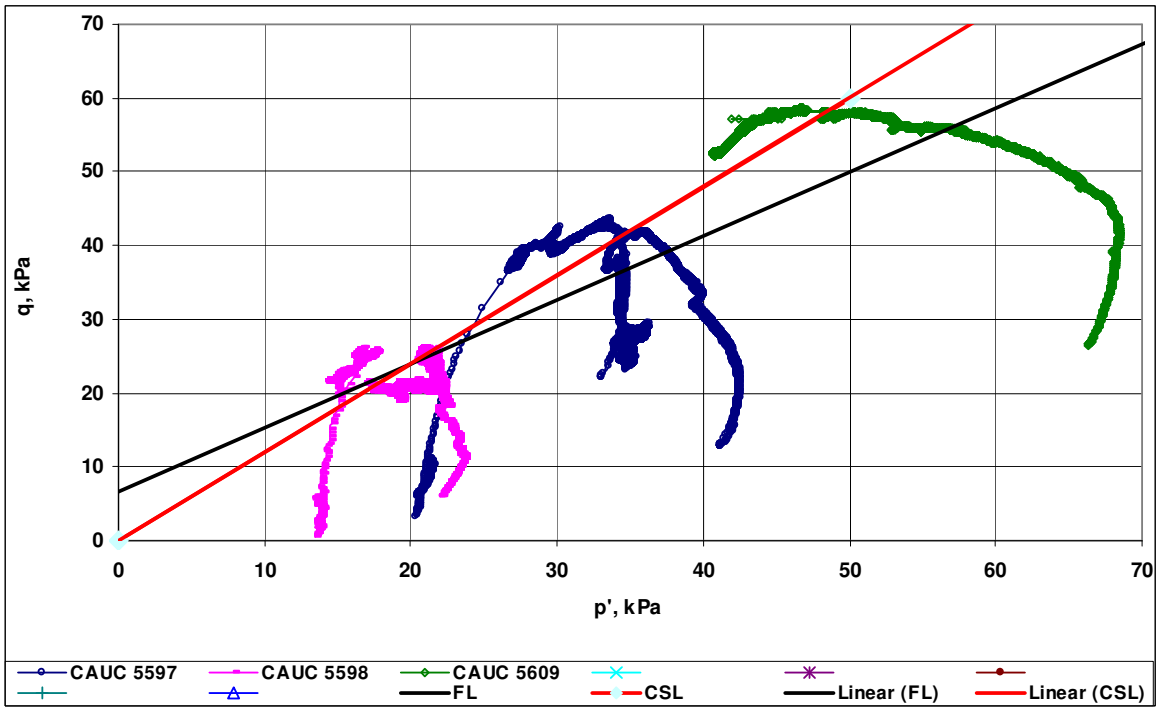

----- Failure line **-----Critical state line**

Figure 6.20 *a) ε_1-q-plot and b) p`-q-plot when* $\dot{\varepsilon}$ *= 0,06 %/h*

6.3.1.2 Tests performed with strain rate $\dot{\varepsilon}$ = 0,6 %/h on undisturbed samples

Four undrained triaxial tests, CAUC 5580, CAUC 5581, CAUC 5591, CAUC 5595, were performed with strain rate $\dot{\varepsilon}$=0,6 %/h. Stress ratio was 0,4 in all the tests. As it can be seen from the Figure 6.21 a) the cell pressures were: CAUC 5591- 20 kPa, CAUC 5595- 20 kPa, CAUC 5580- 40 kPa and CAUC 5581-60 kPa.

In test CAUC 5591 shearing was continued with strain rate $\dot{\varepsilon}$ = 0,6 %/h until the strain reached value 2,6 % and then strain rate was increased to $\dot{\varepsilon}$ = 6 %/h. This strain rate was kept until ε_1 = 4,6 % and then strain rate was reset to $\dot{\varepsilon}$ = 0,6 %/h . When ε_1 = 4,77 % shearing was stopped and sample was let to relax. There were suspicions that sample CAUC 5591 had already broken down during consolidation but without clear evidences the test was continued to shearing phase.

In test CAUC 5595 shearing was carried out with strain rate $\dot{\varepsilon}$ = 0,6 %/h until the strain ε_1 = 3,8%. Then strain rate was decreased to $\dot{\varepsilon}$ = 0,06 %/h. During the night time there was power failure and thus there is a cap in the graph. Shearing was started again in the morning with strain rate $\dot{\varepsilon}$ = 0,06 %/h and when strain reached value 6,3 % the strain rate was increased to $\dot{\varepsilon}$ = 0,6 %/h. Strain rate was increased again when ε_1 = 7,5 % to $\dot{\varepsilon}$ = 6 %/h and decreased to $\dot{\varepsilon}$ = 0,6 %/h when ε_1 = 14 %. Shearing was stopped when ε_1 = 15,7 % and sample was let to relax. The shearing action was not so clear in this test and only sample deformation to barrel shape could be observed.

In test CAUC 5580 strain rate was altered more often and “jumps” are easy to observe from the graph. Shearing was continued with strain rate $\dot{\varepsilon}$ = 0,6 %/h until ε_1 = 3,09 % and then the strain rate was decreased to $\dot{\varepsilon}$ = 0,06 %/h. When ε_1 = 4,16 % the strain rate was increased to $\dot{\varepsilon}$ = 0,6 %/h and was continued until ε_1 = 4,4 %. Then strain rate was in-

creased to value $\dot{\varepsilon}$ = 6 %/h was continued like that until ε_1 = 4,8 %, when the strain rate was again decreased to $\dot{\varepsilon}$ = 0,6 %/h. The strain rate was changed once more when ε_1 = 8,78 % to $\dot{\varepsilon}$ = 0,06 %/h and that was continued until ε_1 = 9,9 %. Then sample was allowed to relax.

In test CAUC 5581 the alteration of the strain rate was pretty similar to alteration in test CAUC 5580. Shearing was carried out with strain rate $\dot{\varepsilon}$ = 0,6 %/h until ε_1 = 2,94 % and then strain rate was decreased to $\dot{\varepsilon}$ = 0,06 %/h. When the strain reached the value ε_1 = 3,86 % the strain rate was reset to initial value $\dot{\varepsilon}$ = 0,6 %/h and the test was continued with this strain rate until ε_1 = 4,13 %. Then the strain rate was increased to $\dot{\varepsilon}$ = 6 %/h and continued like that until ε_1 = 4,55 % when strain rate was decreased to $\dot{\varepsilon}$ = 0,6 %/h. The last alteration of the strain rate to $\dot{\varepsilon}$ = 0,06 %/h was done when ε_1 = 8,42 %. Shearing was stopped when ε_1 = 9,35 % and sample was allowed to relax.

In Figures 6.21 a) and 6.21 b) the behaviour of samples in triaxial tests is presented when strain rate was 0,6 %/h. In Figure 6.21 b) the failure line is illustrated.

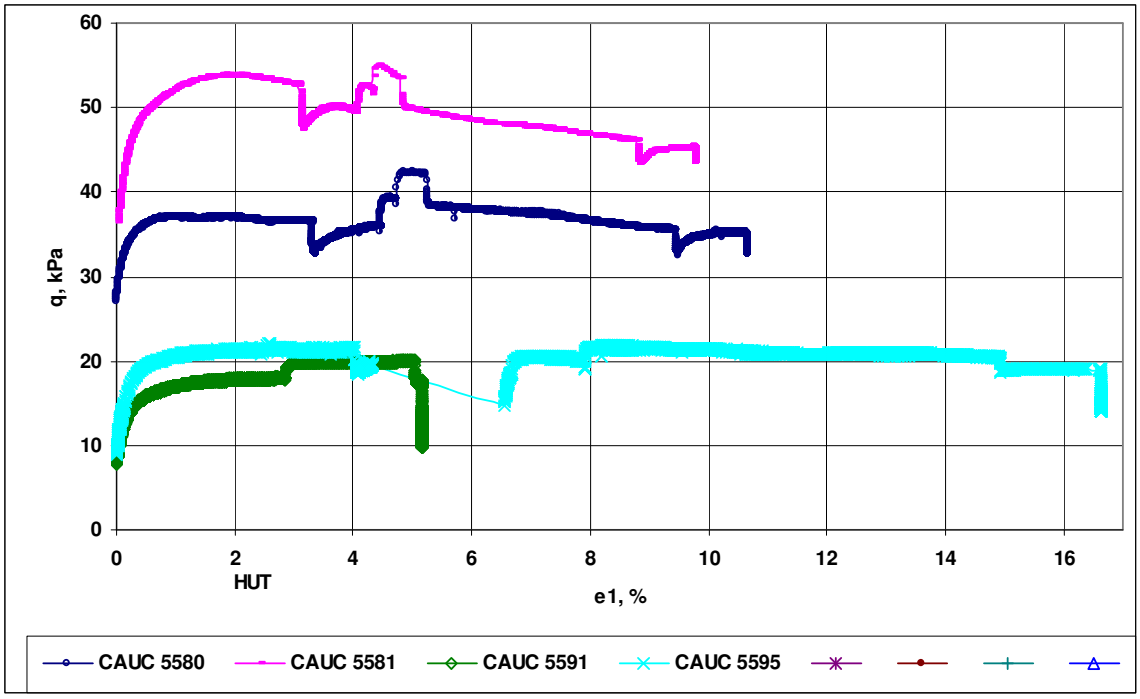

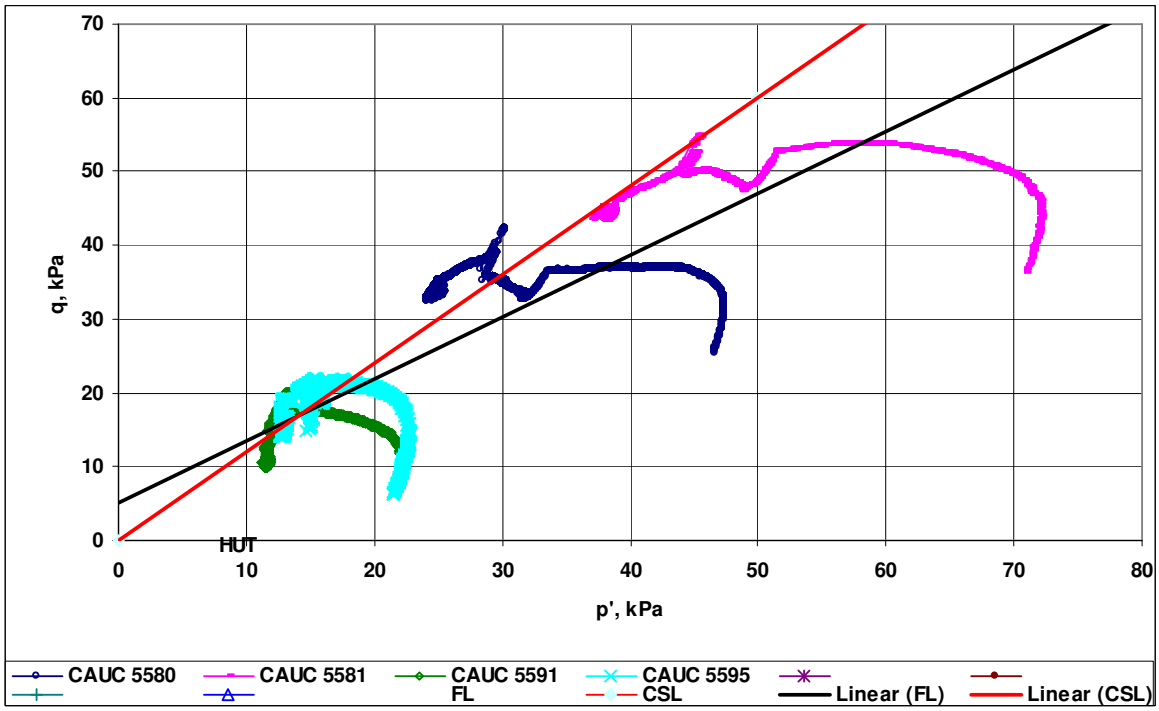

----- Failure line **-----Critical state line**

Figure 6.21 *a) ε1-q-plot and b) p`-q-plot when* $\dot{\varepsilon}$ *= 0,6 %/h*

6.3.1.3 Tests performed with strain rate $\dot{\varepsilon}$ = 6 %/h on undisturbed samples

Three tests were performed with strain rate $\dot{\varepsilon}$ = 6 %/h, but only two tests, CAUC 5592 and CAUC 5596, are presented in Figures 6.22 a) & b) because test CAUC 5608 was failed. As it can be seen from the Figure 6.22 a) the used cell pressures were: CAUC 5592- 20 kPa, CAUC 5596- 40 kPa. Stress ratio was 0,4 in both of the tests.

Test CAUC 5592 was carried out with strain rate $\dot{\varepsilon}$ = 6 %/h until ε_1 reached value 8,09 % and then strain rate was decreased to $\dot{\varepsilon}$ = 0,6 %/h. Test was continued with that strain rate until ε_1 = 10,58 % and then sample was let to relax. The shearing action occurred approximately when ε_1 was 3,9 %.

In test CAUC 5596 shearing was performed with strain rate $\dot{\varepsilon}$ = 6 %/h as long as the strain rate ε_1 was 2,15 %. At this point strain rate was decreased to $\dot{\varepsilon}$ = 0,6 %/h. Test was carried out with that strain rate until ε_1 = 3,53 % and then decreased to $\dot{\varepsilon}$ = 0,06 %/h. There was power failure during night time and due that there is discontinuity in the graph. Shearing was started again in the morning with strain rate $\dot{\varepsilon}$ = 0,06 %/h and continued like that until ε_1 = 6,17 %. After that strain rate was increased to $\dot{\varepsilon}$ = 0,6 %/h and was continued until ε_1 = 9,5 %. Then sample was allowed to relax. Two minor spikes in the graph (ε_1 = 7,38 % and ε_1 = 8,07 %) are followed by short stops in shearing. Stops were done to change computer programs reading frequency. The shearing action was clearly observed when ε_1 = 8,39 %.

In Figures 6.22 a) and 6.22 b) the behaviour of samples in triaxial tests is presented when strain rate was 6 %/h. In Figure 6.22 b) the failure line is illustrated.

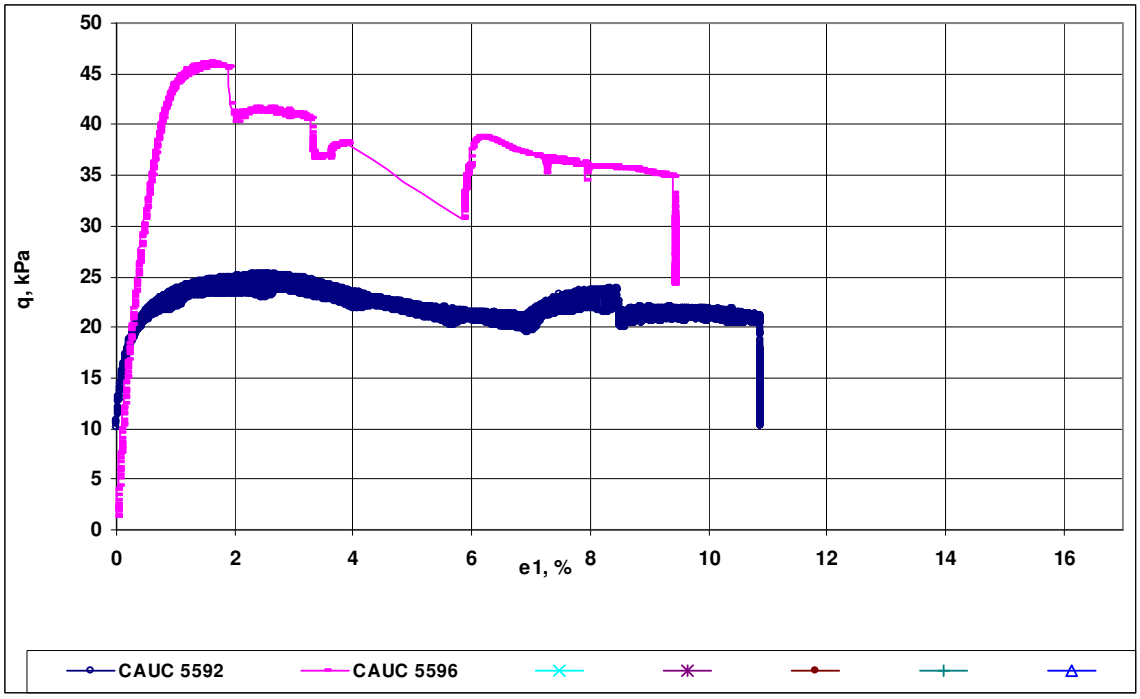

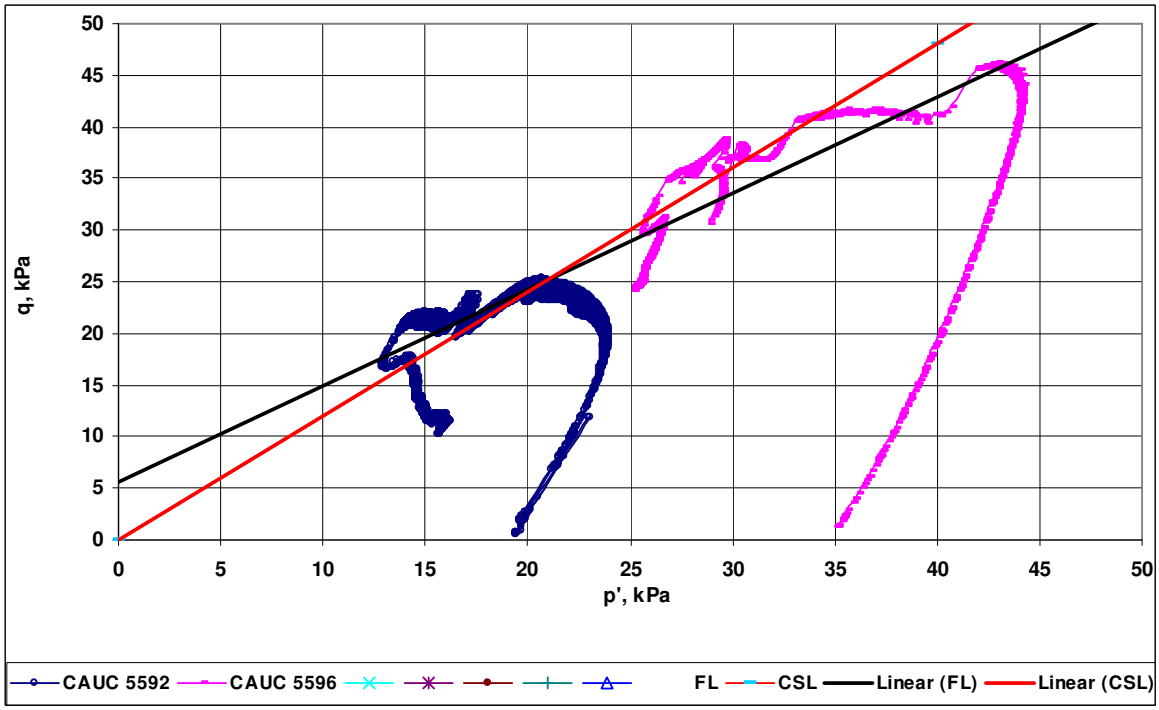

----- Failure line **-----Critical state line**

Figure 6.22 *a) ε1-q-plot and b) p`-q-plot when* $\dot{\varepsilon}$ *=6 %/h*

6.3.1.4 Tests performed with strain rate $\dot{\varepsilon}$ = 0,6 %/h on reconstituted samples

Four tests, CAUC 5602REC, CAUC 5603REC, CAUC 5606REC and CAUC 5607REC, were performed with strain rate $\dot{\varepsilon}$ = 0,6 %/h on reconstituted samples. Stress ratio was 0,4 in all the tests. As it can be interpreted from the Figure 6.23 a) the used cell pressures were: CAUC 5603REC- 20 kPa, CAUC 5602REC- 40 kPa, CAUC 5607REC- 40 kPa, CAUC 5606REC- 60 kPa.

Test CAUC 5603REC was performed with strain rate $\dot{\varepsilon}$ = 0,6 %/h through the whole test. Fracturing of the sample was not clear, sample only deformed to barrel shape when ε_1 = 3,66 %. Shearing was stopped at the moment when ε_1 = 13,91 % and sample was not allowed to relax.

In test CAUC 5602REC shearing was performed with strain rate $\dot{\varepsilon}$ = 0,6 %/h through the whole test. Samples shape deformed to barrel when ε_1 = 3,42 %. Shearing was stopped when ε_1 reached the value 13,69 % and sample was not let to relax.

Whole test CAUC 5607REC was carried out with strain rate $\dot{\varepsilon}$ = 0,6 %/h and the shearing was stopped when ε_1 = 15,9 % and sample was allowed to relax almost three hours. Fracturing of the sample was not possible to observe clearly.

Also whole test CAUC 5606REC was performed with strain rate $\dot{\varepsilon}$ = 0,6 %/h and shearing was stopped when ε_1 = 16,3 %. Then sample was let to relax similar to test CAUC 5607REC.

In Figures 6.23 a) and 6.23 b) the behaviour of reconstituted samples in triaxial tests is presented when strain rate was 0,6 %/h. In Figure 6.23 b) the failure line is illustrated.

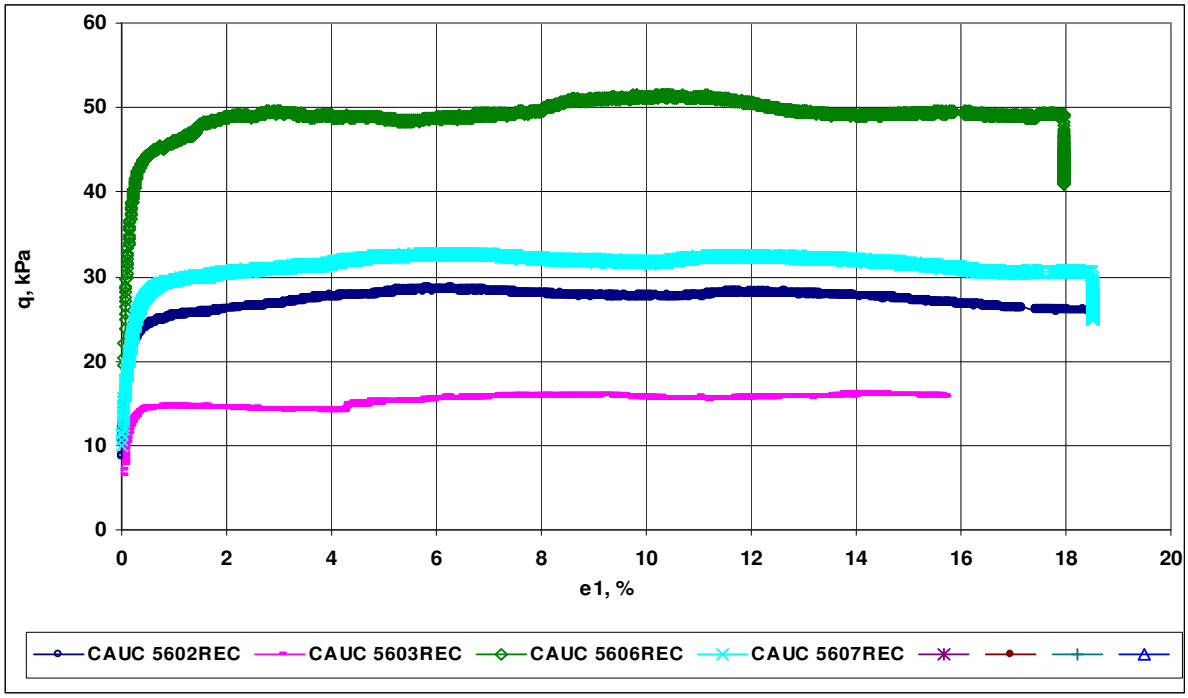

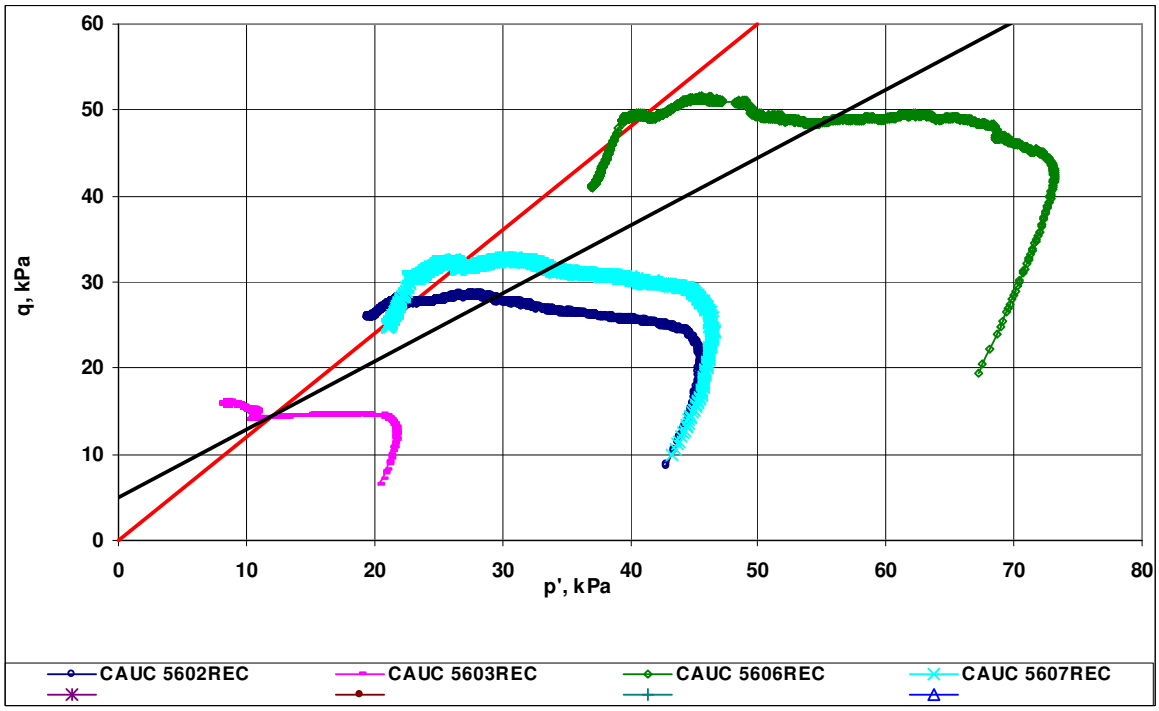

----- Failure line **-----Critical state line**

Figure 6.23 *a) ε_1-q-plot and b) p`-q-plot for reconstituted samples when* $\dot{\varepsilon}$ *= 0,6 %/h*

When comparing the strength of the natural and reconstituted samples tested with same strain rate, it can be observed that the strength of the natural samples is higher than the strength of the reconstituted samples according to q_{max} values from the Figures 6.21a) and

6.23a). q_{max}-values for natural samples reach the used cell pressure or even higher, whereas the q_{max}-values for reconstituted samples stay significantly smaller than used cell pressures.

6.3.2 Determination of strength parameters from triaxial test results

The basic data from triaxial tests is presented in Table 6.14.

Table 6.14 *Basic data from triaxial tests.*

Test n:o	Depth	Cell pressure	Shearing rate	Water content	Unit weight	Void ratio	Satura-tion	Volume initial	Height initial	Volume after cons.	Height after cons.	Void ratio
	z	σ_3	ε_1	w_0	γ_0	e_0	S_r	V_0	h_0	V_1	h_1	e_1
	m	kPa	%/h	%	kN/m^3		%	cm^3	cm	cm^3	cm	
CAUC 5580	1,79-1,89	40	0,60	75,3	15,17	2,13	98	199,11	10,00	178,31	9,30	1,80
CAUC5581	1,69-1,79	60	0,60	74	15,36	2,07	99	199,11	10,00	181,71	9,60	1,80
CAUC5591	1,79-1,90	20	0,60	77	15,51	2,09	100	199,11	10,00	186,41	9,27	1,89
CAUC5592	1,68-1,79	20	6,00	68	14,92	2,05	92	199,11	10,00	191,01	9,72	1,92
CAUC5595	1,83-1,94	20	0,60	75,3	15,38	2,09	100	199,11	10,00	187,91	9,44	1,91
CAUC5596	1,72-1,83	40	6,00	78,3	15,18	2,18	99	199,11	10,00	186,81	9,76	1,98
CAUC5597	1,50-1,61	40	0,06	78,1	15,95	2,02	100	199,11	10,00	187,11	9,63	1,84
CAUC5598	1,61-1,72	20	0,06	65,3	15,59	1,87	96	199,11	10,00	191,01	9,77	1,75
CAUC 5608	1,68-1,79	60	6,00	79,5	15,15	2,21	99	198,71	10,00	171,91	9,42	1,78
CAUC5609	1,57-1,68	60	0,06	75	15,52	2,05	100	198,71	10,00	178,81	9,48	1,75
CAUC5602REC	1,3-2,1	40	0,60	88,5	15,05	2,39	100	176,71	9,00	142,01	7,43	1,73
CAUC5603REC	1,3-2,1	20	0,60	87,4	15,38	2,30	100	196,35	10,00	170,75	8,92	1,87
CAUC5606REC	1,3-2,1	60	0,6	86	15,33	2,28	100	196,35	10,00	153,40	9,26	1,57
CAUC5607REC	1,3-2,1	40	0,60	82,3	15,5	2,18	100	180,64	9,20	148,64	8,76	1,62

The determination of strength parameters was based on the Figures 6.20 b), 6.21 b), 6.22 b) and 6.23 b). For the failures lines, illustrated in these pictures, the slope of the FL line k_1 and interception with q-axis q_0 was defined. From the grounds of k_1 and q_0, effective friction angle φ' and effective cohesion c' was possible to define with following formulas:

$$\sin\varphi' = \frac{3k_1}{6+k_1} \tag{6.5}$$

$$c' = q_0 \frac{3-\sin\varphi'}{6+\cos\varphi'} \tag{6.6}$$

Defined strength parameters are presented in Table 6.15.

Table 6.15 *Defined strength parameters.*

Test n:o	**Strain rate** $\dot{\varepsilon}$	**Shearing point ε_1=0**			**Fail-ure line**			
		q [kPa]	p` [kPa]	u_w [kPa]	q_0[kPa]	k_1	φ`	c` [kPa]
CAUC5597	0,06	13,5	41,6	2,9	6,7	0,87	22,2	2,5
CAUC5598	0,06	6,1	22,1	0,0	6,7	0,87	22,2	2,5
CAUC5609	0,06	27,1	66,6	2,5	6,7	0,87	22,2	2,5
CAUC5580	0,6	16,8	44,2	1,4	5,0	0,84	21,6	1,9
CAUC5581	0,6	26,5	68,1	0,8	5,0	0,84	21,6	1,9
CAUC5591	0,6	7,3	22,0	0,4	5,0	0,84	21,6	1,9
CAUC5595	0,6	6,3	21,5	0,6	5,0	0,84	21,6	1,9
CAUC5592	6	8,6	21,7	1,2	5,6	0,93	23,8	2,1
CAUC5596	6	2,0	35,3	5,3	5,6	0,93	23,8	2,1
CAUC5602REC	0,6	8,8	42,9	0,1	5,0	0,79	20,4	1,9
CAUC5603REC	0,6	6,4	20,3	1,8	5,0	0,79	20,4	1,9
CAUC5606REC	0,6	19,5	67,2	-0,7	5,0	0,79	20,4	1,9
CAUC5607REC	0,6	9,9	43,3	0,0	5,0	0,79	20,4	1,9

Slope of the critical state line M is illustrated in figures and it is defined as M = 1,2 for HUT clay according to numerous earlier researches. According to formula (6.4) the critical state friction angle can be defined as 30° when M = 1,2. From critical state friction angle coefficient of the earth pressure at rest, $K_{0,}$ can be defined according to Jaky´s formula $K_0^{'} = 1 - \sin\phi_c^{'}$. For HUT clay $K_0 = 0{,}5$. The stress ratio η_{k0} for K_0-line can be defined from $\eta_{K_0} = \frac{q}{p^{'}}$. For the samples researched here $\eta_{K_0} = 0{,}75$.

When comparing the critical state line and the failure line it can be observed that the slope of the critical state line (M=1,2) is steeper than the slope of the failure line, which was approximately 0,8-0,9.

As it can be seen from the Table 6.15 there is a small difference between the strength parameters whether the used strain rate was 0,06 %/h, 0,6 %/h or 6 %/h. According to previous researches the logical result would have been that with higher strain rate clay would have strengthen and thus strength parameters would have been higher for higher strain rates. Strength parameters are higher for tests carried out with strain rate $\dot{\varepsilon}$ = 6 %/h than tests carried out with strain rate $\dot{\varepsilon}$ = 0,6 %/h. However, for the tests carried out with lowest strain rate $\dot{\varepsilon}$ = 0,06 %/h strength parameters are little higher than for tests with strain rate $\dot{\varepsilon}$ = 0,6 %/h. That does not follow the commonly assumed behaviour of soft clay. Regardless, the variation of strain rate in individual tests increases the strength of clay as can be seen from test CAUC 5580 and CAUC 5581 in Figure 6.21. Although the strengthening of the clay do not seem to follow any logic in these tests when compared with chancing the strain rate. Obviously, the strength parameters are lower for reconstituted samples due to destructuration.

7. CONCLUSIONS AND RECOMMENDATIONS

The main purpose of this work was to collect more test data from behaviour of Finnish soft clay and that way lighten the definition of the parameters of EVP-SCLAY1S and ACM models. With proper parameters the performance of EVP-SCLAY1S and ACM could be improved. This was done by testing both reconstituted and natural samples with oedometer and triaxial equipment and then determining desired parameters.

A large testing program with HUT clay included seven oedometer tests, two triaxial consolidation tests and 14 undrained triaxial tests. With short- and long-term oedometer tests the influence of settlement time to values of critical state parameters was examined and it was observed that the influence of settlement time was not significant. It was also observed from oedometer test results that destructuration of reconstituted samples influences little on critical state parameters as a decreasing factor. Very small differences between intact and intrinsic λ-values indicate that clay is not very structured and the reasons for that could be: intact samples may have been disturbed or from dessicated layer that have been subject to drying-wetting cycles in the past. Also the stress state of HUT clay was managed to determine. Little uncertainty to some oedometer test results was caused by weekends and summer holidays, because it was impossible to maintain the duration of the loading steps as a constant, but this has been taken into account when handling the results.

The triaxial consolidation tests were performed to determine the yield points of the samples and also to define some same critical state parameters than in oedometer tests. Unfortunately, we were not able to define yield surfaces with existing test data but hopefully later in this project the data provided in this work can be used. Definition of the critical state parameters was managed but as it took so much time, it would be logical to define these parameters with oedometer. Critical state parameters from consolidation tests and oedometer tests were not comparable due to different stress ratios that were used. In consolidation tests we had some difficulties with other dial gauge that tended to stuck and that could have had some influence on results.

Undrained triaxial tests were carried out to research the influence of strain rate to strength parameters. The influence of strain rate was small. Strength parameters were defined with the help of failure lines and critical state lines that were illustrated in p'-q-graphs. The position of failure line was determined with the similar method that is used in practical design. First the q_{max}-value for the tests in same series was detected and then fitted the failure line according to these values. Also strains in failure point were checked and it was ensured that the strains were reasonable, because samples are not usable if they are already broken. Any membrane correction was not performed. Also the graphs describing the behaviour of pore pressure (ε_1-u_w, ε_1-q and ε_1-q/p) were used to define the failure line. The position of the critical state line was defined according to numerous earlier performed drained triaxial tests on HUT clay. According to these tests the slope of the critical state line M=1,2. When defining failure line and critical state line, the results that were generated when samples shape was clearly deformed, were not used in determination. Strength parameters were very similar for test groups performed with strain rates 0,06 %/h, 0,6 %/h and 6 %/h. Only strength parameters in tests performed with the highest strain rate 6 %/h were a bit higher. For individual tests the strain rate alteration during the test was investigated and it was observed that higher strain rate strengthens the sample and vice versa. It can be stated that the strain rate has the influence on the strength of the clay and higher the strain rate higher the strength. However, the strengthening and weakening of the samples did not seem to follow any logic in this research. During the triaxial tests there were several power failures in Helsinki University of Technology and due to that there is discontinuity in some test results.

When comparing the strength of the natural and reconstituted samples tested with same strain rate, it was observed that the strength of the natural samples is higher than the strength of the reconstituted samples according to q_{max} values. q_{max}-values for natural samples reached the used cell pressure or grow even higher, whereas the q_{max}-values for reconstituted samples stay significantly smaller than used cell pressures.

It is obvious that in order to improve the performance of EVP-SCLAY1S and ACM models further research is required and to define model´s parameters reliably, wider database of test results must be gathered. For example, to research the influence of strain rate on strength parameters it is recommended to perform undrained triaxial tests with different stress ratios. In this research used stress ratio was 0,4 and in the future it would be interest-

ing to see what happens when used stress ratio is either lower or higher. Working machines and continuous power supply are also essential to ensure success in laboratory tests.

The definition of selected parameters was viable and in the future when archive of the test results is wider, EVP-SCLAY1S and ACM models will surely be user-friendly design tools for geotechnical engineers.

REFERENCES

Aalto A., Lojander M. & Ravaska O. 2004. *On the stress-dependence of settlement parameters of Finnish Clays.* XIV Nordic Geotechnical Meeting, Ystad, Sweden 19-21 May 2004. Linköping 2004, Swedish Geotechnical society, pp. I 27- I 38.

Bengtsson, P.E., & Larsson R. 1994, *Användarhandbok Program Embankco, version 1.02.* Statens Geotekniska Institut och Vägverket, Linköping.

Bjerrum L. 1974. Publication Nr.100- *Problems of soil mechanics and construction on soft clays*. Norwegian Geotechnical Institute, Oslo.

Bjerrum, L. 1967. Engineering geology of Norwegian normally-consolidated marine clays as related to settlements of building. Geotechnique vol.17, no.2, pp.81-118

Boudali, M., Leroueil, S.& Murthy, B.R.S. 1994. *Viscous behaviour of natural soft clays*. Proc. 13th ICSMFE, New Dekhi, pp.411-416.

Brinkgreve R.B.J., Broere W. & Waterman D. 2004. *Soft-Soil-Creep model.* Plaxis v.8, Material Models Manual, Netherlands, pp. 6-1 – 6-18.

Buisman A.S.K. 1936. *Results of long duration settlement tests.* 1st International Conference on Soil Mechanics and Foundation Engineering, Cambridge, Massachusetts, 1936. Proceedings, Vol.1, p.103-106.

Burland, J.B. 1990. On the compressibility and shear strength of natural clays. Geotechnique 40: 329-378.

CEN Technical Specification. 2004. CEN ISO/TS 17892-5. Geotechnical investigation and testing- Laboratory testing of soil- Part 5: Incremental loading oedometer test.

CEN Technical Specification. 2004. CEN ISO/TS 17892-9. Geotechnical investigation and testing- Laboratory testing of soil- Part 9: Consolidated triaxial compression tests on water saturated soil.

Claesson P. 2003. *Long term settlements in soft clays,* Department of geotechnical engineering, Chalmers University of technology, Goteborg, chapter 2.

Flaate K. et al. 2003. *Laurits Bjerrum- more than an engineer*. Norway: Gjovik bokbinderi. 192s.

Floquet V. 2006. *Modelling creep of soft finnish clay*. Final Project. Helsinki University of technology, Department of Civil and Environmental Engineering. Espoo. 96p.

Graham, J., Crooks, J.H.A., Bell, A.L. 1983. *Time effects on the stress-strain behaviour of natural soft clays.* Geotechnique, vol 33, no.3, pp.327-340.

Graham J., Noonan M.L., Lew K.V. 1983. *Yield states and stress-strain relationship in a natural plastic clay.* Canadian Geotechnical Journal. Vol.20. The National Research Council of Canada. 502-516.

Gardemeister R. 1975. *On engineering geological properties of fine-grained sediments in Finland.* Technical Research Centre of Finland, Publication 9. ISBN 951-38-0185-3.

Hassan M. 2009. *Engineering characteristics of cement stabilized soft finnish clay- a laboratory study.* Licentiate thesis. Helsinki University of Technology, Department of Civil and Environmental Engineering. Espoo. 72p.

Head K.H. 1992. *Manual of soil laboratory testing, Volume 3: Effective stress tests*. John Wiley & Sons, New York. 247-329.

Hoikkala S. 1991. *Jatkuvapuristeinen ja portaittainen ödömetrikoe.* Master´s thesis. Helsinki University of Technology, Faculty of Civil Engineering and Surveying.

Janbu N. 1967. *Settlement calculations based on the tangent modulus concept.* The technical University of Norway, Soil mechanics and Foundation Engineering. Trondheim. 57p.

Karstunen M., Yin Z.Y., Koskinen M., Leoni M.& Vermeer P.A. 2008. *Some recent developments in constitutive modelling of soft clays.* Proc. of The 12th International Conference on Computer Methods and Advances in Geomechanics, 966-975.

Karstunen M. 2008. Modelling progressive failure of embankments and slopes. Research plan.

Karstunen M., Krenn H., Wheeler S.J., Koskinen M.& Zentar R. 2005. *Effect of Anisotropy and Destructuration on the Behavior of Murro Test Embankment.* International Journal of Geomechanics (ASCE); 5(2), 87-97.

Kim Y.T., Leroueil S. 2001. Modelling the viscoplastic behavior of clays during consolidation: Application to Berthierville clay in both laboratory and field conditions. Canadian Geotechnical Journal, 38(3), 484-497.

Korhonen, K-H. 1985. *Muodonmuutosominaisuudet*. RIL 157-1 Geomekaniikka 1. Helsinki, Finland : Otapaino. S.259-307. ISBN 951-758-086-X

Koskinen M. & Karstunen M. 2004. *The effect of structure on the compressibility of Finnish clays.* Proc. of XIV Nordic Geotechnical Meeting, Volume 1, A11-A22.

Koskinen M., Karstunen M. & Lojander M. 2003. *Yielding of "ideal" and natural anisotropic clays.* International Workshop on Geotechnics of Soft Soils- Theory and Practice. Vermeer, Schweiger, Karstunen & Cudny (eds.).

Larsson, R. 1981. *Drained behaviour of Swedish clays*. Swedih Geotechnical Institute. Report No.12. Linköping.

Larsson, R. 1986. *Consolidation of soft soils- Report 29*, Swedish Geotechnical Institute, Linköping

Larsson R., Eriksson, L., Bengtsson, P-E. 1993. *Sättningsprognoser för vägbankar på lös finkornig jord. Beräkning av sättningars storlek och tidsförlopp.* Statens Geotekniska Institut, Information 13. Linköping.

Larsson R., Bengtsson P-E, Eriksson L . 1997. Prediction of settlements of embankments on soft, fine-grained soils. Calculation of settlements and their course with time. Swedish geotechnical institute, Linköping.

Leoni M., Karstunen M. & Vermeer P.A. 2008. *Anisotropic creep model for soft soils*. Geotechnique 58, No. 3, 215-226

Leoni, M., Vermeer P.A.& Karstunen M. 2009. *Validation of anisotropic creep model for soft soils.* Geotechnics of Soft Soils- Focus on Ground Improvement. Karstunen & Leoni(eds). Taylor & Francis Group. London. ISBN 978-0-415-47591-4.

Leoni, M. & Vermeer P.A. 2009. *Numerical modelling of creep in soft clays*. Proc. 17th Int. Conf. Soil Mech. Geotech. Engng, Alexandria, 1, 578-581.

Leroueil S. & Vaughan P.R. 1990. The general and congruent effects of structure in natural soils and weak rocks. Geotechnique, vol 40, no.3, pp.467-488.

Leroueil S., Kabbaj M., Tavenas F., Bouchard R. 1985. *Stress-strain-strain-rate relation fot the compressibility of sensitive natural clays.* Geotechnique, vol. 35, no. 2, pp.159-180.

Leroueil S., Tavenas F., Brucy F., La Rochelle P. & Roy M. 1979. *Behaviour of destructured natural clays.* ASCE Journal of Geotechnical Engineering, vol. 105, no.6, pp.759-778.

Länsivaara T. 2001. *Painuman ennustaminen painumahavaintojen perusteella*. Tiehallinnon selvityksiä 49/2001. Helsinki : Edita Oyj. 87s. ISBN 951-726-797-5.

Mesri, G. & Castro, A. 1987. *C_α /C_c concept and K_0 during secondary compression.* Journal of Geotechnical Engineering, Vol.113, no.2, March, pp.230-247.

Mesri G. & Godlewski P.M. 1977. *Time and stress-compressibility interrelationship.* ASCE Journal of Geotechnical Engineering, vol.103, no. 5, pp.417-430.

NovaPoint GeoCalc. 2009. Version 2.0. Help. Painuma.teoria. Vianova Systems Finland Oy.

Ohde, J. 1939. *Zur Theorie der Druckverteilung im Baugrund Bauingenieur.* 14 (1939): 33/34: 451-458

Ojala K.A.E., Ikävalko O., Palmu J.P., Vanhala H., Valjus T., Suppala I., Salminen R., Lintinen P.& Huotari T. 2007. *Espoon Suurpellon alueen maaperän ominaispiirteet.* Geologinen tutkimuskeskus. [Referred 28.10.2009] Available: http://arkisto.gtk.fi/p22/p22_4_2007_39.pdf

Ortigao, J.A.R. 1995. *Soil mechanics in the light of critical state theories.* Rotterdam, Netherlands: Balkema. 299s. ISBN 90-5410-1946.

Schofield A. & Wroth P. 1968. *Critical State Soil Mechanics*. Berkshire, England. McGraw-Hill.306p.

SFS-Käsikirja 179-2. 2008. *Geotekninen tutkimus ja koestus. Osa 2: Maan laboratoriokokeet 2008*. Suomen standardisoimisliitto SFS RY. Helsinki. ISBN 978-952-5650-59-4.

Sheahan T.C., Ladd C.C., Germaine J.T.1996. *Rate- dependent undrained shear behaviour of saturated clay.* ASCE Journal of the Geotechnical Engineering, vol. 122, no. 2, pp.99-108.

Stapelfeldt T., Vepsäläinen P.& Yin Z.Y. 2009. *Numerical modelling of a test embankment on soft clay improved with vertical drains.* Geotechnics of Soft Soils- Focus on Ground Improvement. Karstunen & Leoni(eds). Taylor & Francis Group. London. ISBN 978-0-415-47591-4.

Suklje, L. 1969. *Rheological aspects of soil mechanics*. Bath, United Kingdom: Pitman Press. 571s. SBN 471-83550-1

Svano G. & Christensen S. 1991. *A soil model for consolidation and creep*. The Norwegian Institute of Technology, Norway.

Takala, J. 1995. *Kerroksellisen maan painuman laskeminen.* Master´s thesis. The Helsinki University of Technology.

Tavenas, F.& Leroueil, S. 1977. *Effects of stresses and time on yielding of clays*. 9th International Conference on Soil Mechanics and Foundation Engineering ICSMFE, vol. 1, pp.319-326.

Taylor, D. 1948. *Fundamentals of soil mechanics.* New York, USA: John Wiley & Sons, inc. 700p.

Terzaghi, K. & Peck R.B. 1948. *Soil mechanics in engineering practice.* New York, USA: John Wiley & Sons, inc. 566p.

Tidfors, M.& Sällfors, G. 1989. *Temperature effects on the preconsolidation pressure.* Geotechnical Testing Journal, Vol.12, No. 1, pp.93-97.

Vaid, Y.P.& Campanella, R.G. 1977. *Time-dependent behaviour of undisturbed clay.* ASCE Journal of the Geotechnical Engineering, vol. 103, no. 7, pp.693-709.

Wheeler S.J., Näätänen A., Karstunen M., Lojander M. 2003. *An anisotropic elastoplastic model for soft clays.* Canadian Geotechnical Journal, 40 (2): 403-418.

Yin J.H. & Graham J. 1989. *General elastic viscous plastic constitutive relationship for 1-D straining in clays.* Proceedings of the 3rd NUMOG 1989. University of Manitoba. Winnipeg, Canada.

Yin Z.Y. & Karstunen M. 2008. *Influence of Anisotropy, Destructuration and Viscosity on the Behavior of an Embankment on Soft Clay.* Proc. of The 12th International Conference on Computer Methods and Advances in Geomechanics, 4728-4735.

Yin Z.Y., Hicher P.Y. 2008. *Identifying parameters controlling soil delayed behavior from laboratory and in situ pressometer testing.* International Journal for Numerical and Analytical Methods in Geomechanics; 32, 1515-1535.

APPENDICES

1. ε_1-q and ε_1-u_w graphs from all triaxial tests

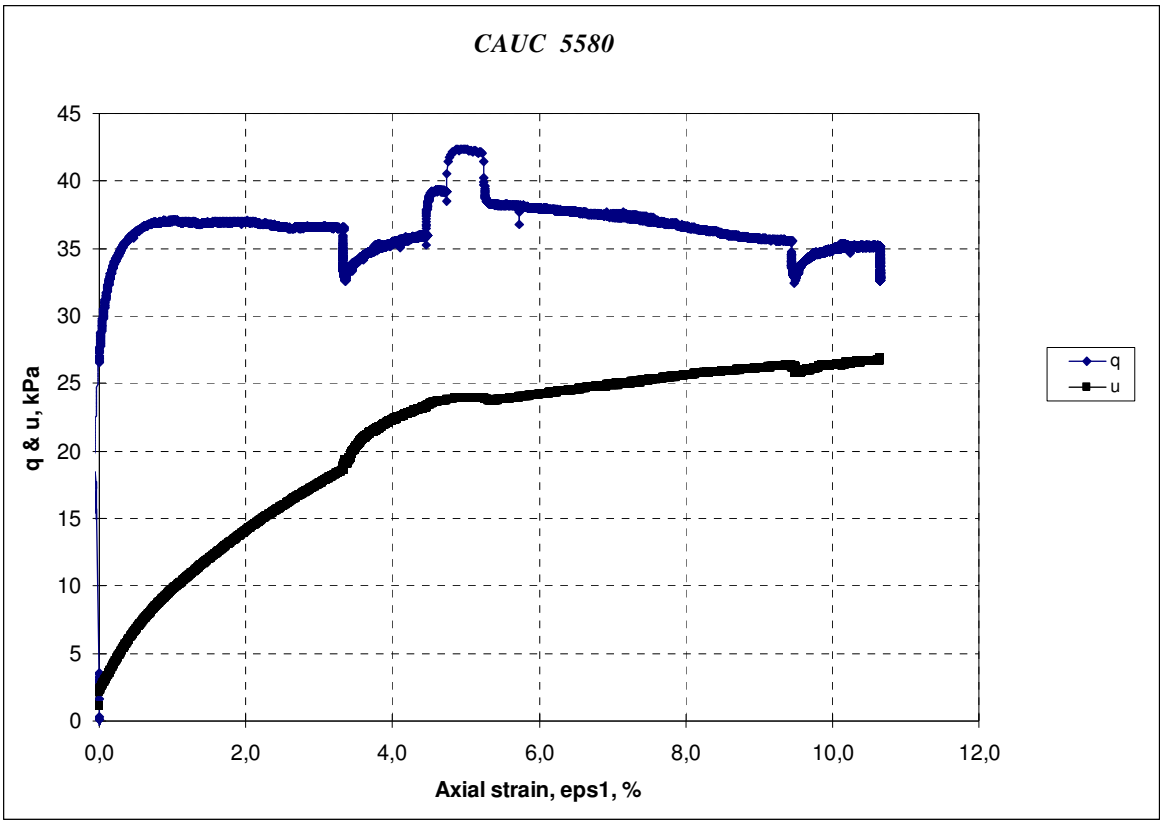

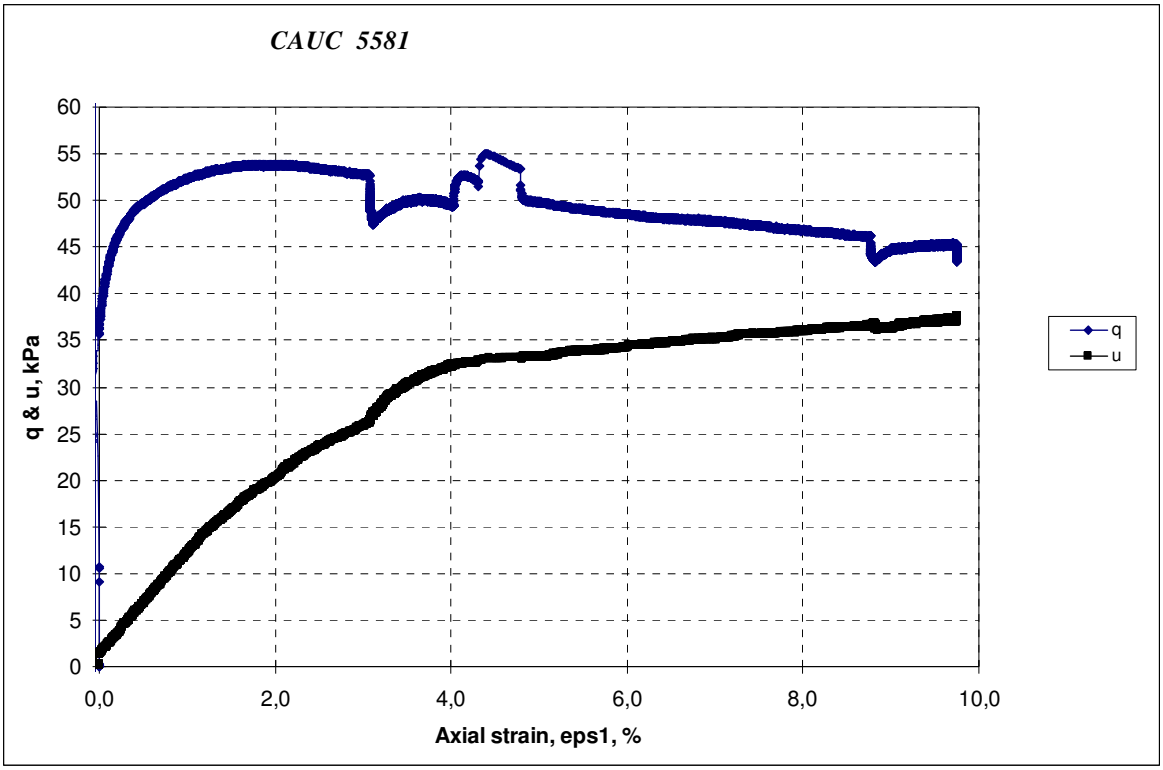
CAUC 5581
q & u, kPa
Axial strain, eps1, %
q
u
0
5
10
15
20
25
30
35
40
45
50
55
60
0,0
2,0
4,0
6,0
8,0
10,0

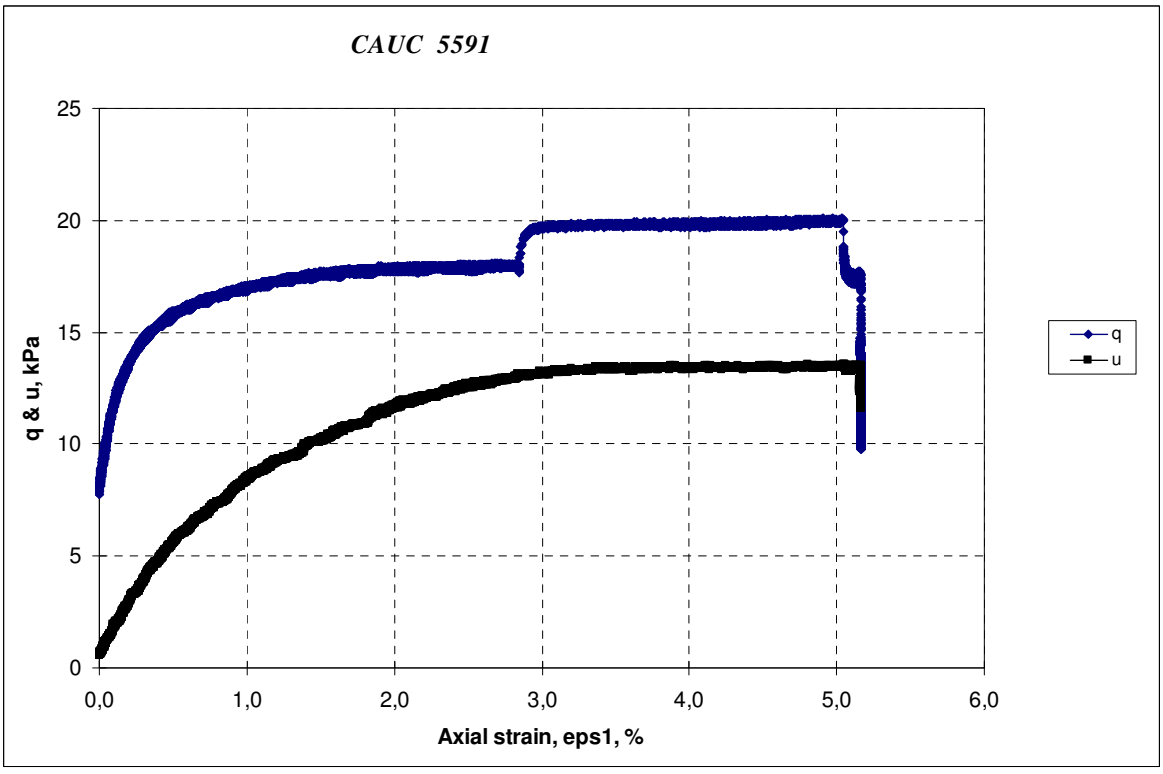
CAUC 5591
q & u, kPa
Axial strain, eps1, %
q
u
0
5
10
15
20
25
0,0
1,0
2,0
3,0
4,0
5,0
6,0

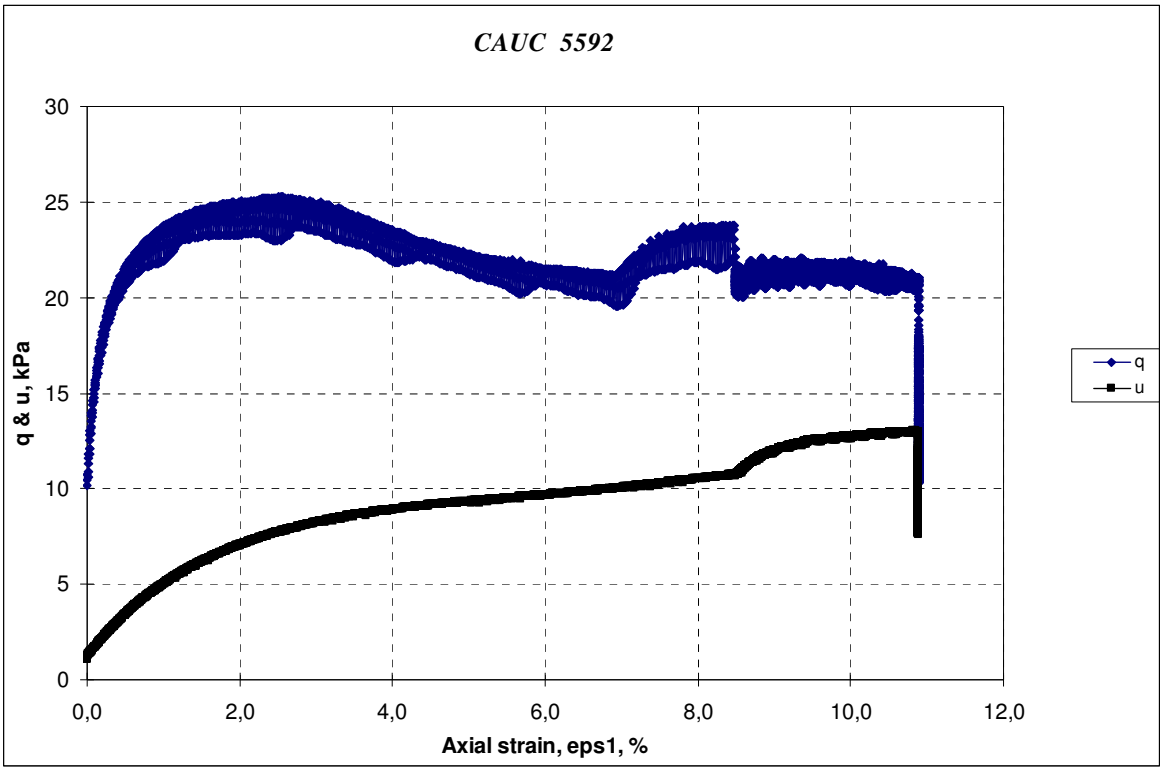
CAUC 5592
30
25
20
15
10
5
0
q & u, kPa
0,0
2,0
4,0
6,0
8,0
10,0
12,0
Axial strain, eps1, %
q
u

,

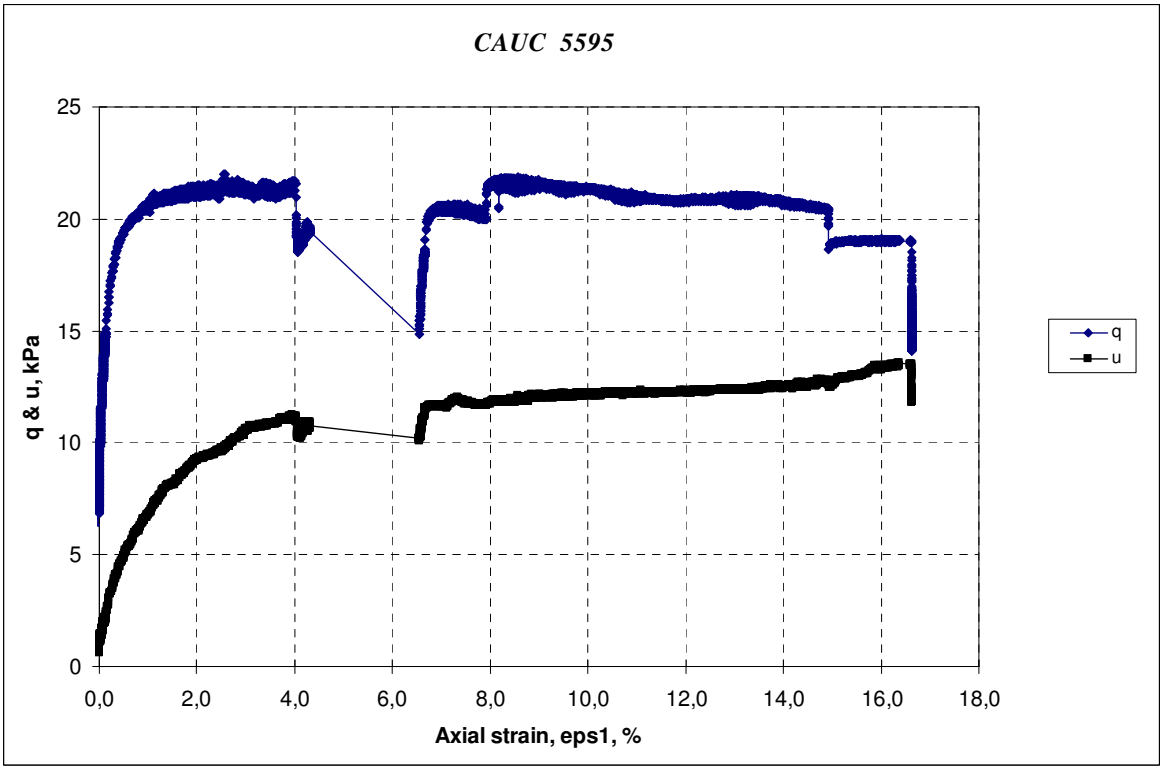
CAUC 5595
25
20
15
10
5
0
q & u, kPa
0,0
2,0
4,0
6,0
8,0
10,0
12,0
14,0
16,0
18,0
Axial strain, eps1, %
q
u

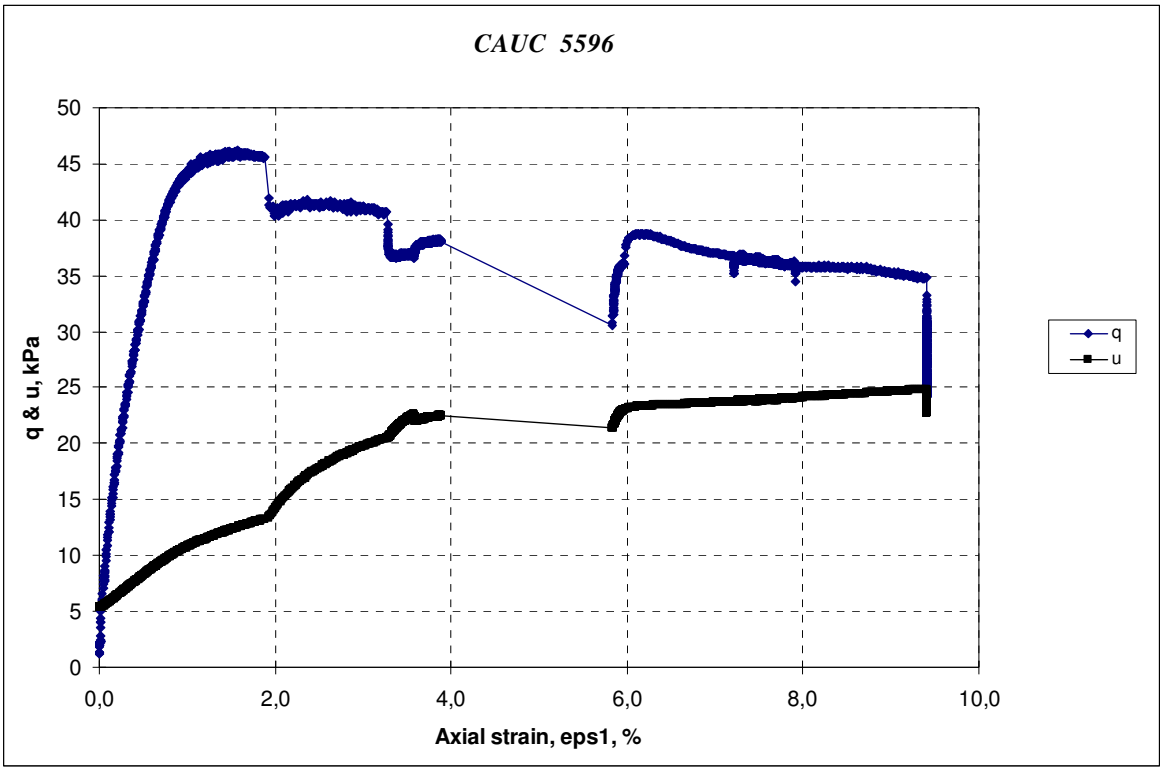
CAUC 5596
q & u, kPa
Axial strain, eps1, %
q
u
0
5
10
15
20
25
30
35
40
45
50
0,0
2,0
4,0
6,0
8,0
10,0

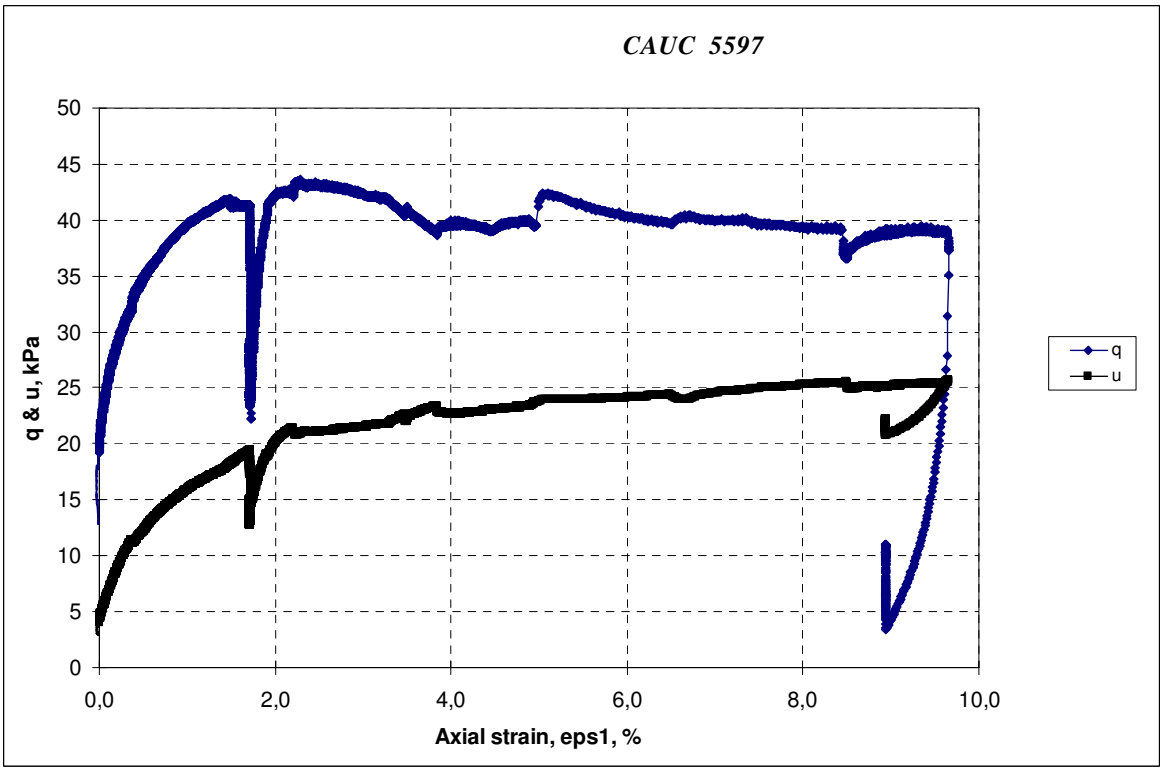
CAUC 5597
q & u, kPa
Axial strain, eps1, %
q
u
0
5
10
15
20
25
30
35
40
45
50
0,0
2,0
4,0
6,0
8,0
10,0

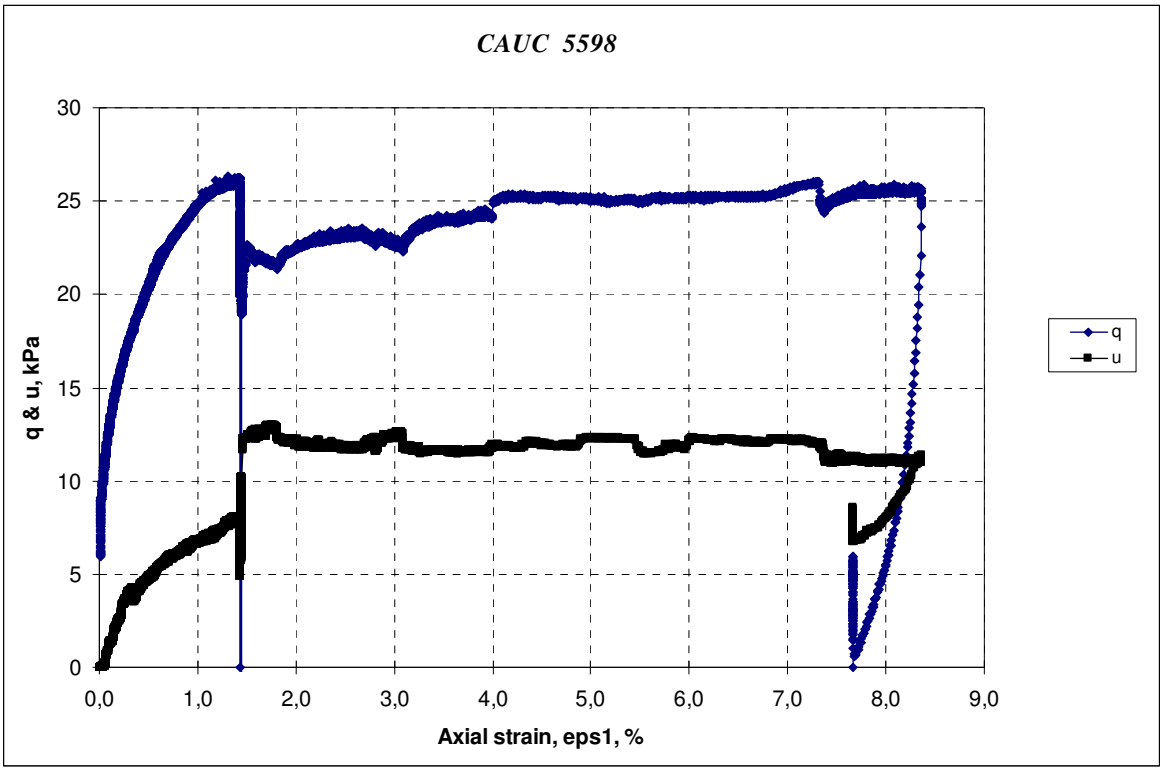
CAUC 5598
q & u, kPa
Axial strain, eps1, %
q
u
0
5
10
15
20
25
30
0,0
1,0
2,0
3,0
4,0
5,0
6,0
7,0
8,0
9,0

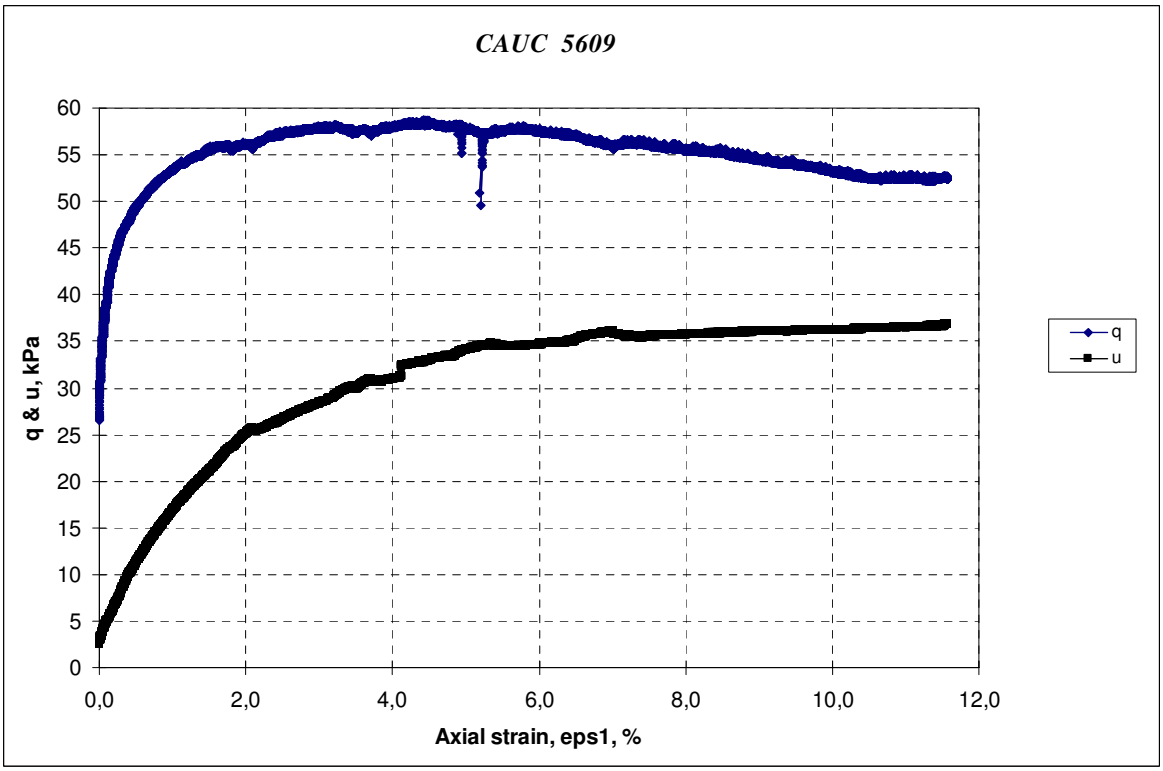
CAUC 5609
q & u, kPa
Axial strain, eps1, %
q
u
0
5
10
15
20
25
30
35
40
45
50
55
60
0,0
2,0
4,0
6,0
8,0
10,0
12,0

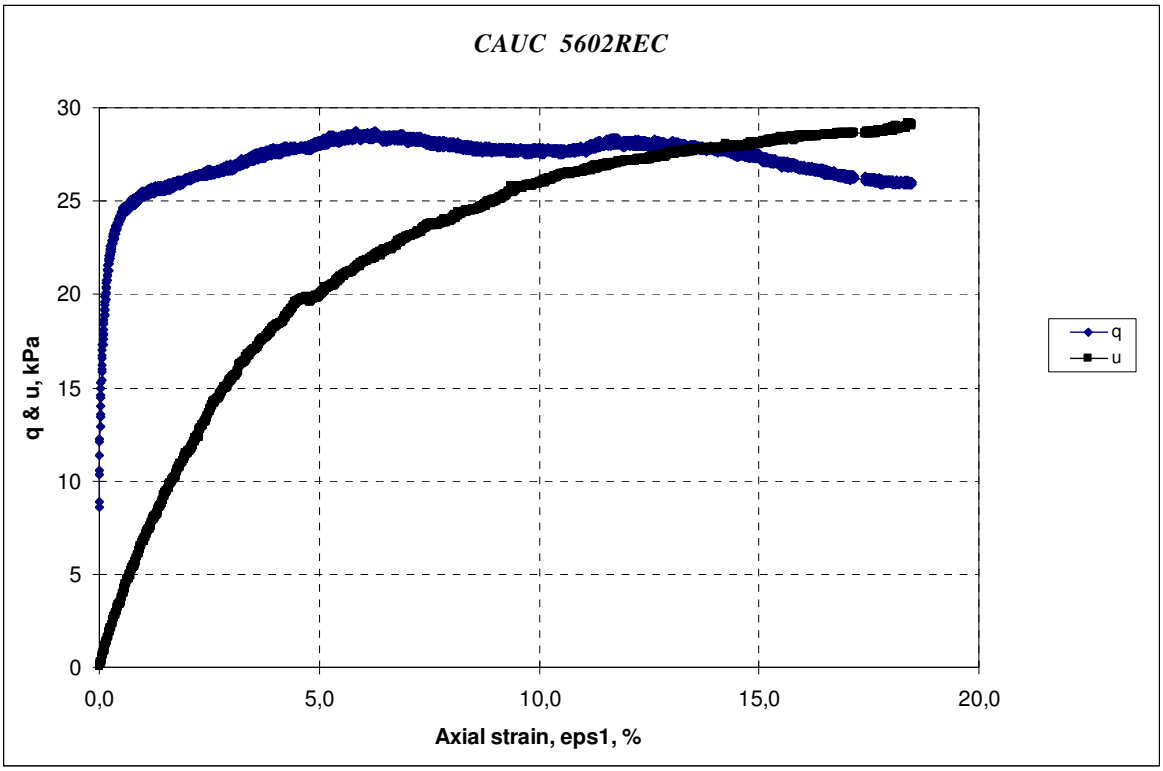
CAUC 5602REC
30
25
20
15
10
5
0
q & u, kPa
0,0
5,0
10,0
15,0
20,0
Axial strain, eps1, %
q
u

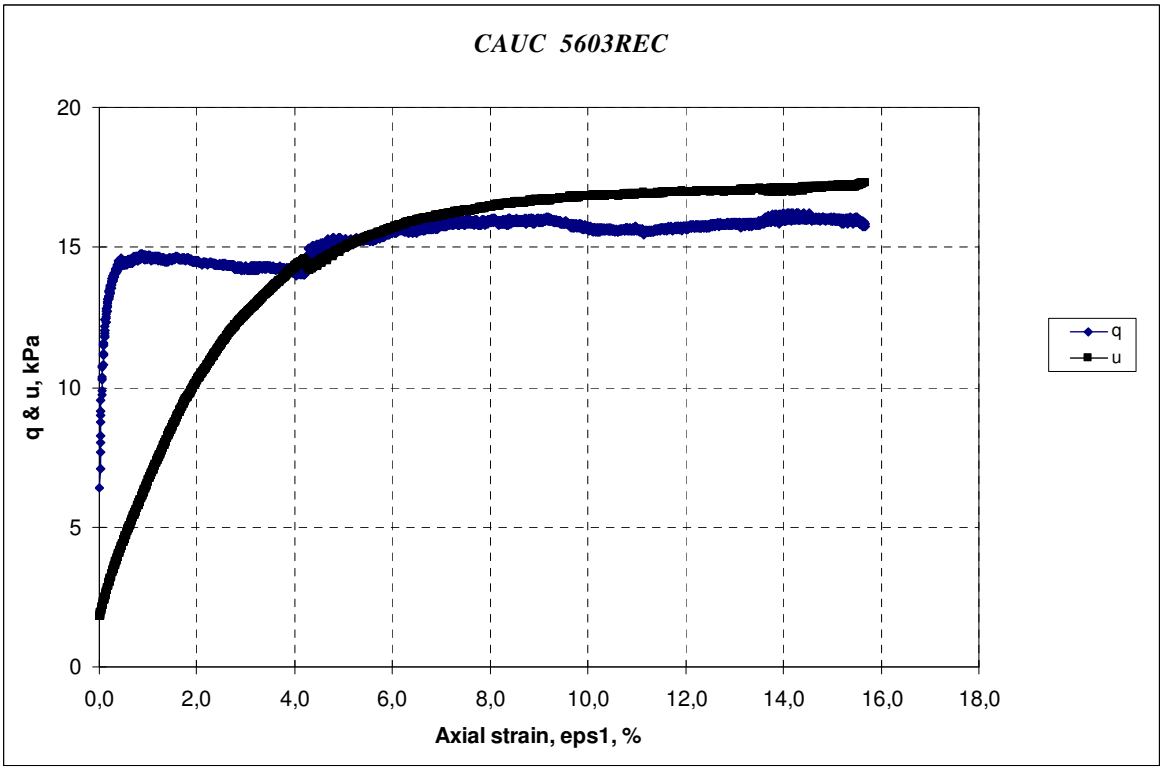
CAUC 5603REC
20
15
10
5
0
q & u, kPa
0,0
2,0
4,0
6,0
8,0
10,0
12,0
14,0
16,0
18,0
Axial strain, eps1, %
q
u

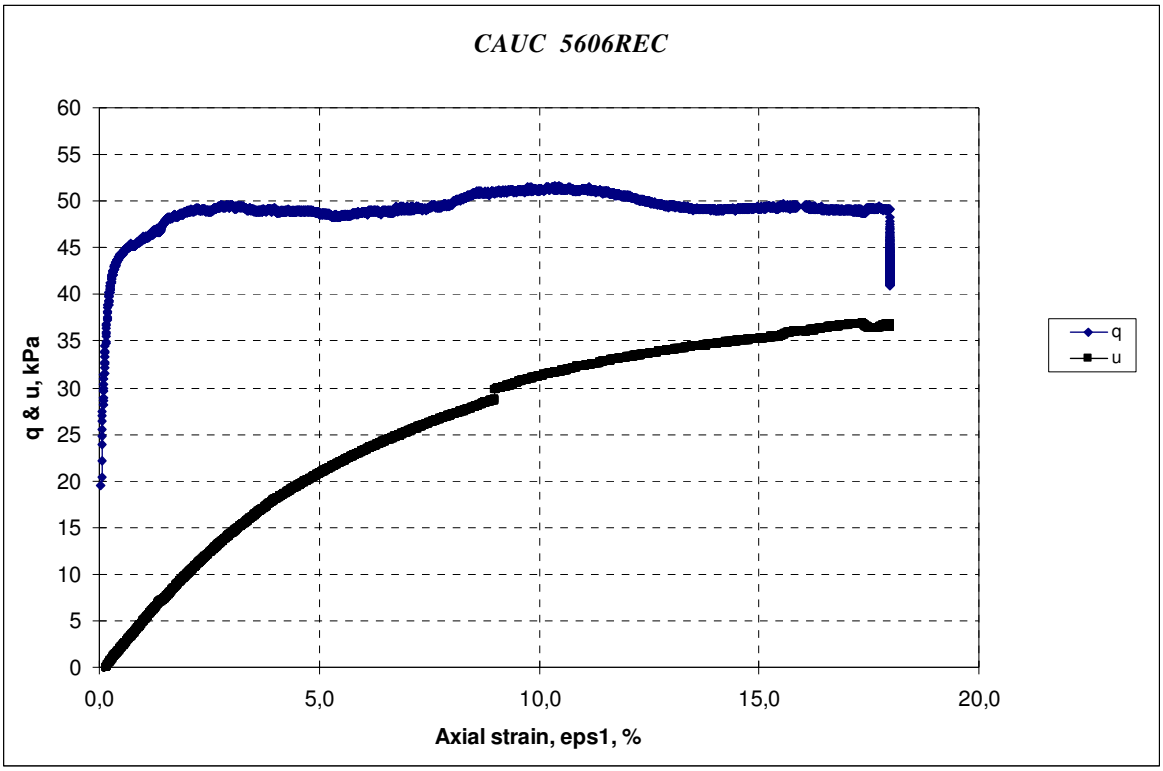
CAUC 5606REC
q & u, kPa
60
55
50
45
40
35
30
25
20
15
10
5
0
0,0
5,0
10,0
15,0
20,0
Axial strain, eps1, %
q
u

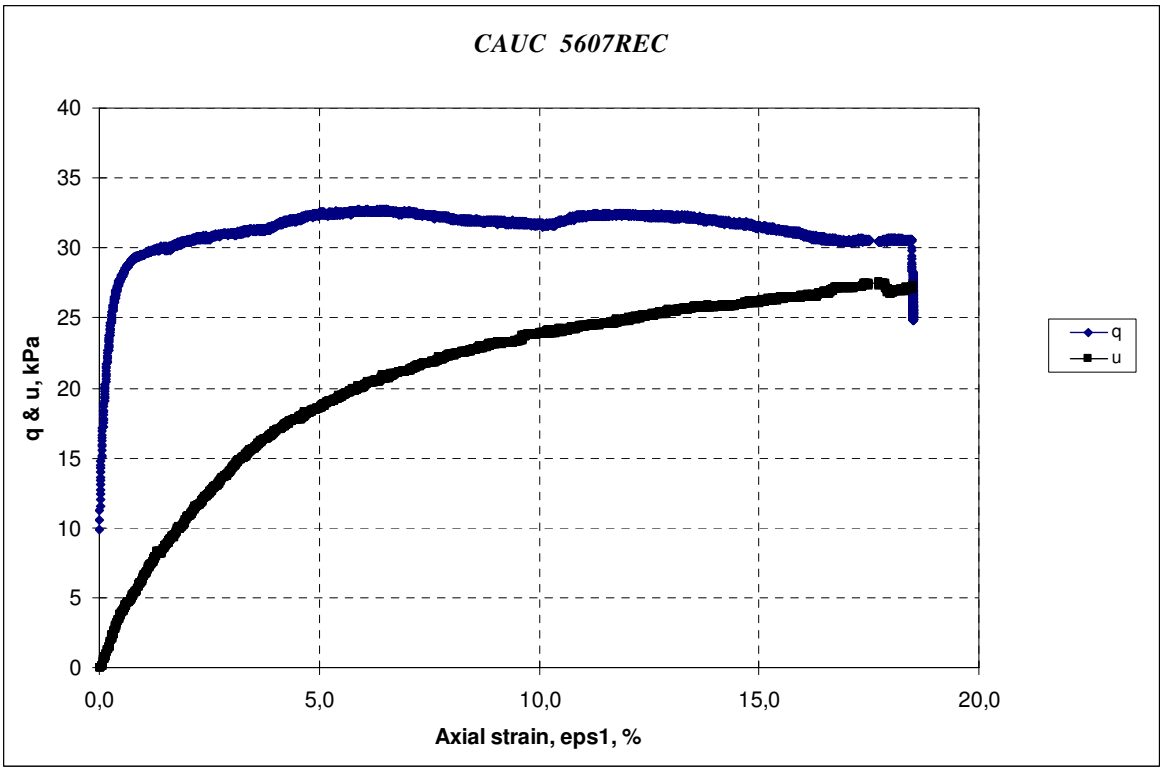
CAUC 5607REC
q & u, kPa
40
35
30
25
20
15
10
5
0
0,0
5,0
10,0
15,0
20,0
Axial strain, eps1, %
q
u

2. ε_1-q/p graphs from all test series

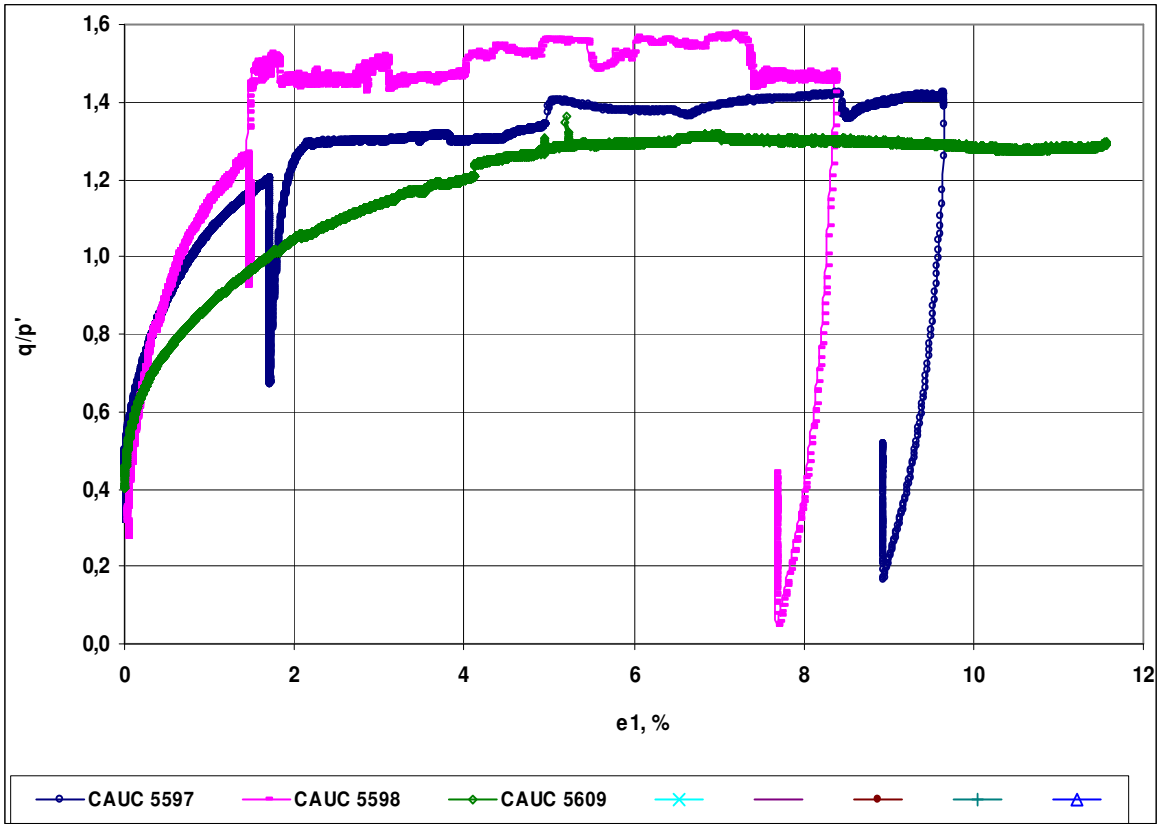

ε_1-q/p-plot and when $\dot{\varepsilon}$ *= 0,06 %/h*

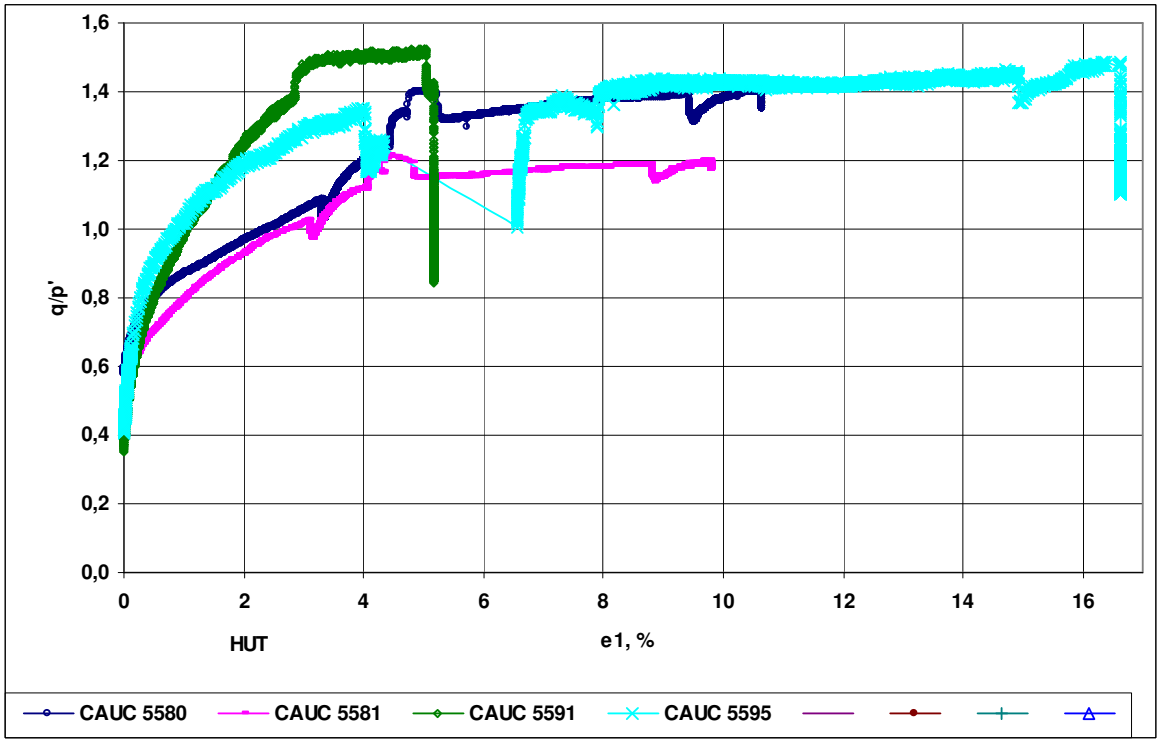

ε_1-q/p-plot and when $\dot{\varepsilon}$ *= 0,6 %/h*

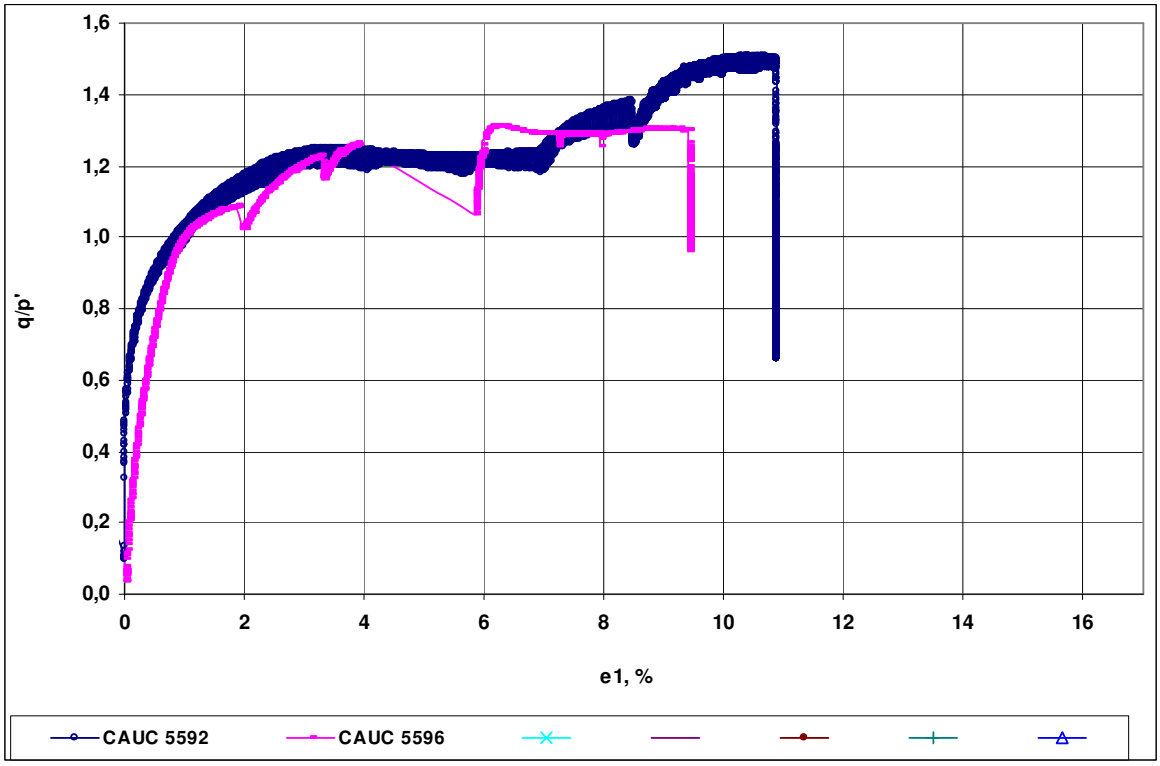

ε_1-q/p-plot and when $\dot{\varepsilon}$ =6 %/h

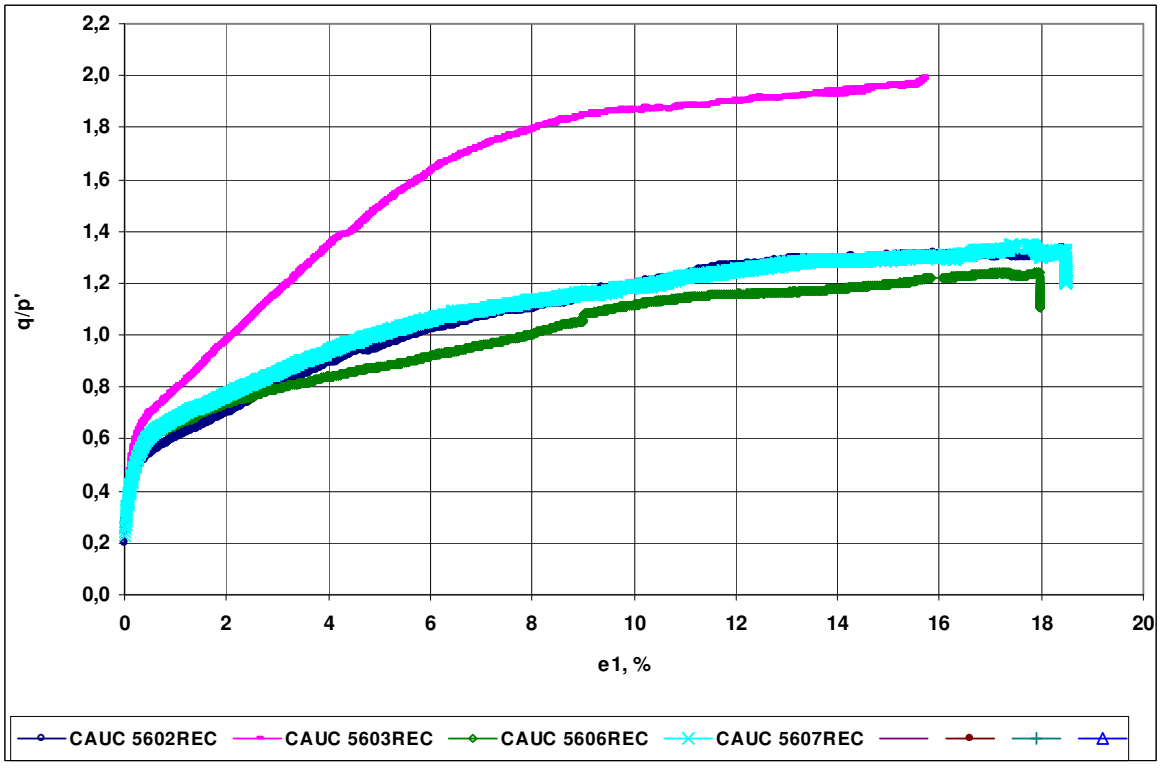

ε_1-q/p-plot for reconstituted samples and when $\dot{\varepsilon}$ =0,6 %/h